Role of one-carbon metabolism in neocortex development

Sulov Saha

RÉPUBLIQUE FRANÇAISE
Liberté Égalité Fraternité

Université de Toulouse

Doctorat de l'Université de Toulouse

préparé à l'Université Toulouse III - Paul Sabatier

ROLE DU METABOLISME ONE-CARBONE DANS LE DEVELOPPEMENT DU NEOCORTEX

Thèse présentée et soutenue, le 7 mars 2024 par

Sulov SAHA

École doctorale
BSB - Biologie, Santé, Biotechnologies

Spécialité
NEUROSCIENCES

Unité de recherche
MCD - Molecular, Cellular and Developmental Biology Unit

Thèse dirigée par
Alice DAVY

Composition du jury
M. Laurent NGUYEN, Rapporteur, Université de Liège - Belgique
M. Alexandre BAFFET, Rapporteur, INSERM de Paris - Institut Curie
Mme Gaia NOVARINO, Examinatrice, Institute of Science and Technology Austria - Autriche
M. Julien COURCHET, Examinateur, INSERM de Lyon - Institut NeuroMyoGène
Mme Pascale DUFOURCQ, Présidente du jury, Université de Toulouse III - Paul Sabatier
Mme Alice DAVY, Directrice de thèse, CNRS de Toulouse - MCD - CBI

Acknowledgement

This research would not have been possible without the support of a number of people. First of all, big thanks to Alice Davy for providing me the opportunity to work together on such an exciting project. She has been a tremendous inspiration and support, enabling me to achieve something for which I am truly grateful.

Special thanks to Laurent Nguyen and Alexandre Baffet for helping to meticulously check my work, and guiding me to a stronger conclusion. I would like to show my sincere gratitude to Gaia Novarino, Julien Courchet, and Pascale Dufourcq for serving on the thesis defense committee and providing helpful feedback and suggestions. I am also grateful to the thesis committee members, Isabelle Ader and Julien Ferent, for their enduring support and much-appreciated advice.

I am thankful to the entire Davy team for their invaluable guidance that made this project possible. This thesis builds on initial work done by Mohamad-Ali Fawal, Christophe Audouard, and Thomas Jungas. To all of you, thanks for the special “black & white result” and “American method”. Without the ongoing support of David Ohayon and Clémence Debacq, this thesis would miss “la cerise sur le gateau”. I also extend my gratitude to Clément Chapat for sharing his expertise and fruitful collaboration.

This work is supported by the French Ministry of Higher Education and Research (MESR) and the French National Center for Scientific Research (CNRS). I am deeply grateful to the Paul Sabatier University and MCD unit at the CBI Toulouse for facilitating access to the resources and support throughout this research project. I would also like to thank the anonymous peer reviewers and editorial board members at Development for their valuable insights in the published manuscript.

To Vicente, Damien, Maha, Vishnu, Cheryn, Iulia, Clement, Clair, Lea, Meritxell, Aurore, Delhia, Alexandra, and Alid – you are the best colleagues. Together, we have navigated the challenges and celebrated the triumphs, and I appreciate having you by my side. Finally, I would like to thank my parents, brother, and friends around the world for supporting and motivating me on this incredible journey.

To all those mentioned and those that have slipped my mind: ধন্যবাদ

Table of contents

Summary

The neocortex is unique for its evolutionary innovations such as developmental expansion and higher cognitive functions in mammals. This requires a proper coordination on the generation of neurons and glia by a pool of neural progenitor cells (NPC) consisting of apical radial glial cells (aRGC) and intermediate progenitor cells (IPC). NPC pool is spatiotemporally regulated to balance proliferation and commitment to specific fates. Both intrinsic programs and extrinsic cues can influence NPC fate dynamics. Cellular metabolism allows the NPC to establish an integration of the intrinsic and extrinsic factors to better adapt to different environments. Emerging evidences suggest that NPC metabolism is crucial for the maintenance of NPC proliferation, but how metabolism may facilitate in vivo differentiation into distinct neuronal subtypes remain elusive. For modeling in vivo differentiation under one carbon (1C) metabolic deficiency, I aimed to characterize the contributions of folate and methionine cycles that provides biosynthetic metabolites predominantly in the NPC. We used quantitative immunofluorescence to perform a detailed analysis of neuronal production under 1C metabolic deficiency during neocortical development. First, we assessed the effects of folate metabolic deficiency using a genetically mutant mouse line and human organoids. Second, we investigated the impacts of gestational methionine dietary restriction on organ-specific growth outcomes in mice.

In the first project, we found that folate metabolism is active in aRGC at the onset of neurogenesis. This spatiotemporal activity appears to be necessary for direct neurogenesis, an important step of development. Specifically, we show that targeting dihydrofolate reductase (DHFR) enzyme delays direct neuronal differentiation of aRGC at early stages, followed by increased production of IPC that promotes the onset of indirect neurogenesis with accelerated neuronal differentiation at mid-to-late stages in both mouse and human models. Mechanistically, we found that DHFR activity contributes to the steady-state levels of THF and SAM metabolites, and that has critical consequences on the histone methylation (H3K4me3) dynamics, implicating folate metabolism as a novel spatiotemporal regulator in the generation of neurons.

In the second project, we sought to explore the consequences of methionine restriction (MR) on fetal organ growth and development. We targeted methionine metabolism with a MR diet given for 5 days to the pregnant mice and analyzed the growth of fetal organs, including the brain, liver, and heart. Our data shows that the supply of methionine throughout the gestation is necessary for brain growth and neocortical neurogenesis. In contrast, growth of the liver and heart is unaffected highlighting an organ-specific response to MR. In addition, we quantified global DNA methylation, translation, and cell cycle kinetics and found that those parameters are differentially affected in the organs. Strikingly, MR leads to neocortical growth retardation with reduced neuron numbers that is completely compensated at birth with the reintroduction of control diet for 5 days. Using cell cohort tracing, I identified the NPC pool that is responsible for this catch-up growth. Further, my data indicates that MR promotes direct neuronal differentiation of aRGC at early stages, followed by delay in the production of IPC and neuronal differentiation at mid-to-late stages in mouse neocortex. This unexpected result is in sharp contrast with the outcomes of folate metabolic deficiency, suggesting shared metabolites in the 1C metabolism might act independently. In conclusion, this study revealed that the brain is highly sensitive to MR, and methionine metabolism is a major regulator of brain growth.

Collectively, the results of this PhD thesis provide new perspectives on how 1C metabolism contributes to NPC proliferation and differentiation outputs throughout neocortex development.

Résumé

Le neocortex des mammifères est unique en raison d'innovations évolutives telles que l'augmentation de sa taille et l'apparition de capacités cognitives complexes. Ces attributs nécessitent la mise en place de circuits neuronaux qui s'appuient sur une production stéréotypée de neurones et de cellules gliales à partir de progéniteurs neuraux (NPC). Des études pionnières ont montré que des programmes intrinsèques et des facteurs extrinsèques régulent le devenir des NPC pour équilibrer leur prolifération et leur différentiation en sous types cellulaires distincts. Le métabolisme cellulaire intègre ces différents facteurs et permet ainsi l'adaptation des NPC à leur environnement. Un nombre croissant d'études indiquent que le métabolisme des NPC est crucial pour leur maintien en prolifération mais comment ces cascades métaboliques interviennent pour contrôler la différentiation en sous types cellulaires spécifiques est encore mal compris. Au cours de mon doctorat, je me suis concentré sur le métabolisme du One carbone (1C). En particulier, j'ai cherché à caractériser le développement du neocortex lors d'une restriction du métabolisme 1C. Je me suis intéressé aux cycles du folate et de la Methionine qui produisent des métabolites importants pour la prolifération et les réactions de méthylation. J'ai utilisé une approche d'immunofluorescence quantitative pour analyser en détail la production des sous types de neurones lors d'une restriction du métabolisme 1C. Dans un premier temps j'ai analysé une lignée de souris génétiquement modifiée et un modèle d'organoide humain traité avec un agent pharmacologique. Dans un deuxième temps, j'ai évalué l'impact d'une restriction alimentaire en Methionine pendant la gestation sur la croissance et le développement du foetus.

Au cours du premier projet, en ciblant spécifiquement l'enzyme Dihydrofolate reductase (DHFR), mes travaux montrent que le métabolisme du folate est actif dans les progéniteurs apicaux au début de la neurogenèse et que la diminution de cette activité dans les NPC entraîne le basculement d'une neurogenèse directe à indirecte. Ceci a des conséquences sur la production neuronale et la composition en neurones du cerveau postnatal. Au niveau mécanistique, la diminution de l'activité de DHFR entraîne une diminution des métabolites THF et SAM, avec des conséquences sur la méthylation de l'histone H3. Globalement, ce travail indique que le

métabolisme du folate joue un rôle important dans la dynamique de la neurogenèse dans le neocortex.

Lors du deuxième projet, nous avons cherché à caractériser les conséquences d'une restriction alimentaire de Methionine (MR) courte (5 jours) au cours de la gestation sur trois organes foetaux, le cerveau, le foie et le coeur. Nos travaux montrent que l'apport régulier en Methionine est indispensable à la croissance du cerveau, mais pas du foie ni du coeur, revélant une sensibilité différentielle de ces organes. Nous avons mesuré des paramètres, tels que la méthylation de l'ADN, la traduction et le cycle cellulaire et montré que ces trois organes réagissent différemment à la MR. Par ailleurs, en analysant plus spécifiquement le neocortex, nous avons observé que la production neuronale est fortement impactée par la MR. Cependant, le retour à un régime alimentaire complet pendant les 5 jours suivants la MR permet de restaurer la production neuronale, soulignant la très grande plasticitié du neocortex au cours du développement. En utilisant des approches de traçage de cohortes cellulaires, j'ai pû visualiser les progéniteurs à l'origine de cette croissance de rattrapage. Cette étude indique que le cerveau en développement est particulièrement vulnérable au déficit en Methionine qui se manifeste par un retard de croissance et une production neuronale réduite.

Collectivement, les résultats obtenus durant ce travail de doctorat apportent un nouvel éclairage sur l'importance du métabolisme 1C pour la croissance et le développement du neocortex.

Introduction

A human fetus inside the mother's womb needs adequate nutritional supply to meet the growth demands for an appropriate birth size. Maternal supply fails to provide nutrients and oxygen efficiently due to genetic or environmental factors in about 5% of human pregnancies, resulting in abnormal fetal growth (Romo et al., 2009). This can induce metabolic stress to the developing organs, often causing growth asymmetry in the fetus. In many of these cases, the growth defects are associated with compromised outcomes in the vital organs, including the brain (Sharma et al., 2016).

The human brain has undergone dramatic changes during evolution. An adult human brain is composed of 86 billion neurons and 85 billion nonneuronal (~glial) cells (Azevedo et al., 2009). Neurons and glial cells form neuroglial circuits to form the information processing networks that are responsible for sensory-motor and cognitive abilities. During development, progenitor cell populations coordinate brain growth through their proliferation and differentiation rate over time in order to generate appropriate number of neuronal and glial subtypes. Evidences support that the capability of progenitor cells are dependent on the intrinsic and extrinsic factors, including metabolism (Namba et al., 2021). Specifically, one carbon (1C) metabolism, comprised of folate and methionine cycles, is reported to support early brain morphogenesis, including the neural tube formation, through 1C units required for the synthesis of DNA, amino acids, polyamine, phospholipids, and methylation reactions (Keuls et al., 2023). Nevertheless, it remains to be understood how these metabolic cues integrate to maintain the long-term development of the brain in a physiological and malnutrition context. This fundamental knowledge may contribute to the development of therapy options for neurobiological diseases.

In this context, this Ph.D. thesis addresses how 1C metabolic cues impact spatiotemporal regulation of brain development. To address that, I have studied mouse neocortex and human neural organoids to closely mirror the biology of human health and disease. The focus of my project was to quantify the dynamics of cellular production and fate in the context of decreased 1C metabolism through genetic targeting and dietary restriction. These models allow

constitutive and transient perturbation of specific metabolites in the 1C pathway and the originality of this work was to look at the nutritional dependency of cellular specification in the developing neocortex with the help of known cell-type specific markers using conventional confocal imaging. Two projects were run in parallel:

In the first project, we made use of a CRISPR-Cas9 engineered mouse mutant for dihydrofolate reductase (DHFR) and methotrexate (MTX)-mediated inhibition of DHFR in human neural organoids, on the production of different neuronal subtypes during neocortex development. This work was published in Development, on 04 September 2023.

Dihydrofolate reductase activity controls neurogenic transitions in the developing neocortex.

Sulov Saha, Thomas Jungas, David Ohayon, Christophe Audouard, Tao Ye, Mohamad-Ali Fawal, Alice Davy.

The second project assesses whether methionine restriction impact neocortex development. It unravels diet-induced microcephaly and the possibility of catch-up growth with the reintroduction of methionine, reflecting the vulnerability and plasticity of the developing brain. This work is in preparation and will lead to a scientific publication.

Acute dietary methionine restriction highlights sensitivity of neocortex development to metabolic variations.

Sulov Saha, Clemence Debacq, Christophe Audouard, Thomas Jungas, Mohamad-Ali Fawal, Clement Chapat, David Ohayon, Alice Davy.

The framework of my Ph.D. project will be introduced in the following order:

• A brief introduction to metabolism with a special focus on the physiological, developmental and pathological aspects.

• A focus on the key developmental and evolutionary processes involved in the mouse and human brain development.

• A comparative analysis of in vivo and in vitro modeling of brain development.

Chapter 1: Metabolism

1.1 A brief history of metabolism

Metabolism is derived from the Greek word, metabolē meaning “to change” and comprises a series of biochemical reactions that take place in the cells of living organisms. These reactions may lead to the synthesis and degradation of complex macromolecules, utilizing or generating energy in the process. The earliest record of metabolic studies has been traced to Santorio Sanctorius’s noted work “Ars de statica medecina” published in 1614 (Figure 1), in which he weighed himself before each meal and then stopped eating and found that the ingested food was lost through what he called “insensible perspiration”.

Figure 1: Santorio Sanctorius sitting in his steelyard balance.

However, the macromolecular constituents of foods had not been identified until Justus von Liebig classified foodstuffs into protein, fat, and carbohydrates in 1840s. Later, pioneering studies led by Wilhelm Kühne, Eduard Buchner, and James Sumner in the late 19th and early 20th centuries marked the beginnings of metabolism with the identification of enzymes involved in biological processes. These discoveries led to the “golden age of biochemistry”, spanning from approximately the 1920s to the 1960s, which established the foundational understanding of the metabolic network governing the utilization of nutrients and the generation of energy in various organisms, including humans. Key contributions during this era were driven by Gustav Embden, Otto Fritz Meyerhof, and Jakub Karol Parnas on glycolysis, Otto

Warburg on respiration, Hans Krebs on tricarboxylic acid (TCA) and urea cycle, Carl and Gerty Cori on glycogen catabolism, and Peter Mitchell on oxidative phosphorylation. These metabolic pathways helped to understand the fundamental aspects of core metabolism, which predominantly encompass essential nutrients, including the carbohydrates, amino acids, and fatty acids (Figure 2).

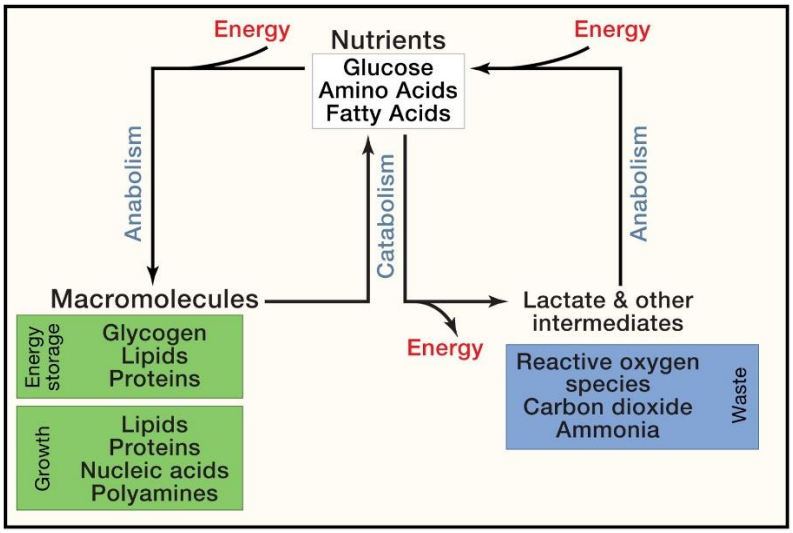

Figure 2: An overview of core metabolism of major nutrients (carbohydrates, amino acids, and fatty acids) for energy homeostasis and growth. Image adapted from (DeBerardinis & Thompson, 2012).

These pathways were identified vital for maintaining macromolecule synthesis in tissues (known as anabolism) or breaking down macronutrient into metabolite and release energy (known as catabolism). However, metabolic research was gradually overshadowed with the quest for genetic and molecular basis of human diseases. An intricate link between metabolic states in health and disease remained incomplete by the end of the 20th century.

1.2 Metabolism in physiology, development, and disease

1.2.1 Overview of metabolism in physiological contexts

In physiology, metabolism serves as a central hub for energy production and utilization, enabling the coordination of anabolism and catabolism for adult homeostasis. Various mechanisms are employed to facilitate energy storage and to ensure the availability of stored energy in the fed, fasting, or starvation state (MacDonald & Webber, 1995).

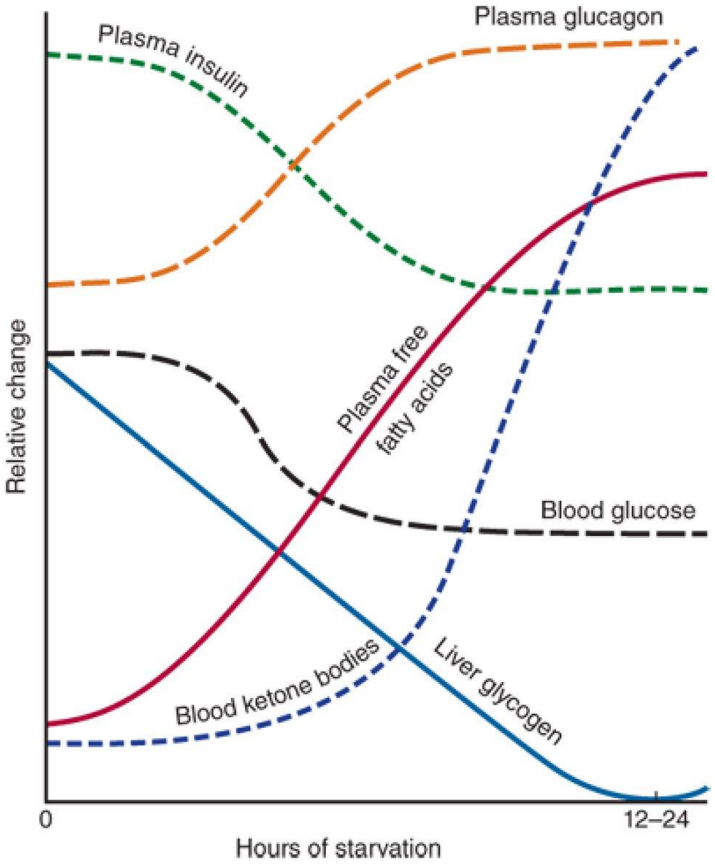

Figure 3: Fasting effects on different hormones and nutrients. Fasting leads to the release of glucose, fatty acids, ketone bodies, and glucagon into the bloodstream to fulfill the body's daily energy requirements. Image adapted from (Karimi et al., 2021).

The fed state, occurring after a meal, entails the digestion of food and absorption of nutrients, with an emphasis on anabolism outweighing catabolism. The digestion of carbohydrate begins

in the salivary glands, while protein and fat digestion occur in the stomach and small intestine. The digested micronutrients are transported across the intestinal wall and enter the blood circulation (glucose and amino acids) or the lymphatic system (lipids) for reaching the target tissues, such as the liver, adipose tissue, or muscle. The glucose and lipids are promptly consumed in case of immediate energy requirements. Otherwise, glucose and amino acids are stored as glycogen and proteins in liver and muscle tissues, and lipids are stored in adipose tissues. Subsequently, the fasting state takes into effect. This state that typically occurs during overnight fasting or by skipping a meal, stimulates the body to rely on stored glycogen. In contrast, prolonged periods of fasting prompts the body to enter "survival mode", prioritizing the provision of sufficient glucose for the brain, followed by the conservation of amino acids for protein synthesis. The body also utilizes ketones to meet the energy demands of the brain and other glucose-dependent organs, while ensuring the lipids and proteins as alternative sources in the events of long-term starvation (Figure 3). These metabolic states are orchestrated as whole-body energy balance and metabolic homeostasis under the regulation of endocrine system, including the actions of insulin, glucagon, and cortisol, modulates metabolic pathways to maintain blood glucose levels, control lipid storage and mobilization, and support protein synthesis. However, these physiological processes adapt during pregnancy in pursuit of a complex endocrine-metabolic rearrangement (Parrettini et al., 2020).

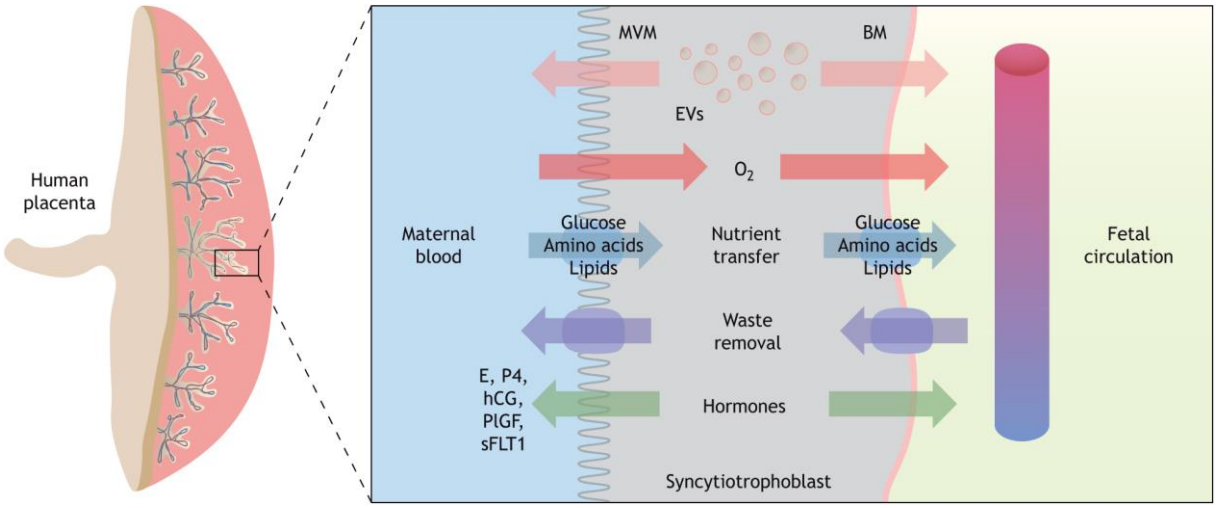

Figure 4: Macromolecules and waste products transport across the human maternal-fetal interface. Key components include BM (basal plasma membrane), E (estrogen), P4 (progesterone), hCG (human chorionic gonadotropin), MVM (microvillous membrane), plGF (placental growth factor), and sFLT1 (soluble fms-like tyrosine kinase). The

syncytiotrophoblast facilitates transport through passive and facilitated diffusion, active transport, as well as endo- and exocytosis. Image adapted from (Kramer et al., 2023).

The initial stage of pregnancy (first and second trimesters) is marked by an anabolic phase of lipid deposition in maternal stores to meet the demands of the developing fetus. As the pregnancy progresses in the third trimester, maternal metabolism enters into a catabolic phase, marked by increased levels of glucose and fatty acids for facilitating fetal growth. The transfer of these nutrients from maternal to fetal circulation is regulated at the placenta, an extra-embryonic specialized tissue that harbors distinct transporting systems for the uptake of specific nutrients (Figure 4). Glucose serves as a vital source of energy for the developing fetus, thereby the demand for glucose transfer elevates during the course of pregnancy. In the case of amino acids, fetal concentrations tend to surpass those in the maternal compartment. Maternal fatty acid metabolism undergoes modifications, particularly during the third trimester, with an increase in fatty acid concentrations in the plasma. The contributions of such maternal supports in fetal growth is a fundamental question in the field of developmental biology.

1.2.2 Metabolism in fetal development

The concept of developmental metabolism was pioneered in the 1950s with the observations on glycolytic activity and developmental progressions in chick embryonic tissues (O'Connor, 1950, 1952). In the 20nd and 21st centuries, studies on animal models have established the notion that metabolism is not just a homeostatic process, but instead an active effector of physiological and developmental changes (Miyazawa & Aulehla, 2018). As our understanding of the developmental metabolism is improving through better in vivo measurements, we can transition from in vitro correlative investigations to more functional in vivo studies. During early embryonic development following fertilization, the single-cell embryo relies primarily on pyruvate metabolism. As the embryo progresses to form a blastocyst, its dependence shifts to glucose metabolism for augmenting biomass and cellular proliferation (Tippetts et al., 2023). Subsequent postimplantation development is characterized by successive waves of proliferation and differentiation for proper organ development over the course of gestation. As cells undergo proliferation or differentiation, their metabolic processes shift to fulfill the biosynthetic or specific energy requirements associated with the new cell fate. A recent study revealed that fetal tissues exhibit varying mitochondrial fuel preferences during mid-gestation (Solmonson

et al., 2022). Exploring these metabolic patterns defining embryonic stages is crucial in revealing metabolism's role in the developmental process.

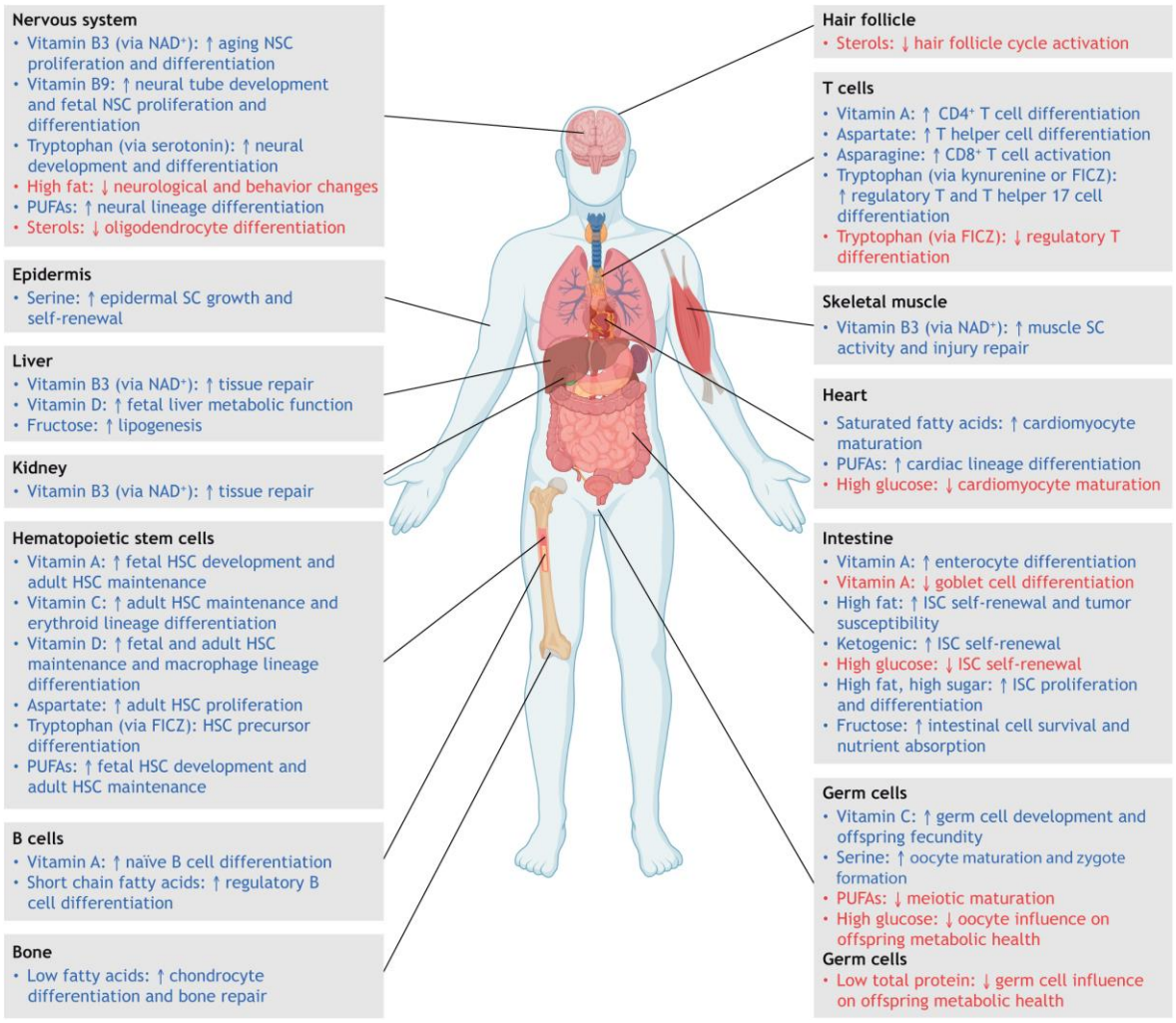

Figure 5: Nutritional positive and negative impacts (highlighted in blue and red) on tissue-specific processes. Image adapted from (Tu et al., 2023).

With the recent technological advances, it has been possible to perturb metabolic pathways by targeting enzymes and metabolites in animal models, revealing how regulatory mechanisms link cell signaling to the orchestration of metabolic cues, such as epigenetic and posttranslational modifications. Work in all of these areas emphasizes that no cellular functions occur independently of metabolism. Thus, current developmental biology has begun to describe the crosstalk between metabolic profile of the cell and developmental conditions at the whole-organism level (Figure 5). This will help to understand the concept of “fetal programming”,

which states that organ development is composed of critical periods in utero. An adequate maternal diet is essential to ensure proper development of the organs. As such, it is often recommended that pregnant women take a daily supplement, containing vitamins, minerals, and omega-3 fats (Brown & Wright, 2020).

1.2.3 Metabolism goes awry in disease states

The concept of metabolic basis of inherited disease was first introduced about a century ago (Garrod, 1908). This emphasizes that metabolic perturbations accompany common human diseases. The advent of the "omics" revolution in the 21st century empowered laboratories to examine genetic and metabolic imprints in bodily tissues and fluids, aiding in the identification of genotype-phenotype correlations. Metabolic irregularities, such as impaired insulin signaling, dyslipidemia, and aberrant nutrient sensing, contribute to the onset of insulin resistance, hyperglycemia, and lipid accumulation, serving as the underlying foundation for a spectrum of disorders, including metabolic syndromes, diabetes, cardiovascular diseases, and cancer (D. J. Hoffman et al., 2021; Huang, 2009). Furthermore, deviations in metabolic states are implicated in fostering inflammatory reactions, oxidative stress, and mitochondrial dysfunction, thereby fueling the advancement of chronic diseases and age-related pathologies (Guo et al., 2022). However, many cases of metabolic disorders appear to be asymptomatic or mild biochemical and phenotypical abnormalities (Edmondson et al., 2016; Ganetzky et al., 2016), suggesting that a systemic compensation exists in the inter-connected metabolic networks.

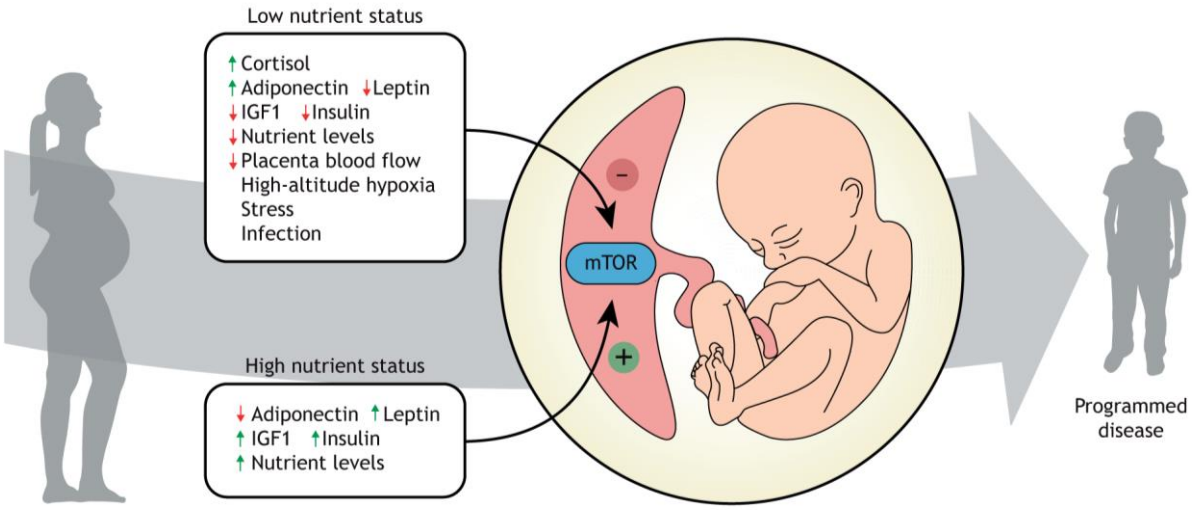

Figure 6: Maternal nutrition in fetal health outcomes. Mechanistic target of rapamycin (mTOR) signaling is one of the key regulatory loops that can sense available nutritional resources and regulate fetal growth accordingly. Image adapted from (Kramer et al., 2023).

Accumulating evidences suggests that the parental environment before and during pregnancy can significantly impact the health and well-being of offspring. Norbert Freinkel first introduced the concept and proposed that over-nutrition during gestation could have consequences on the progeny (Freinkel, 1980). In recent years, this concept has evolved into the theory of the "developmental origins of health and disease" (Barker, 2004), which defines that when the fetus encounters a poor environment, it undergoes irreversible alterations in its developmental path, leading to growth restriction. Subsequently, during childhood or later stages, the organism loses its ability to adapt to a more resourceful environment, setting the stage for the emergence of adult-onset diseases (Figure 6).

1.2.4 1C metabolism: a diet-dependent health and disease outcomes

The discovery of methionine and folate were accomplished in 1920s and 1941, respectively (Barger & Coyne, 1928; Mitchell et al., 1941; Mueller, 1921). Deficiency in folate intake was implicated in human developmental processes, including neural tube defects (NTDs) and anemia during pregnancy (Emery et al., 1969; Hibbard et al., 1965). Since then emphasis is given to the underlying molecular mechanisms, which demonstrated that 1C metabolism plays integral roles on the regulation of methylation reactions, nucleotide synthesis, and amino acid

metabolism. This intricate metabolic pathway heavily relies on folate and methionine, which only come from a balanced dietary intake (Figure 7). Dietary patterns rich in folate have been associated with reduced risks of NTDs (MRC Vitamin Study Research Group, 1991). Conversely, excess in folate intake have been recently implicated in various health complications (Bahous et al., 2017; Kintaka et al., 2020). Methionine has been receiving great attention because its dietary restriction exhibits positive outcomes on metabolic health and life span (Fang et al., 2022). However, a complete understanding of the contributions of methionine in health is still missing.

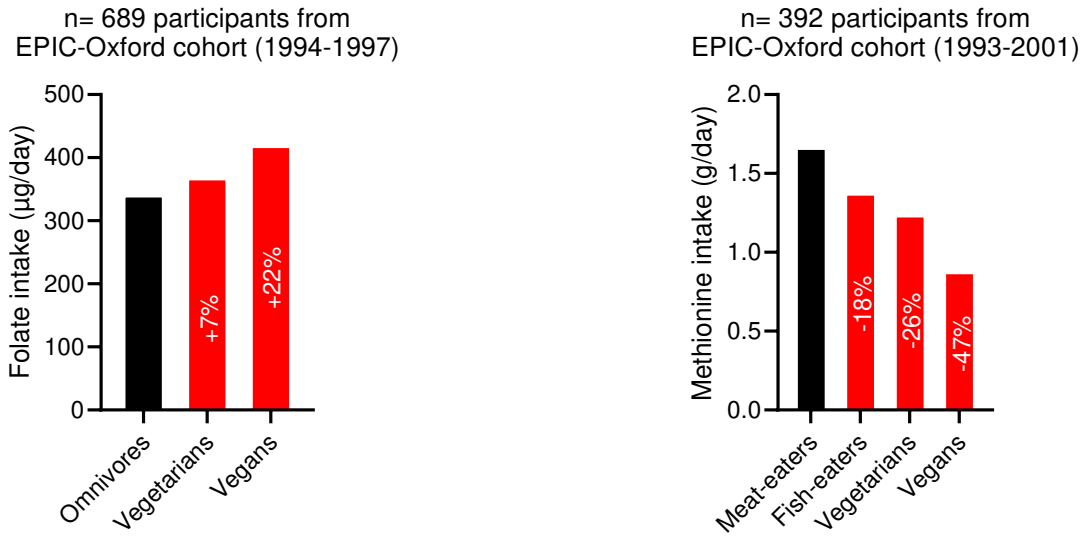

Figure 7: Dietary intake of folate and methionine in male participants (non-supplemented) from EPIC-OXFORD study. Data adapted from (Gilsing et al., 2010; Schmidt et al., 2016) with GraphPad Prism.

The 1C metabolism encompasses the folate cycle, methionine remethylation, and transsulfuration pathways, which are compartmentalized within the cytoplasm, nucleus, and mitochondria (Ducker & Rabinowitz, 2017). The presence of such compartmentalized pathways may allow for a complete oxidative/reductive cycle. This intricate metabolic network facilitates the transfer of 1C moieties, such as methenyl, formyl, and methyl groups, essential for various cellular processes, including regulation of nucleotide pools, biosynthesis of macromolecules (e.g., proteins, polyamines, creatine, phospholipids), epigenetic modulation of gene expression via methylation, and redox homeostasis (Figure 8).

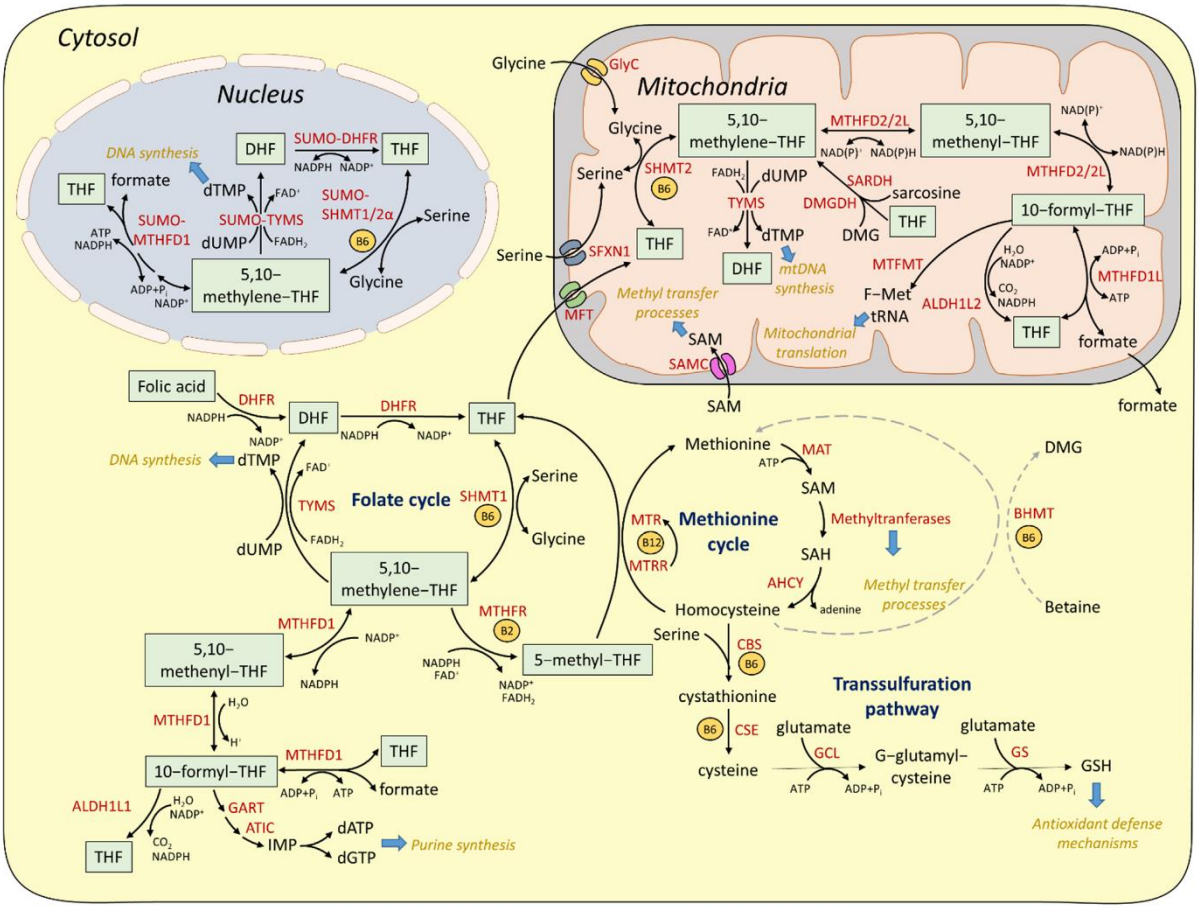

Figure 8: Products and compartmentalization of 1C metabolism in cytosol, nucleus, and mitochondria. The folate forms are illustrated in green boxes, enzymes are indicated in red, and functional output is colored in orange. Image adapted from (Lionaki et al., 2022).

Folates function as versatile methyl donors, transporting and activating 1C units. Folates in diet can be present as naturally reduced form or as folic acid (synthetic form). The DHFR enzyme converts both forms into a biologically active form, tetrahydrofolate (THF). THF undergoes transformation to 5,10-methylene-tetrahydrofolate (5,10-CH2-THF) through the B6-dependent enzyme serine hydroxymethyltransferase (SHMT1) and is subsequently irreversibly reduced to 5-methyltetrahydrolate (5-mTHF) by the B2-dependent enzyme methylenetetrahydrofolate reductase (MTHFR). Alternatively, a series of reactions catalyzed by methylenetetrahydrofolate dehydrogenases (MTHFD1) converts 5-mTHF to 10-formyl-tetrahydrofolate (10-f-THF) for the synthesis of purines. The folate cycle ends with the demethylation of 5-mTHF, wherein 1C unit is donated for the remethylation of homocysteine

(HCY) to methionine, a reaction facilitated by the B12-dependent enzyme methionine synthase (MTR). Methionine undergoes adenylation by methionine adenosyltransferase (MAT) to form S-adenosylmethionine (SAM), a universal methyl donor. During the process of methyl transfer, SAM converts to S-adenosylhomocysteine (SAH), which, in turn, is hydrolyzed back to HCY and adenosine through a reversible reaction catalyzed by S-adenosylhomocysteine hydrolase (AHCY), thus completing the methionine cycle. When methionine and folate levels are adequate, elevated levels of SAM trigger the degradation of HCY through a two-step transsulfuration pathway, which relies on vitamin B6 as a cofactor (Figure 8).

Sydney Farber initially acknowledged the significance of 1C metabolism in cancer outcomes in 1948. He noted that a deficiency of dietary folate in children with acute leukemia resulted in a reduction of leukaemic cell count (Farber & Diamond, 1948). The dependency of cancer on 1C metabolism were identified with the development of metabolic inhibitors, including MTX. MTX is a competitive inhibitor of DHFR enzymatic activity, which is essential for high nucleotide synthesis in proliferating and transformed cells (Nilsson et al., 2014). MTX demonstrates high sensitivity to the hematological cancer cell lines (Yang et al., 2013), however application of MTX in cancer treatments is limited due to resistance mechanisms in cancer cells (Horns et al., 1984; Pizzorno et al., 1988). In contrast, all cancer cell lines show increased consumption of methionine, and cancer is dependent on methionine (R. M. Hoffman, 1984).

Chapter 2: Key regulatory mechanisms of brain development

2.1 Overview of basic cellular mechanisms

The brain is composed of the cerebrum/cerebral cortex, cerebellum, and brainstem. The cerebral cortex, largest part of the brain, is characterized by the presence of neuronal cells organized in a layered structure. In mammals, these neurons exist in six layers in the neocortex, while in birds and reptiles, they primarily populate the dorsal and dorsolateral ventricular ridges (S. D. Briscoe et al., 2018). The neocortical development begins with the formation of the telencephalic vesicles, composed of a monolayer of neuroepithelial cells (NEC). These NEC, the earliest type of NPC, with two radial processes extending from the soma, self-amplify and transform into apical radial glial cells (aRGC; also known as RGC) within the ventricular zone (VZ) (Sahara & O'Leary, 2009; Sidman & Rakic, 1973). Throughout each cell cycle, the nucleus undergoes a consistent movement spanning the entire apical-basal length, referred to as interkinetic nuclear migration (INM) (Takahashi et al., 1993). Mitotic division takes place at the apical surface, with the nucleus transitioning towards the basal side during the G1 phase, maintaining its position during DNA synthesis (S phase), and returning from the basal to the apical side at G2. RGC, which divides at the apical surface and expresses the paired-box transcription factor 6 (PAX6) (Götz et al., 1998), serves as the primary type of NPC for generating all cortical excitatory neurons in the dorsal telencephalon (Malatesta et al., 2003). The remaining RGC fractions undergo a transition from neurogenic to gliogenic progressively (Hippenmeyer, 2023), producing various types of glial cells (astrocytes and oligodendrocytes) and establishing the postnatal NPC niche.

At the onset of neurogenesis, aRGC divisions give rise to both additional aRGCs and a small proportion of neurons. As development progresses, aRGC starts to generate a secondary type of progenitor cells, known as basal progenitors (BP) in the subventricular zone (SVZ) (Noctor et al., 2004). These BP include intermediate progenitor cells (IPC) and outer radial glia cells (oRGC, also known as basal radial glial cells). In mice, most BPs manifest as IPC, which express the T-box transcription factor 2 (TBR2) (Englund et al., 2005). IPCs can generate excitatory neurons across all layers (Kowalczyk et al., 2009). In contrast, species with larger and folded brains, such as primates, exhibit abundant oRGCs with high proliferative capabilities marked by a unique expression of the homeodomain-only protein homeobox (HOPX) (Pollen et al., 2015), with a significant proportion co-expressing PAX6 and TBR2 (Reillo et al., 2011).

oRGC share similarities with aRGC, including PAX6 expression and the presence of a radially extended basal process, but they lack apical processes and INM, instead undergo mitotic somal translocation (MST) (Figure 9).

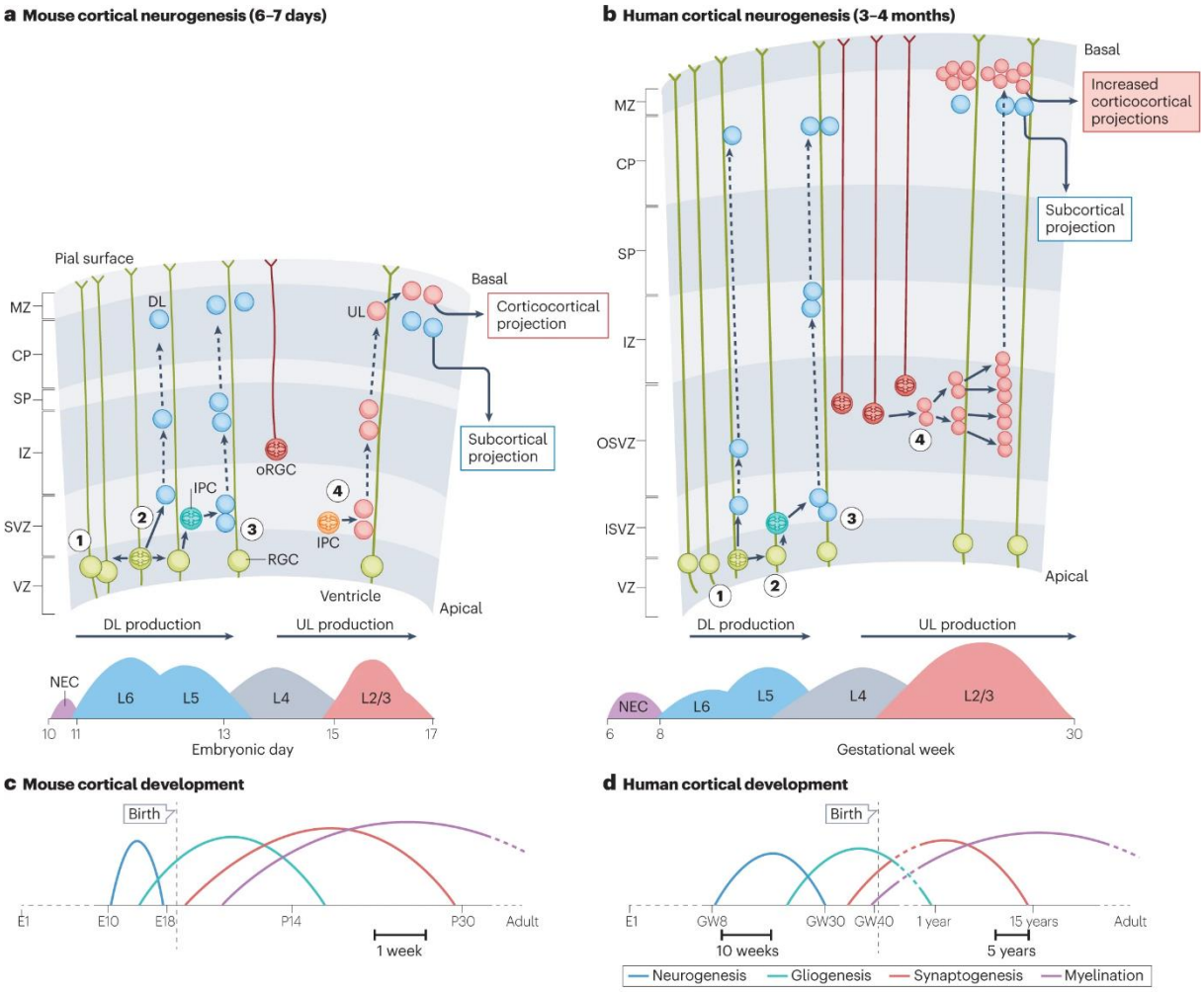

Figure 9: Species-specific specification of excitatory neurons in the neocortex. Mouse neurogenesis spans about one week, and oRGC is rarely found. In contrast, human neurogenesis extends for four months, and a higher prevalence of oRGC contributes to the increased neuronal production and brain expansion. Image adapted from (Vanderhaeghen & Polleux, 2023).

The six layers of excitatory projection neurons in the neocortex, numbered 1 to 6, are generated in a sequential 'inside-out' manner (except for early-born uppermost layer 1 neurons). The process of neurogenesis occurs through both direct neurogenesis, where a fraction of deep layer (DL) neurons are directly produced by aRGC, and indirect neurogenesis, where upper layer (UL) neurons are predominantly generated indirectly through BP (Cárdenas et al., 2018;

Laguesse et al., 2015). Due to the amplifying nature of BP, indirect neurogenesis significantly increases neuron production in primates (Kriegstein et al., 2006). Newborn neurons embark on a journey by radial migration toward their ultimate destination in the cortical plate (CP). Excitatory neurons follow two primary modes of migration: somal translocation, primarily used by the early-born neurons, and glia-guided locomotion, which is more commonly used by pyramidal cells. On the other hand, inhibitory neurons, originating in the ventral telencephalon, employ a distinct mode of migration (Lepiemme et al., 2022; Nadarajah & Parnavelas, 2002). During this phase, excitatory projection neurons develop specialized axonal projections to distant brain targets based on their specific subtypes, including corticothalamic projection neurons (CThPN), subcerebral projection neurons (SCPN), and callosal projection neurons (CPN). The appropriate differentiation of CThPN, SCPN, and CPN neurons are regulated by the expression of the T-box brain protein 1 (TBR1), COUP-TF-interacting protein 2 (CTIP2; also known as BCL11B), and special AT-rich sequence binding protein 2 (SATB2), respectively (Figure 10). This specialization of identity is area-specific and gradually refined during the developmental stages (Greig et al., 2013).

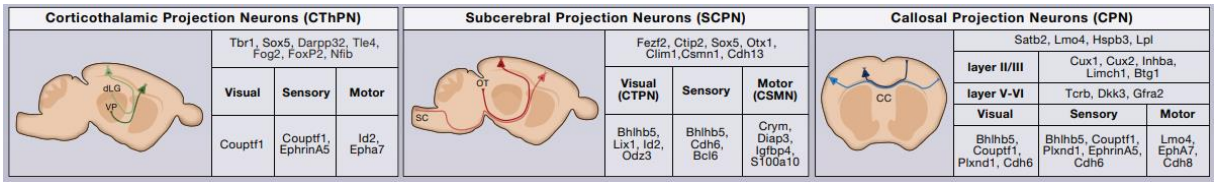

Figure 10: Excitatory projection neuron diversity in the neocortex. The excitatory projection neurons are classified into three major subtypes on the basis of their projection pattern: CThPN in layer 6 project axons to the thalamus (VP, ventral posterior nucleus; dLG, dorsal lateral geniculate nucleus); SCPN located in layer 5 send axons to the optic tectum (OT), brainstem, or spinal cord (SC); and translaminar CPN project axons to the contralateral cortex (CC, corpus callosum). Notably, a combinatorial expression of transcription factors during development determines both subtype and area identity. Image adapted from (Woodworth et al., 2012).

Unlike excitatory projection neurons, cortical interneurons originate in the ventral telencephalon, from where they tangentially migrate to the dorsal telencephalon (Anderson et al., 1997). Interneurons are primarily derived from three progenitor regions: medial ganglionic eminence (MGE), caudal ganglionic eminence (CGE), and the preoptic area (POA) (Figure 11). The interneurons are classified into three major subtypes: parvalbumin (PV)-, somatostatin

(SST)-, and the serotonin receptor 3A (5HT3aR)-expressing interneurons (Lim et al., 2018). Around the same onset of neurogenesis as in the dorsal telencephalon, ventral VZ progenitors undergo spatiotemporal fate programming to generate the interneuron subtypes. The laminar distribution of interneurons is partially influenced by both their birthdate and origin; however, this arrangement can be modulated by the populations of excitatory projection neurons (Lodato et al., 2011). In humans, RGC can generate both excitatory projection neurons and interneurons (Delgado et al., 2022), which is not the case in mouse neocortex (Bandler et al., 2022). During development, neocortical neurons are generated in excess numbers, and some are later eliminated (up to 40%) by programmed cell death (Southwell et al., 2012; Verney et al., 2000). This process refines neocortical circuits and adjusts the neuron numbers, of which excitatory projection neurons constitute approximately 80% of the population (Douglas & Martin, 2004).

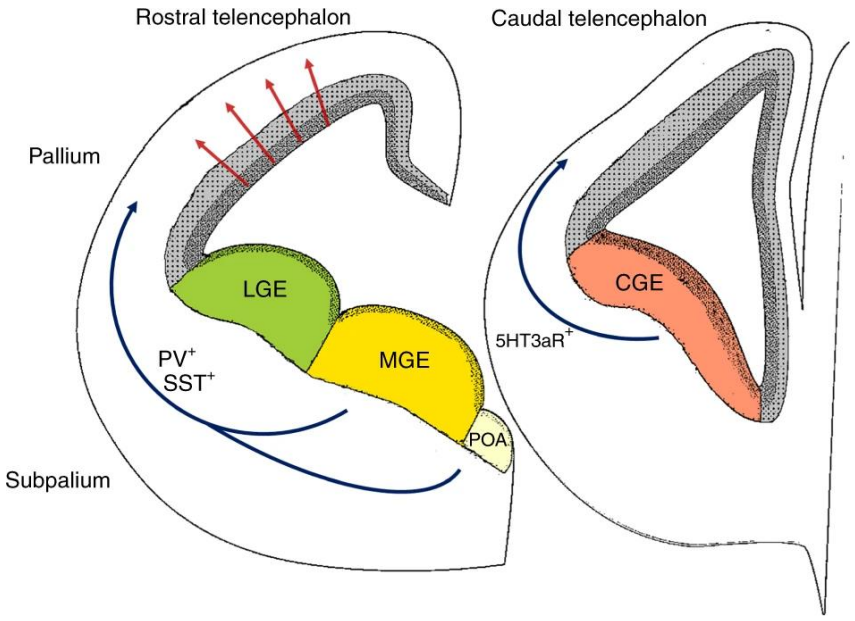

Figure 11: Distinct telencephalic progenitor domains in the mouse neocortex. The newborn excitatory neurons migrate radially from the dorsal VZ (red arrows) and subtypes of interneurons migrate long distances tangentially toward the neocortex (blue arrows). Image adapted from (Lunden et al., 2019).

Apart from neurons, the mature neocortex consists of two glial subtypes: macroglia and microglia. Macroglia, including astrocytes and oligodendrocytes, originate from distinct NPC pools (Beattie et al., 2017; Z. Shen et al., 2021), while microglia are of mesodermal origin derived from primitive yolk-sac-derived myeloid precursors (Ginhoux et al., 2010; Kierdorf et

al., 2013). Astrocytes and excitatory neurons share the same NPC pools and astrocytes generation is spatiotemporally promoted by extrinsic signals and epigenetic regulation at the end of neurogenesis (Molné et al., 2000; Takizawa et al., 2001). Conversely, oligodendrocyte precursor cells (OPC) originating in the ventral telencephalon and responsible for generating oligodendrocytes share common developmental origins and migration profiles with the interneurons (Kessaris et al., 2006; Lepiemme et al., 2022).

2.2 Cell-extrinsic and intrinsic regulation

Neocortical neurogenesis primarily relies on a temporal patterning in comparison with a spatial patterning of NPC in the spinal cord (J. Briscoe et al., 2000; Telley et al., 2019), meaning that the different subtypes of neurons are generated in a sequential temporal order from the same location. This process is controlled by cell-intrinsic mechanisms as well as by cell-extrinsic cues that originate in the neighboring niche. These cues influence the fate of NPC via precise modulation of gene expression, ultimately contributing to the growth and final size of the neocortex. Fundamental studies from mouse models have contributed to the understanding of key developmental cues in the NPC, which are stated below.

Signaling molecules: Extrinsic signaling cues, such as fibroblast growth factors (FGFs), sonic hedgehog (SHH), wingless-related integration site (WNTs), and bone morphogenetic proteins (BMPs)/ transforming growth factor-beta (TGF-β) (Figure 12), participate in the regionalization of telencephalic vesicles into a dorsal or pallial and a ventral or subpallial territory (Campbell, 2003).

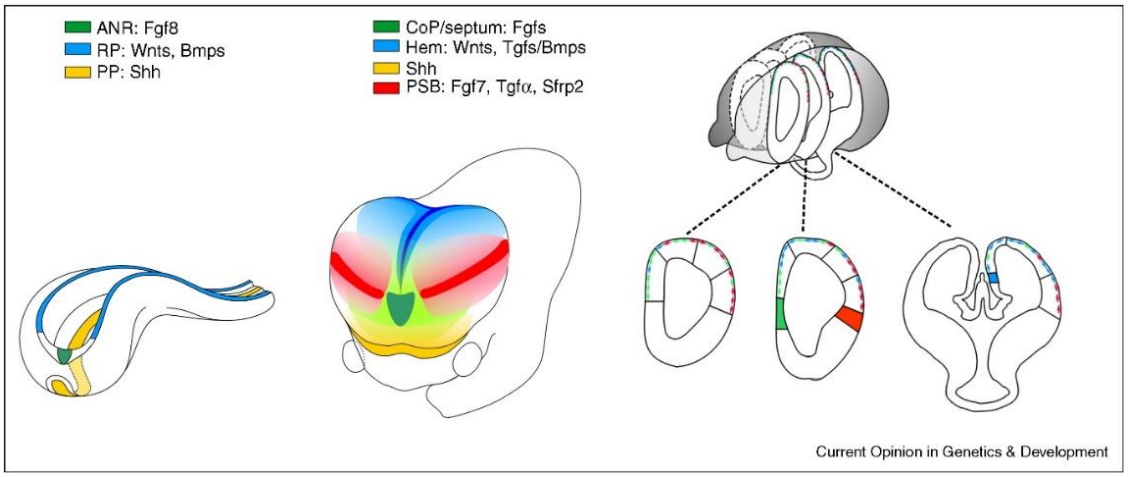

Figure 12: Signaling centers in the patterning of early telencephalon. During neurulation, three patterning centers are localized in anterior neural ridge (ANR), roof plate (RP), and prechordal plate (PP). At the onset of neurogenesis, patterning centers and migrating signaling units are distributed in commissural plate (CoP), septum, hem, ventral telencephalon, and pallial–subpallial boundary (PSB/anti-hem). Image adapted from (Borello & Pierani, 2010).

During early neurodevelopment, FGF8 secretion at the rostral midline acts as a center for anterior forebrain patterning (Fukuchi-Shimogori & Grove, 2001). SHH is secreted at the ventral midline for the specification of ganglionic eminence (Rallu et al., 2002). WNTs/BMPs secretion at the dorsal/caudal midline plays instructive role for the patterning of the hippocampus (Furuta et al., 1997; Grove et al., 1998). Following the formation of telencephalic vesicles, two additional signaling centers are established along the mediolateral axis: the hem serves as the organizer of the hippocampus and the anti-hem segregates the pallial/subpallial boundary (Assimacopoulos et al., 2003). These secreted morphogens induce anterior-posterior (AP) and dorsal-ventral (DV) axes of the forebrain through direct or indirect interactions between the signaling centers and their downstream transcription factors, may further promote the precise identity and specification programs in the NPCs.

Transcription factors: Intrinsic genetic programs are driven by the coordinated action of morphogenetic signals on the NPC. In the dorsal telencephalon, SHH and FGF8 induces the positional identity of the NPCs via expression of specific transcription factors, including PAX6, empty spiracles homeobox 1 (EMX1), GS homeobox 2 (GSH2/GSX2), and NK2 homeobox 1 (NKX2.1) (Muzio & Mallamaci, 2003; Puelles et al., 2000). PAX6 is highly expressed in the

VZ and activates the expression of the proneural basic helix–loop–helix (bHLH) transcription factor neurogenin-2 (NGN2/NEUROG2) (Gunhaga et al., 2003; Scardigli et al., 2003). Together with the winged-helix transcription factor forkhead box G1 (FOXG1) (Hanashima et al., 2002), they promote neurogenesis and specification of excitatory neurons. Several transcription factors, including NGN2, zinc-finger transcription factor insulinoma-associated 1 (INSM1), and activating enhancer binding protein 2 gamma (AP2γ/TFAP2C), have been implicated in the generation of TBR2 progenitors (Farkas et al., 2008; Miyata et al., 2004; Pinto et al., 2009). These transcription factors act in a spatiotemporal manner for the generation of excitatory neurons in the neocortex. Afterwards, signal transducer and activator of transcription 3 (STAT3) promotes astrocytic gene expression at the onset of gliogenesis (Fan et al., 2005). In addition to STAT3, SRY-box transcription factor 9 (SOX9) and nuclear factor 1 (NFIA) acts together as transcriptional determinants of gliogenesis (P. Kang et al., 2012). NPC in the ventral telencephalon expresses distal-less homeobox 1/2 (DLX1/2), which subsequently gives rise to migrating interneurons towards the neocortex (Anderson et al., 1997). DLX1/2 coordinates interneuron differentiation and restricts OPC formation through oligodendrocyte transcription factor 2 (OLIG2) repression at the time of neurogenesis (Petryniak et al., 2007).

Cell-intrinsic timing: Neocortical NPC undergoes distinct transitions during excitatory neuronal specification, suggesting NPC adopts a distinct strategy for the sequential production of neuronal subtypes. There are two distinct hypotheses that support a deterministic strategy involving the existence of homogenous and heterogeneous populations of the NPC. On the one hand, the progressive restriction hypothesis argues for the existence of a homogeneous population of multipotent NPC that lose their potency gradually; therefore, the fate of NPC evolves with time (Gao et al., 2014; McConnell & Kaznowski, 1991; Oberst et al., 2019; Q. Shen et al., 2006). On the other hand, the fate-restricted hypothesis states that the pool of heterogeneous NPC is diverse from the earliest stages and that specific NPC will give rise to specific neurons (Fabra-Beser et al., 2021; Franco et al., 2012; Llorca et al., 2019). Nevertheless, both hypotheses identified either a temporal code or a genetic program as the mechanisms responsible for fate transitions during neurogenesis. Neurogenic programs proceeds until the end of the gestation, at which point a pool of remaining NPC switches to gliogenic programs for the production of glial subtypes onwards (Barnabé-Heider et al., 2005; Fan et al., 2005; Petryniak et al., 2007). These programs are orchestrated by global and specific

transcriptional and epigenetic changes for regulating time-dependent gene expression in the NPC (Albert et al., 2017; Sanosaka et al., 2017).

Cell-extrinsic mechanisms: Progressive changes of cell-extrinsic cues drive the early-to-late temporal progression of the NPC fate. These non cell-autonomous cues facilitate the proliferation and temporal transitions in the NPC. For instance, during early neurogenesis, FGF signaling promotes the acquisition and maintenance of RGC state (W. Kang et al., 2009; Sahara & O'Leary, 2009). The secretion of retinoic acid (RA) from the meninges joins in the maintenance and proper differentiation of aRGC (Siegenthaler et al., 2009). Furthermore, feedback signals of WNT and neurotrophin 3 (NTF3) from newborn neurons regulate the RGC fate decisions and the subtype of progeny (Parthasarathy et al., 2014; Wang et al., 2016). Another non cell-autonomous feedback mechanism is cell-cell interactions influencing the identity and differentiation timing of RGC locally. For instance, EPH (erythropoietin-producing hepatocellular carcinoma):EPHRIN (EPH receptor-interacting proteins) signaling is required for the maintenance and proper differentiation of the RGC (Arvanitis et al., 2013; Qiu et al., 2008) and for pacing neuronal production in the neocortex (Kischel et al., 2020). We recently identified a direct link between EPH:EPHRIN, 1C metabolism, and epigenetic state in the aRGC (Fawal et al., 2018), underlying the significance of metabolic pathways in the control of temporal fate transitions.

2.3 Metabolic regulation of brain development

Nutritional needs are increased during pregnancy; however, whether that heightened nutritional support has to be continuous or sufficient for critical brain growth is unclear. In addition to their bioenergetics function, recent work showed that nutrients can influence developmental programs by acting as systemic cues (Miyazawa & Aulehla, 2018). The ability to compare different metabolic states in specific cell types led to an understanding of developmental metabolism, and highlighted that stem/progenitor cell metabolism and brain growth are intricately intertwined in a synergistic manner. Brain develops from prenatal to adolescence periods, which are considered critical and sensitive for normal brain function (Figure 13). At this time windows, the plasticity is driven by environmental influence to establish the

stereotypic number of cells (neurons and glia) and their connectivity (synapses) (Dehorter & Del Pino, 2020).

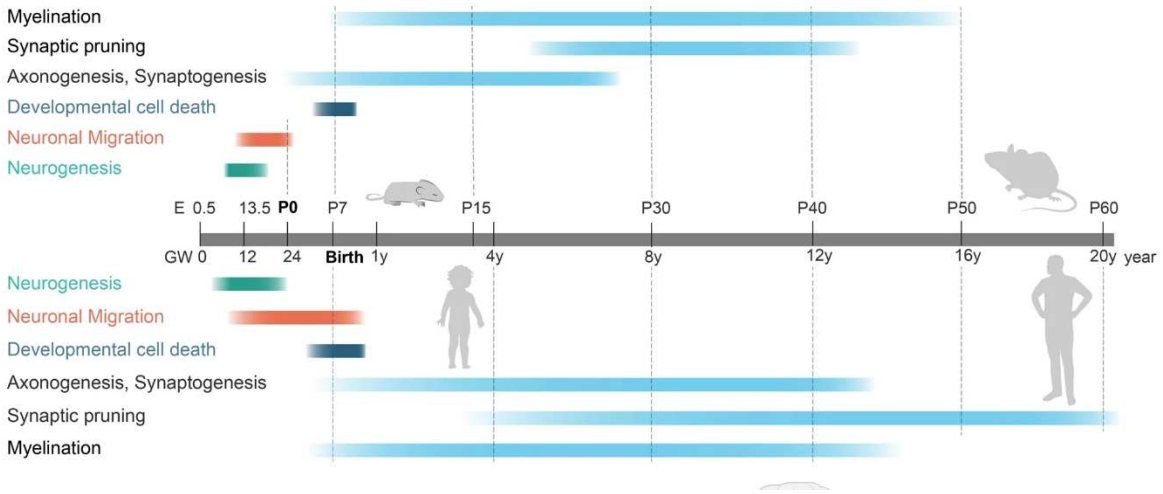

Figure 13: Critical and sensitive stages extend to the peak of axonogenesis, synaptogenesis, and myelination. Image adapted from (Khodosevich & Sellgren, 2023).

Nutritional supplies along the critical and sensitive stages affect neurodevelopmental outcomes in relation to brain structure and function (Cheatham, 2020; Cusick & Georgieff, 2016). In many mammals, a key neurodevelopmental feature is the completion of neocortical neurogenesis during embryonic brain development, resulting in fetal NPC metabolism relying exclusively on maternal nutritional sources. The ability to adapt to environmental fluctuations of specific nutrients that fuel the fetal NPC metabolic network (Figure 14), is still less understood.

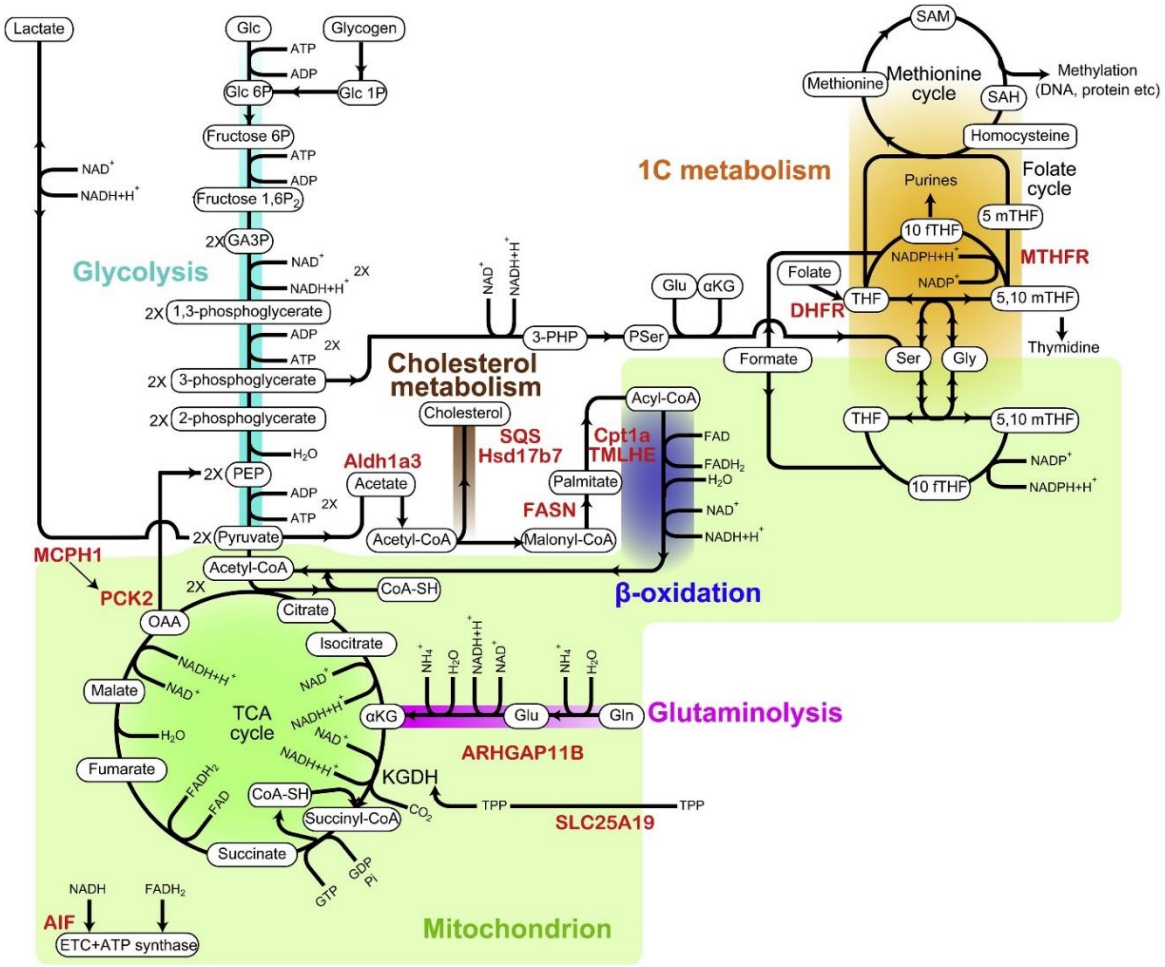

Figure 14: Core metabolic pathways in the NPC are color-coded as follows: turquoise for glycolysis, blue for β-oxidation, brown for cholesterol metabolism, orange for 1C metabolism, purple for glutaminolysis, and green for the TCA cycle. The mitochondrial compartment and key proteins are highlighted in light green and red, respectively. Image adapted from (Namba et al., 2021).

Existing data suggests that NPC populations exhibit distinct cellular metabolism during neocortical development (Figure 15). This evidence strongly suggests that NPC metabolism may affect species-specific proliferation and differentiation output.

Table 1. Summary of Metabolic Pathway Activities in Mouse and Human NPCs

	APs		BPs				
	aRG		bIPs		bRG		
	Mouse	Human	Mouse	Human	Mouse	Human	References
Glycolysis	high	ND	low	ND	ND	ND	Khacho et al., 2016
Glutaminolysis	high	high	low	ND	ND	high	Journiac et al., 2020; Namba et al., 2020
β-oxidation	high	ND	low	ND	ND	ND	Xie et al., 2016; Knobloch et al., 2017
Fatty acid synthesis	low	high	low	ND	ND	ND	Bowers et al., 2020
Cholesterol metabolism	high	ND	low	ND	ND	ND	Saito et al., 2009; Driver et al., 2016
1C metabolism	high	ND	low	ND	ND	ND	Fawal et al., 2018

The table lists the extent of the activity of the indicated metabolic pathways either as deduced from changes in NPC abundance upon manipulation of the respective metabolic activity or as deduced from metabolic activity measurements. Note that (1) the current knowledge for human NPCs is less than that for mouse NPCs, and (2) the metabolic regulation of behavior and fate of mouse NPCs is only partially understood. ND, no data.

Figure 15: NPC metabolic activities vary across species and across progenitor subtypes (APs: apical progenitors, aRG: apical radial glial cells, BPs: basal progenitors, bIPs: basal intermediate progenitor cells, bRG: basal/outer radial glial cells). Image adapted from (Namba et al., 2021).

In a recent study, differential mitochondrial metabolic activities were identified as a driving force influencing the rate of neuronal maturation (Iwata et al., 2023; Rangaraju et al., 2019). In newborn excitatory neurons, there is a limited number of mitochondria with low metabolic activity, gradually increasing as the neurons mature. Elevated mitochondrial metabolism in human neurons accelerates the maturation process, contributing to many aspects of neurodevelopment (Figure 16).

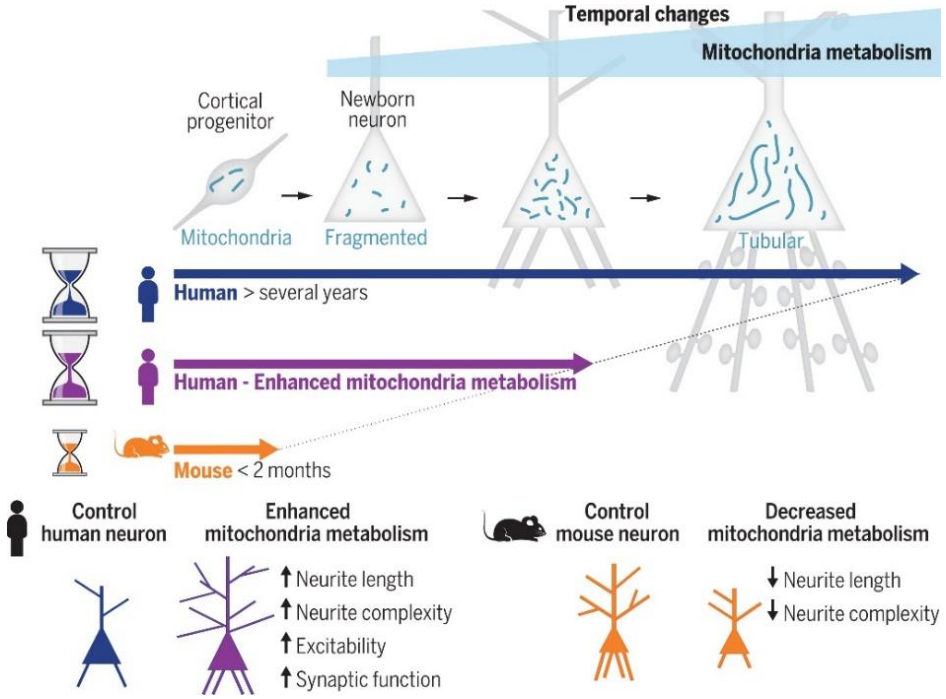

Figure 16: Mitochondrial dynamics during neocortical neuron development. Image adapted from (Iwata et al., 2023).

Despite this progress, one key question remains to be investigated: are metabolic pathways strictly coordinated in the acquisition of specific cell identities (e.g., subtypes of excitatory projection neurons) in normal and delayed developmental contexts. 1C metabolism, like many other core metabolisms, plays integral roles in dictating proliferative and differentiation events in the NPC (Fawal et al., 2018). Moreover, a recent single-cell RNA sequencing data revealed that the expression of several metabolic enzymes, including DHFR, is dynamic in the developing neocortex (Klingler et al., 2021) (Figure 17). Changes in expression levels or activity of DHFR and other enzymes of the 1C metabolism raise the possibility that metabolic programs play a critical role during neurogenesis.

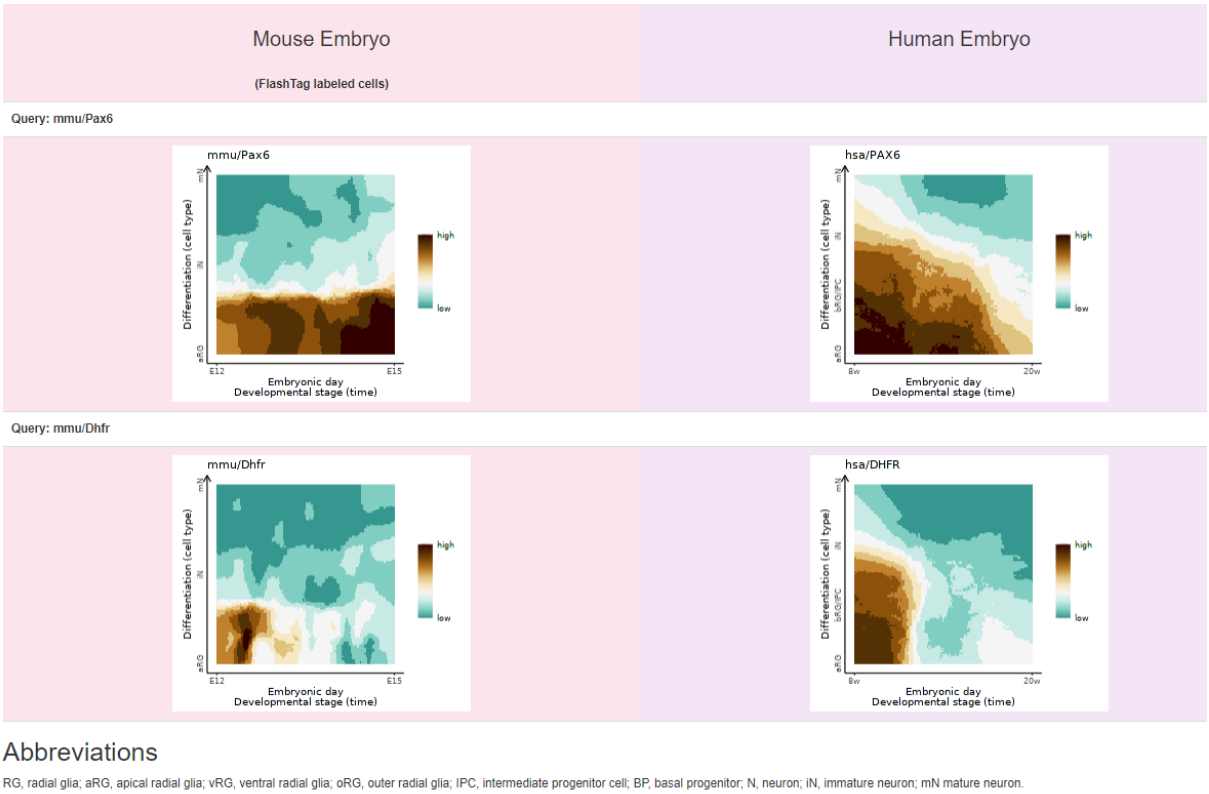

Figure 17: Gene expression pattern of *Pax6* and *Dhfr* during mouse and human embryonic development. Image adapted from (http://www.humous.org/).

As mentioned before, DHFR is a key enzyme in the catalysis of folate into THF using nicotinamide adenine dinucleotide phosphate (NADPH) as the cofactor (Osborn & Huennekens, 1958). The DHFR gene consists of 6 exons which constitutes the loop conformations for the binding and release of cofactor, substrate, and products (Figure 18). Homozygous point mutations in the exons can disrupt this enzymatic activity and have been associated with growth defects (Banka et al., 2011; Cario et al., 2011), characterized by hematological conditions (megaloblastic anemia or pancytopenia) and neurological conditions (microcephaly, brain atrophy, white matter disturbances, refractory seizures, and learning disabilities). However, not all DHFR mutations may result in microcephaly (Kuijpers et al., 2022), and humans possess a second copy of functional DHFR enzyme (DHFRL1/DHFR2) in the mitochondria (Hughes et al., 2015). Additionally, a 19bp-deletion of DHFR and 1C metabolites are implicated in ASD phenotypes (Adams et al., 2007; James et al., 2006), suggesting a complex etiology involving genetic and environmental risk factors that could potentially affect brain growth both prenatally and postnatally. During my PhD, I analyzed a

new DHFR mutant mouse line in which exon 5, which carries the enzymatic activity, was excised.

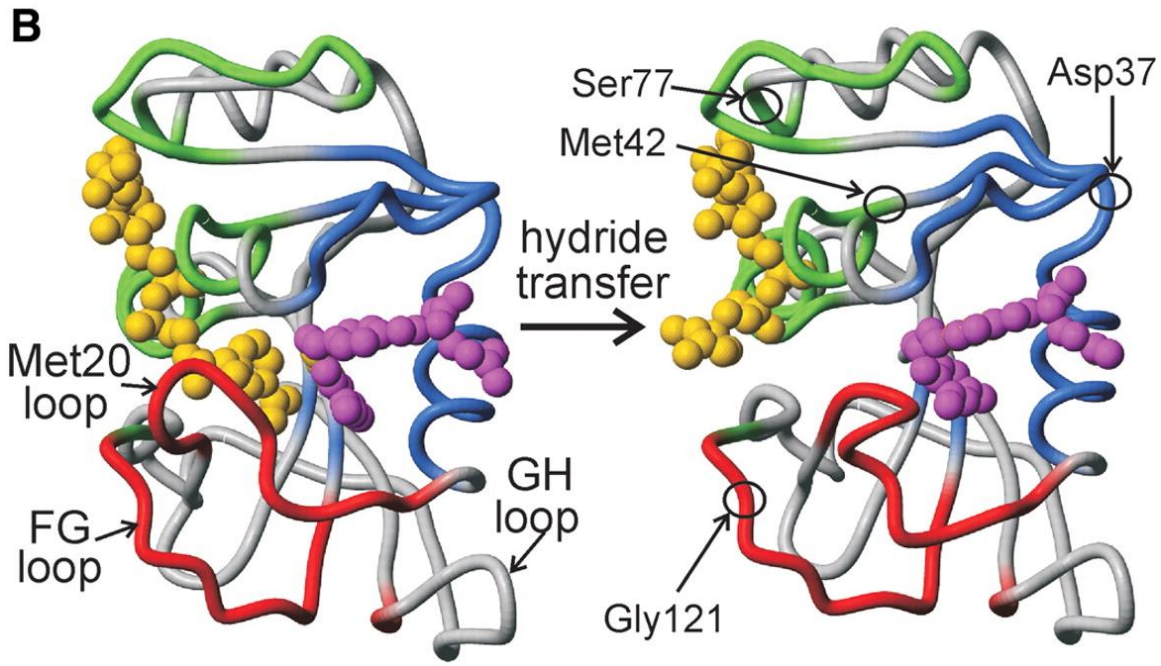

Figure 18: Structures of *Escherichia coli* DHFR enzyme, illustrating the conformational changes that occur upon hydride transfer from NADP+:folate substrate (left) to NADPH:THF product (right). Enzyme residues that define the active site loop, substrate/product-binding, and cofactor-binding are highlighted in red, blue, and green, respectively. The bound folate and THF are shown in magenta, and cofactor is colored gold. Image adapted from (Boehr et al., 2006).

The fetus cannot synthesize essential amino acids (e.g., methionine); they must come from the maternal food sources. The fetal circulatory system is linked to the maternal circulation through a pathway that runs from the placenta to the liver, then to the heart, and finally to the brain. Recent studies revealed alterations in amino acid pools during mid-to-late gestation (Figure 19) and postnatal development (Knaus et al., 2023; Perez-Ramirez et al., 2024). However, the contributions of methionine metabolism remains incomplete due to its complexity involving the methylation and protein synthesis. Therefore, the regulatory signals of methionine at the systemic level on NPC behavior are unclear.

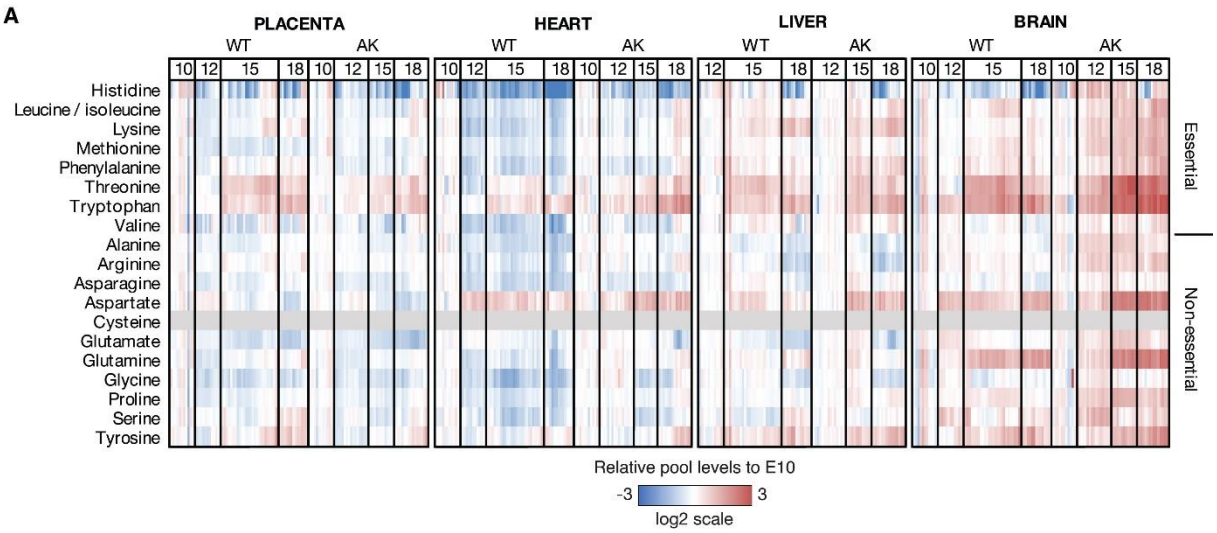

Figure 19: Heatmap illustrating the amino acid levels obtained from wild-type (WT) and Akita (AK, hyperglycemic) dams in relative to E10.5 fetal tissues. Image adapted from (Perez-Ramirez et al., 2024).

Chapter 3: In vitro modeling of brain development

3.1 Early in vitro models

A significant advancement in in vitro studies came with the development of embryonic stem cell (ESC) culture conditions for both mice and humans. Some of the initial efforts to generate neural cells involved the use of floating aggregates of ESC known as embryoid bodies (EB). While EB can generate derivatives of all three germ layers, they do not replicate the organized spatial pattern of organogenesis. In 1995, mouse ESC were first used to obtain cells with neuronal identity from dissociated EB (Bain et al., 1995). It hinted that neural differentiation is an intrinsic mechanism that can be induced in vitro through secreted factors. In fact, in vitro neurogenesis recapitulates the multi-step process observed in the mouse embryo (Eiraku et al., 2008; Gaspard et al., 2008).

When human EB were cultured in a chemically defined medium in the presence of FGF2, they organized into structures resembling neural tubes known as neural rosettes (Shi et al., 2012). These structures were composed of NEC exhibiting polarized apical and basal domains. RGC encircling the lumen demonstrated an INM, limiting mitotic divisions to the apical surface. Within the neural rosettes, a thin SVZ was primarily populated by IPC and a few oRGC, highlighting significant parallels to human progenitor cell types. As the neural precursors underwent differentiation, they predominantly gave rise to excitatory neurons and astrocytes. Although synaptic connections were present in the neural rosettes, the absence of a more complex tissue architecture on these models has limits for comprehensive investigations.

3.2 Organoid in vitro models

Under appropriate culturing conditions, stem/progenitor cells possess the capacity to differentiate and autonomously assemble into intricate three-dimensional tissues, commonly referred to as organoids. These organoids can effectively mimic the microanatomy and functions of diverse organs, including the brain. The discovery of cell reprogramming opened up the possibility to generate organoids from human cells in an ethically acceptable manner. The generation of organoids starts with the aggregation of human ESC or induced pluripotent stem cells (iPSC) into EB. Subsequently, these EB are cultured in a neural induction medium that steers the cells toward a neuroectodermal destiny. EB are then cultured in a neural induction medium, which pushes cells towards a neuroectodermal fate by a spontaneous inhibition of

TGFβ, BMP, and WNT-β-catenin signaling. Once the neuroectoderm is established, the tissue continues to self-organize, forming lumens lined with NEC known as neural rosettes of the organoid. This phase can be facilitated by WNT-β-catenin signaling and matrigel embedding for the expansion and organization of NEC (Eiraku et al., 2008; Lancaster et al., 2013). Within the neural rosettes of the organoid NEC, a layered structure emerges along an apical-basal axis. This structure showcases proliferative VZ-like layers distinct from the overlying SVZ-like layers. RGC exhibit the characteristic INM at the VZ, while IPC and oRGC reside in the SVZ. Excitatory neurons begin to differentiate within 3 weeks of culture and migrate outward, forming a defined CP. With time, human organoids manifest a segregation of DL and UL neurons after approximately 3 months of culture (Figure 20). These organoids effectively replicate the transcriptional profile of fetal brain, as evidenced by comparisons between the age of the organoid and the stage of brain development (Cheroni et al., 2022; Tanaka et al., 2020).

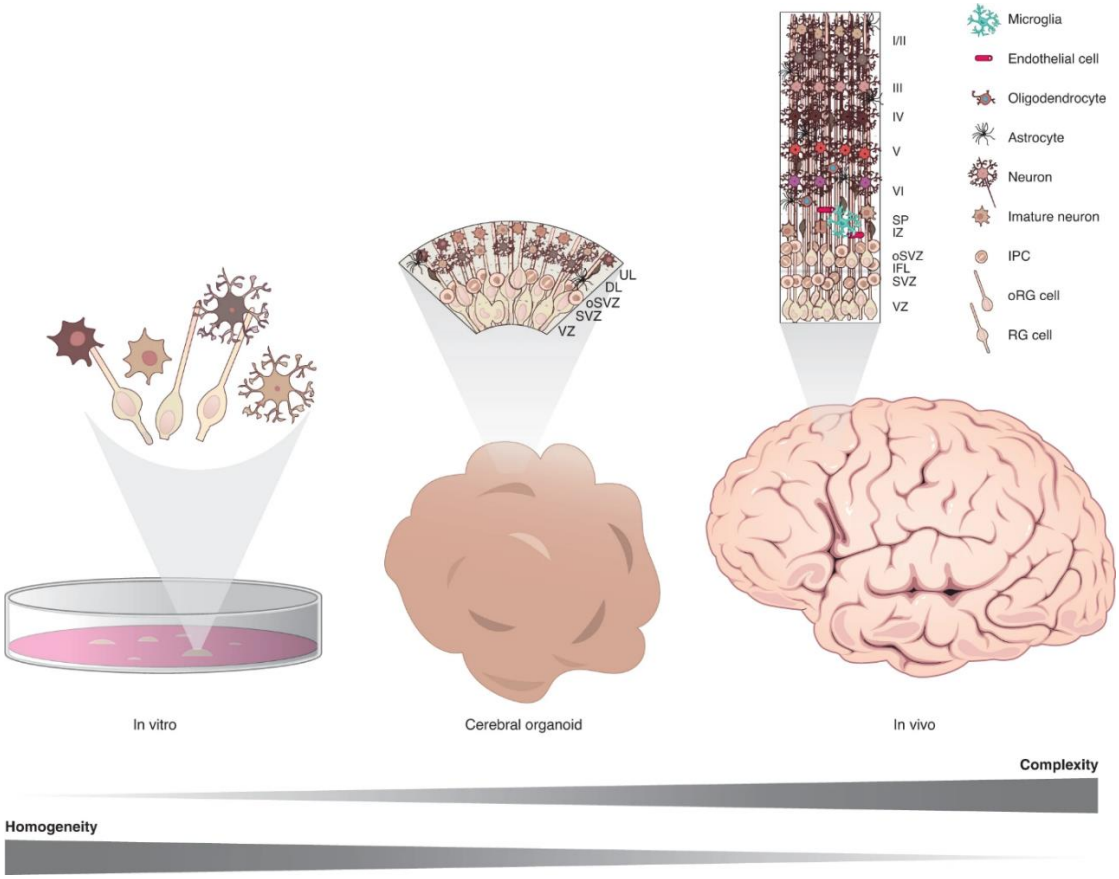

Figure 20: Neural organoid at the interface of in vitro and in vivo. Organoids exhibit characteristics that fall between the homogeneity seen in early in vitro models and the complexity observed in the brain. Image adapted from (Chiaradia & Lancaster, 2020).

This offers a valuable opportunity to investigate the molecular basis of neurodevelopmental fate decisions in the human brain. There are two primary approaches used in the generation of organoids: guided and unguided protocols (Eiraku et al., 2008; Lancaster et al., 2013). Sasai and collegues first established a guided protocol employing a combination of inhibitors targeting the WNT, BMP, and TGFβ pathways, directing the induction of a rostral-dorsal pallial fate (Eiraku et al., 2008). Knoblich and collegues pioneered the unguided protocols following the principles of an intrinsic differentiation capacity of human ESC/iPSC toward the neuroectodermal lineage (Lancaster et al., 2013), which gives rise to organizer-like cell populations and eventually develop distinct brain regions (Renner et al., 2017). Subsequent studies have further modified these protocols to produce organoids with more precise regional brain identities. This is achieved through the incorporation of specific growth factors, signaling molecules, or inhibitors that mimic in vivo regional brain developmental programs (Figure 21). These directed differentiation protocols generate organoids with greater reproducibility and enhanced cellular diversity.

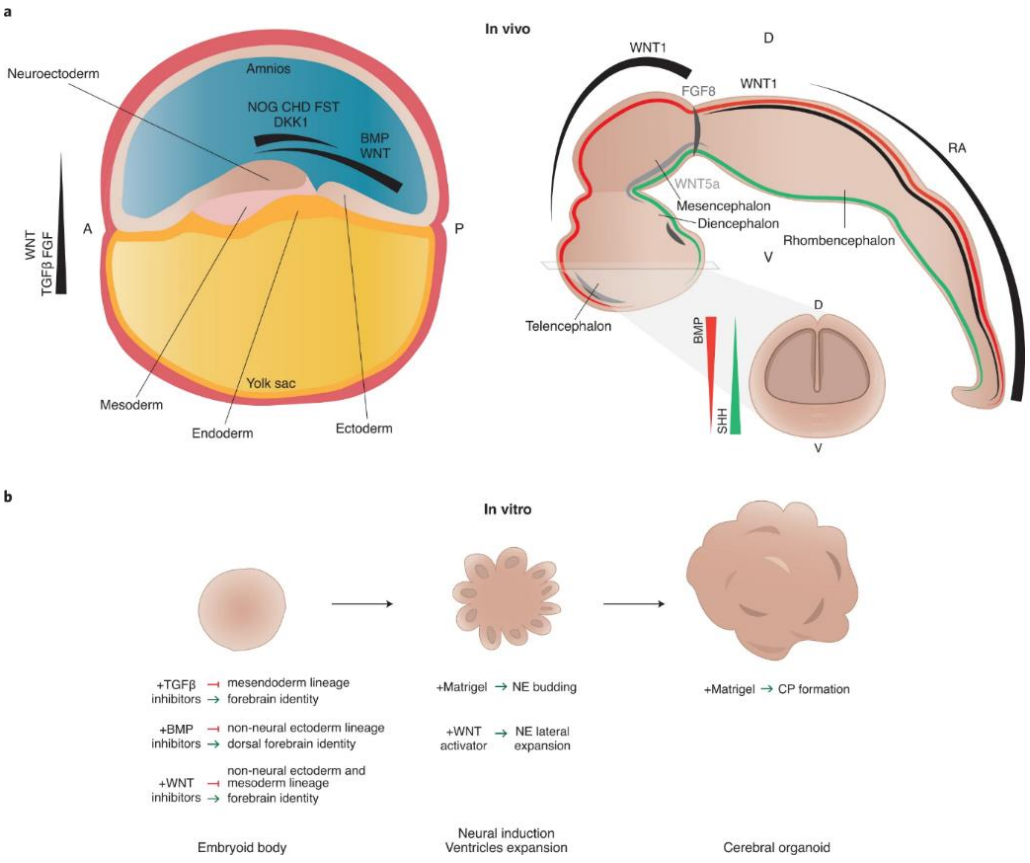

Figure 21: Signaling molecules acting during neurodevelopment. Schematic representing human gastrula (top left), neural tube (top right), and organoid protocols (bottom). Key

signaling components include TGFβ, FGF, Noggin (NOG), Chordin (CHD), Follistatin (FST), Dickkopf-1 (DKK1), BMP, SHH, and anterior (A), posterior (P), dorsal (D), ventral (V) axis. Image adapted from (Chiaradia & Lancaster, 2020).

Across protocols, FOXG1/EMX1 expression is broadly applied for validating differentiation towards forebrain identity. The majority of protocols consist of three common steps: (1) induction (3-18 days), (2) expansion/differentiation (4-20 days), and (3) maturation (Figure 22). The downregulation of pluripotency factors provides a permissive environment for spontaneous neural induction, which may occur at a low efficiency in comparison to directed neural induction. Following neural induction, organoids undergo cultivation in an expansion/differentiation medium supplemented with substances such as N2 or B27. This creates optimal conditions for NPC survival and facilitates the developmental progression into neuron and glial cells. Extracellular matrix-based matrigels and rotational bioreactors are utilized to facilitate morphogenesis and enhance nutrient absorption. The incorporation of lipid concentrate, serum, heparin, and matrigel demonstrated strong reproducibility in both structure and gene expression (Kadoshima et al., 2013; Velasco et al., 2019). Enhanced cortical lamination and functional synaptogenesis were achieved by employing growth factors either during expansion/differentiation (FGF2 and EGF) or maturation (brain-derived neurotrophic factor, BDNF and neurotrophin-3, NT3) (Paşca et al., 2015). Optimized long-term culture of organoids with microfilaments scaffolding and air-liquid interface promotes the transition of NPC towards a neurogenic-gliogenic shift, leading to the generation of astrocytes (Giandomenico et al., 2019). Organoids also demonstrated the presence of interneurons and oligodendrocytes in certain conditions. Additional nutrients, including the platelet-derived growth factor (PDGF), hepatocyte growth factor (HGF), insulin-like growth factor 1 (IGF1), insulin, triiodo-L-thyronine (T3), biotin, L-ascorbic acid (vitamin C), and a cyclic AMP analog (cAMP) were added to promote OPC survival and proliferation (Marton et al., 2019). Consequently, cell-cell interactions contribute to the establishment of neuronal circuits in organoids. Neuronal maturation and spontaneous neuronal activities, a characteristic of fetal brain, has been observed in organoids after a few months in culture (Giandomenico et al., 2019; Trujillo et al., 2019). Therefore, organoids reproduce various features of the developing human brain, encompassing cytoarchitecture, cellular diversity, and maturation.

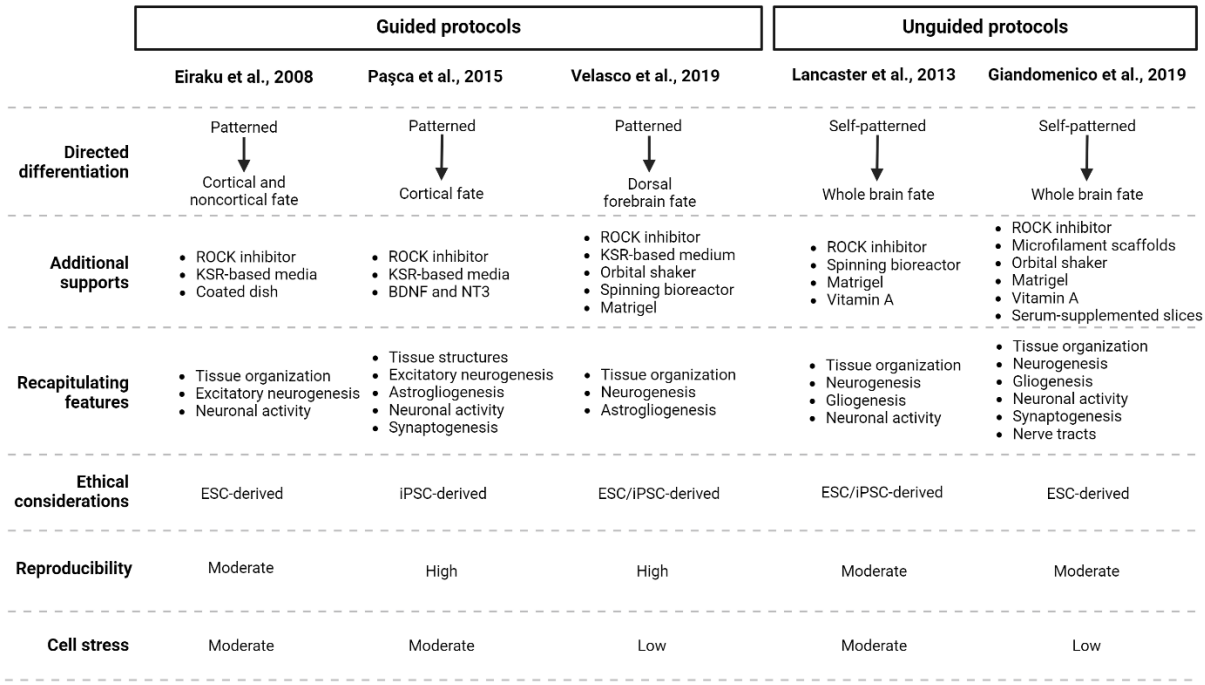

Figure 22: A guide to organoid protocols using different levels of directed patterning and differentiation. Abbreviations: ROCK (Rho-kinase), KSR (knockout serum replacement). Created with BioRender.com.

Despite significant advancements in protocols, organoid models still exhibit several limitations. All existing brain organoids exclusively derive from the neuroectodermal lineage, thus lacking the presence of mesoderm-derived cells, such as microglia and endothelial cells, which can be mitigated through co-culture approaches. The absence of vascularization limits nutrient and oxygen supply via diffusion, which becomes increasingly insufficient and stressful as organoids grow larger (Bhaduri et al., 2020). In terms of differential contribution of direct and indirect neurogenesis, a strategy is recently applied to quantify direct and indirect neurogenic output of BP in the stage-matched human fetal tissue and guided organoids (Coquand et al., 2022). While the BP in organoid largely recapitulate the dynamics of proliferative potential with abundant direct neurogenesis, new methodological approaches will be key to probe and understand the cellular diversity in human.

To analyze the dynamic processes of cell fate transitions during neurogenesis, we used the least directed protocol for the generation of organoids (Lancaster et al., 2013). Then, we have chosen several time points to compare the pace of neurogenesis and its output between our in vivo mouse and in vitro human organoid models (Figure 23).

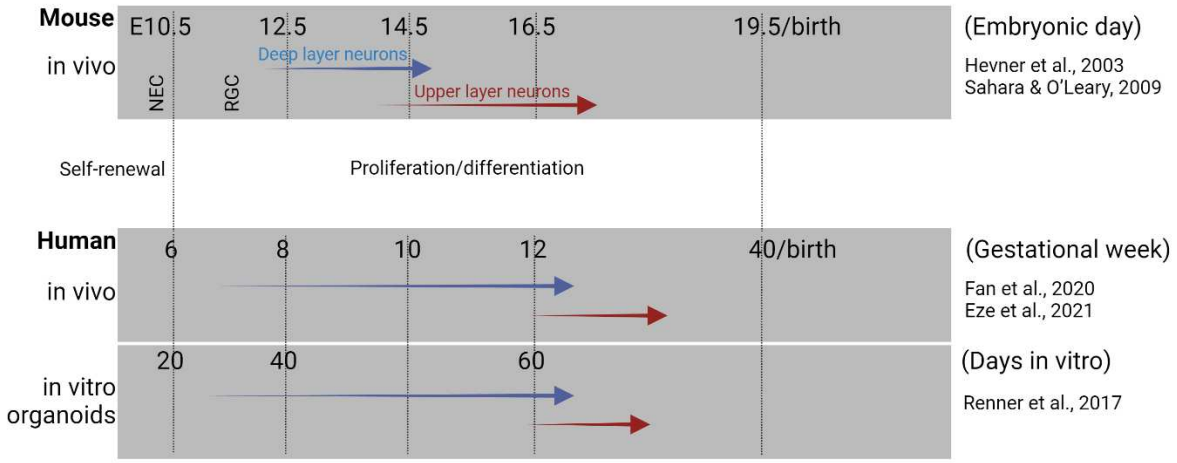

Figure 23: A robust comparison of the timing of excitatory neurogenesis between in vivo and in vitro models. Abbreviations: NEC (neuroepithelial cells), RGC (radial glial cells). Created with BioRender.com.

Objective of the thesis

From the studies discussed here, it seems that molecular mechanisms driving brain development is quite established, while the direct or indirect contributions of metabolic programs to brain development are catching more attention. Metabolism can be modulated and partially studied in animal models; however, species-specificity is a big concern for the benefits of human contexts. Importantly, as metabolism peaks at specific stages of development, many questions remain unanswered: how it is becoming restricted in a time window? How ongoing metabolism ensures proper neurogenesis and brain growth? What metabolic scenarios would lead to severe defects like microcephaly? Finally, how nutrition anticipates developmental growth priorities in the fetus? This thesis aims at providing some answers, which will be outlined in the following chapter.

Results

Manuscript 1: Dihydrofolate reductase activity controls neurogenic transitions in the developing neocortex

Aims: Using mouse genetics and human neural organoids, we assessed the consequences of reducing the activity of DHFR on neocortex development.

Rationale: DHFR is crucial for converting dietary folate into THF, and its downstream folate species are required for both DNA synthesis and methylation reactions. DHFR is classified as a housekeeping gene expressed in all cycling cells, however, we found DHFR is dynamically expressed in human and mouse neural progenitors over the course of neocortex development.

Main results:

1) We observed a loss of CTIP2+ early born neurons associated with an increase in TBR2+ intermediate progenitors and SATB2+ late born neurons in DHFR heterozygous mice.

2) DHFR pharmacological inhibition in neural organoid leads to a depletion in PAX6+ apical progenitors and overproduction of TBR2+ intermediate progenitors resulting in accelerated generation of CTIP2+ early born neurons and SATB2+ late born neurons.

3) Neuronal subtype generation correlates with decreased steady-state levels of THF and SAM metabolites and with a reduction in H3K4me3 marks.

© 2023. Published by The Company of Biologists Ltd | Development (2023) 150, dev201696. doi:10.1242/dev.201696

RESEARCH ARTICLE

Dihydrofolate reductase activity controls neurogenic transitions in the developing neocortex

Sulov Saha[1], Thomas Jungas[1], David Ohayon[1], Christophe Audouard[1], Tao Ye[2], Mohamad-Ali Fawal[1] and Alice Davy[1,*]

ABSTRACT

One-carbon/folate (1C) metabolism supplies methyl groups required for DNA and histone methylation, and is involved in the maintenance of self-renewal in stem cells. Dihydrofolate reductase (DHFR), a key enzyme in 1C metabolism, is highly expressed in human and mouse neural progenitors at the early stages of neocortical development. Here, we have investigated the role of DHFR in the developing neocortex and report that reducing its activity in human neural organoids and mouse embryonic neocortex accelerates indirect neurogenesis, thereby affecting neuronal composition of the neocortex. Furthermore, we show that decreasing DHFR activity in neural progenitors leads to a reduction in one-carbon/folate metabolites and correlates with modifications of H3K4me3 levels. Our findings reveal an unanticipated role for DHFR in controlling specific steps of neocortex development and indicate that variations in 1C metabolic cues impact cell fate transitions.

KEY WORDS: One-carbon metabolism, Neocortex, Neural progenitors, Organoids, Mouse genetics

INTRODUCTION

One-carbon (1C) metabolism is a universal metabolic process composed of two intertwined cycles, the folate cycle and the methionine cycle, that collectively sustain the biosynthesis of purine, thymidine and methyl groups (Clare et al., 2018; Ducker and Rabinowitz, 2017). As such, 1C metabolism is necessary for DNA replication as well as protein and DNA methylation. Although the folate cycle has been extensively studied for its role in cell proliferation, recent studies revealed a role for the methionine cycle in self-renewal of stem cells through the regulation of histone methylation (Fawal et al., 2018, 2021; Shiraki et al., 2014; Shyh-Chang et al., 2013). Specifically, it has been shown that perturbation of the methionine cycle leads to a decrease in H3K4 trimethylation, which in turn impacts gene expression (Fawal et al., 2018; Mentch et al., 2015; Shiraki et al., 2014; Shyh-Chang et al., 2013). Dihydrofolate reductase (DHFR), an enzyme positioned upstream of the two cycles, is crucial for converting dietary folate into tetrahydrofolate (THF), and its downstream folate species are required for both DNA synthesis and methylation reactions. *DHFR* is classified as a housekeeping gene expressed in all cycling cells whose expression varies proportionally to cell growth (Feder et al., 1989). Yet human genetic studies showed that DHFR deficiency leads to hematological and neurological phenotypes in humans (Banka et al., 2011; Cario et al., 2011), indicating that DHFR has tissue-specific functions. Furthermore, a recent single-cell gene expression analysis revealed that *DHFR* mRNA is dynamically expressed in human and mouse neural progenitors over the course of neocortex development (Klingler et al., 2021), suggesting that it could play specific roles in this developmental process.

The mammalian neocortex develops according to an ordered temporal sequence that begins with the amplification of neuroepithelial cells, which are the founder stem cell population. After an active phase of proliferation, neuroepithelial cells transition into apical progenitors that are anchored to both the apical and basal side of the cortical wall, with their cell bodies forming the ventricular zone (VZ) (Noctor et al., 2001; Rakic, 1972). These apical progenitors express the transcription factor PAX6 (Götz et al., 1998) and give rise to glutamatergic projection neurons populating the six layers of the neocortex, numbered I to VI, in a sequential 'inside-out' manner (except for early-born uppermost layer I neurons). In the mouse neocortex, at the onset of neurogenesis, a fraction of $PAX6^+$ apical progenitors generate early-born deep layer (V-VI) neurons by direct neurogenesis (Cárdenas et al., 2018). During the mid-late stages of neurogenesis, $PAX6^+$ apical progenitors generate neurons mostly by indirect neurogenesis, which involves the production of intermediate progenitors expressing the transcription factor TBR2 (Haubensak et al., 2004; Miyata et al., 2004; Noctor et al., 2004; Sessa et al., 2008). Although $TBR2^+$ intermediate progenitors in the subventricular zone (SVZ) symmetrically divide to generate neurons of all layers, at later stages they mainly give rise to late born upper layer (II-IV) neurons (Vasistha et al., 2015). In humans, the number of $TBR2^+$ progenitors and other types of intermediate progenitors is massively expanded (Hansen et al., 2010) and neurogenesis is mostly indirect, although evidence of direct neurogenesis at early developmental stages has been reported for the production of deep layer neurons (Eze et al., 2021). Newborn neurons subsequently migrate radially towards the cortical plate (CP) and express specific factors that control their final positioning and axonal targeting to establish circuit connections, such as TBR1 for layer VI neurons, CTIP2 for layer V neurons or SATB2 for layer II-IV neurons (Molyneaux et al., 2007).

Here, to address whether DHFR plays a role in specific steps of neocortex development, we reduced DHFR activity both in mouse and human models, with, respectively, *in vivo* and *in vitro* approaches. First, we generated haploinsufficient $Dhfr^{+/\Delta}$ mice and observed a loss of $CTIP2^+$ early-born neurons associated with

[1]Molecular, Cellular and Developmental Biology Unit (MCD), Centre de Biologie Intégrative (CBI), Université de Toulouse, CNRS, UPS, 118 route de Narbonne, 31062 Toulouse, France. [2]Institut de Génétique et de Biologie Moléculaire et Cellulaire (IGBMC), INSERM U1258, CNRS UMR7104, Université de Strasbourg, 1 rue Laurent Fries, 67404 Illkirch, France.

*Author for correspondence (alice.davy@univ-tlse3.fr)

A.D., 0000-0003-2134-4526

Handling Editor: Lydia Finley
Received 11 February 2023; Accepted 1 August 2023

Development (2023) 150, dev201696. doi:10.1242/dev.201696

an increase in TBR2$^+$ intermediate progenitors and SATB2$^+$ late-born neurons. Second, we report that DHFR pharmacological inhibition at an early stage of human neural organoid (HNO) development leads to a depletion in PAX6$^+$ apical progenitors and overproduction of TBR2$^+$ intermediate progenitors resulting in accelerated generation of CTIP2$^+$ early-born neurons and SATB2$^+$ late-born neurons. Both findings suggest that DHFR deficiency prematurely initiates indirect neurogenesis and has a functional impact on the generation of neuron subtypes. Mechanistically, we find that these changes in neuronal subtype generation correlate with decreased steady-state levels of THF and S-adenosyl methionine (SAM) metabolites and with a global decrease in H3K4 trimethylation (H3K4me3) marks. Genome-wide analyses revealed changes in this histone methylation mark at genes that are specific to neuronal subtypes.

RESULTS

DHFR haploinsufficient embryos exhibit early neocortex developmental delay

DHFR is classified as a housekeeping enzyme, yet data mining shows that *Dhfr* mRNA is expressed dynamically in the developing mouse neocortex, with a high expression in PAX6$^+$ apical progenitors at early stages of development and a low expression in TBR2$^+$ progenitors and in neurons (Fig. 1A, Fig. S1A,B) (Di Bella et al., 2021; Telley et al., 2019; Visel et al., 2004). By using western blot analyses, we confirmed that expression of DHFR protein is highest at E12.5 in the developing mouse head (Fig. 1B). To investigate the role of DHFR on neurogenesis *in vivo* and the long-term consequences of its inhibition on neocortex development, we generated a *Dhfr* mutant mouse line by deleting exon 5 of the *Dhfr* gene, which harbors the catalytic activity (Fig. 1C). Genotyping of E4.5 embryos revealed a wild-type and a deleted allele, indicating that genome editing was successful (Fig. S1C); RT-PCR and qRT-PCR analyses on wild-type and *Dhfr*$^{+/\Delta}$ heterozygous E12.5 embryos showed that the deleted allele was transcribed (Fig. S1D,E). In tissue extracts from E12.5 embryos, DHFR protein levels were halved in *Dhfr*$^{+/\Delta}$ samples compared with wild type (Fig. 1D) and a similar decrease in DHFR activity was observed in *Dhfr*$^{+/\Delta}$ samples compared with wild type (Fig. 1E). Despite this decreased DHFR activity, *Dhfr*$^{+/\Delta}$ heterozygous mutants were viable and fertile with normal body weight (Fig. S1F).

To gain insight into the role of DHFR in early neocortex development, we assessed progenitor and neuron populations in the *Dhfr*$^{+/\Delta}$ heterozygous mutants at E12.5. This revealed that the number of PAX6$^+$ apical progenitors was reduced in the lateral neocortex of *Dhfr*$^{+/\Delta}$ embryos compared with wild-type embryos, with no change in TBR2$^+$ intermediate progenitors (Fig. 1F,G). In addition, we used TBR1, a marker of immature neurons (predominantly layer VI), CTIP2 (a marker of layer V neurons) and SATB2 (predominantly layer II-IV) to quantify the production of projection neuron subtypes. In the lateral neocortex of E12.5 *Dhfr*$^{+/\Delta}$ embryos, the number of TBR1$^+$ neurons was not significantly changed, the number of CTIP2$^+$ neurons was decreased while no SATB2$^+$ neurons could be detected in either genotype (Fig. 1H-J). DHFR plays a well-known function in cell proliferation; we thus expected that the origin of the decrease in progenitors and CTIP2$^+$ neurons was due to decreased proliferation. However, we observed no significant differences in phospho-histone H3 (pH3)-positive cells at the VZ of *Dhfr*$^{+/\Delta}$ embryos compared with wild type (Fig. S2A,B), suggesting unchanged proliferation rate of apical progenitors. In addition, immunostaining for the apoptotic marker cleaved caspase 3 (CASP3) detected only a few condensed nuclei or CASP3-positive cells in wild-type and *Dhfr*$^{+/\Delta}$ neocortex (Fig. S2C,D), indicating that the decrease in progenitor and neuron populations is not due to cell death. Next, we performed bulk RNA-sequencing at E12.5, comparing wild-type and *Dhfr*$^{+/\Delta}$ embryonic neocortex. PCA analyses with the entire gene set showed that the samples could be partly clustered by genotypes (Fig. 1K). However, a PCA bi-plot analysis using a subset of 258 genes specific for E12.5 neocortex (Di Bella et al., 2021) revealed an association of the majority of these genes with wild-type samples (Fig. 1L), suggesting that the main difference in expression profiles between genotypes is related to genes that define this embryonic stage. Further bioinformatics analyses identified about 250 genes that are differentially expressed in *Dhfr*$^{+/\Delta}$ embryonic neocortex (Fig. S2E), and we confirmed the molecular signature of an immature brain with decreased expression of *Ttr* and *Aldoc* by qRT-PCR in *Dhfr*$^{+/\Delta}$ embryos (Fig. S2F). Altogether, these results reveal a delayed progression of early neocortical development in *Dhfr*$^{+/\Delta}$ embryos.

DHFR deficiency promotes indirect neurogenesis in the mouse neocortex

No significant difference in cortical thickness was observed between wild-type and *Dhfr*$^{+/\Delta}$ heterozygous embryos (Fig. S3A,B), indicating that, despite an initial developmental delay, the general growth of the neocortex is not impaired in *Dhfr*$^{+/\Delta}$ mutant embryos. To investigate the consequences of reduced DHFR activity on neurogenesis at later stages of mouse neocortex development, we quantified progenitor and neuron populations at E14.5 in wild-type and *Dhfr*$^{+/\Delta}$ embryos. Although the number of PAX6$^+$ apical progenitors was unchanged, the number of TBR2$^+$ intermediate progenitors was increased in E14.5 *Dhfr*$^{+/\Delta}$ lateral neocortex (Fig. 2A,B), suggesting that TBR2$^+$ intermediate progenitors were produced at a higher rate from PAX6$^+$ apical progenitors between E12.5 and E14.5. The number of pH3-positive cells within the SVZ was increased (Fig. 2C,D), corresponding to the increased abundance of TBR2$^+$ intermediate progenitors. In terms of neurons, the number of TBR1$^+$ neurons was unchanged in lateral neocortex, but the number of CTIP2$^+$ neurons was decreased while the number of SATB2$^+$ neurons was strongly increased (Fig. 2E-G), indicating a potential switch between direct neurogenesis (generating CTIP2$^+$ neurons) and indirect neurogenesis (generating SATB2$^+$ neurons from TBR2$^+$ progenitors). To test for this hypothesis, we injected EdU (5 mg/ml) at E12.5 and monitored the fate of EdU$^+$ cells at E14.5. In *Dhfr*$^{+/\Delta}$ embryos, the fraction of EdU$^+$/TBR2$^+$ cells and EdU$^+$/SATB2$^+$ was increased whereas the fraction of EdU$^+$/CTIP2$^+$ cells was decreased compared with wild type (Fig. 2H-J). These data indicate that progenitors that were cycling at E12.5 generated more TBR2$^+$ progenitors at the expense of CTIP2$^+$ neurons, thus supporting the notion of a precocious switch from direct to indirect neurogenesis in *Dhfr*$^{+/\Delta}$ mutants.

At E16.5, the number of PAX6$^+$ progenitors is indistinguishable between wild-type and *Dhfr*$^{+/\Delta}$ neocortex whereas the number of TBR2$^+$ progenitors is decreased (Fig. 3A,B), possibly reflecting an accelerated neurogenesis. The imbalance in neuronal composition persists with fewer CTIP2$^+$ and an excess of SATB2$^+$ neurons in *Dhfr*$^{+/\Delta}$ neocortex compared with wild type at E16.5 (Fig. 3C-F). This persisting change of neuronal fate in *Dhfr*$^{+/\Delta}$ neocortex was confirmed at E19.5/P0 using CTIP2 and SATB2 as well as CUX1, which is a marker of late-born, upper layer neurons (Fig. 3G,H). Noticeably, this altered neuronal composition was still observed in *Dhfr*$^{+/\Delta}$ somatosensory neocortex at postnatal P21 stage (Fig. S3C,D), with a decreased number of CTIP2$^+$ neurons and an increased number of SATB2$^+$ neurons, revealing long-term changes in neuronal

Development (2023) 150, dev201696. doi:10.1242/dev.201696

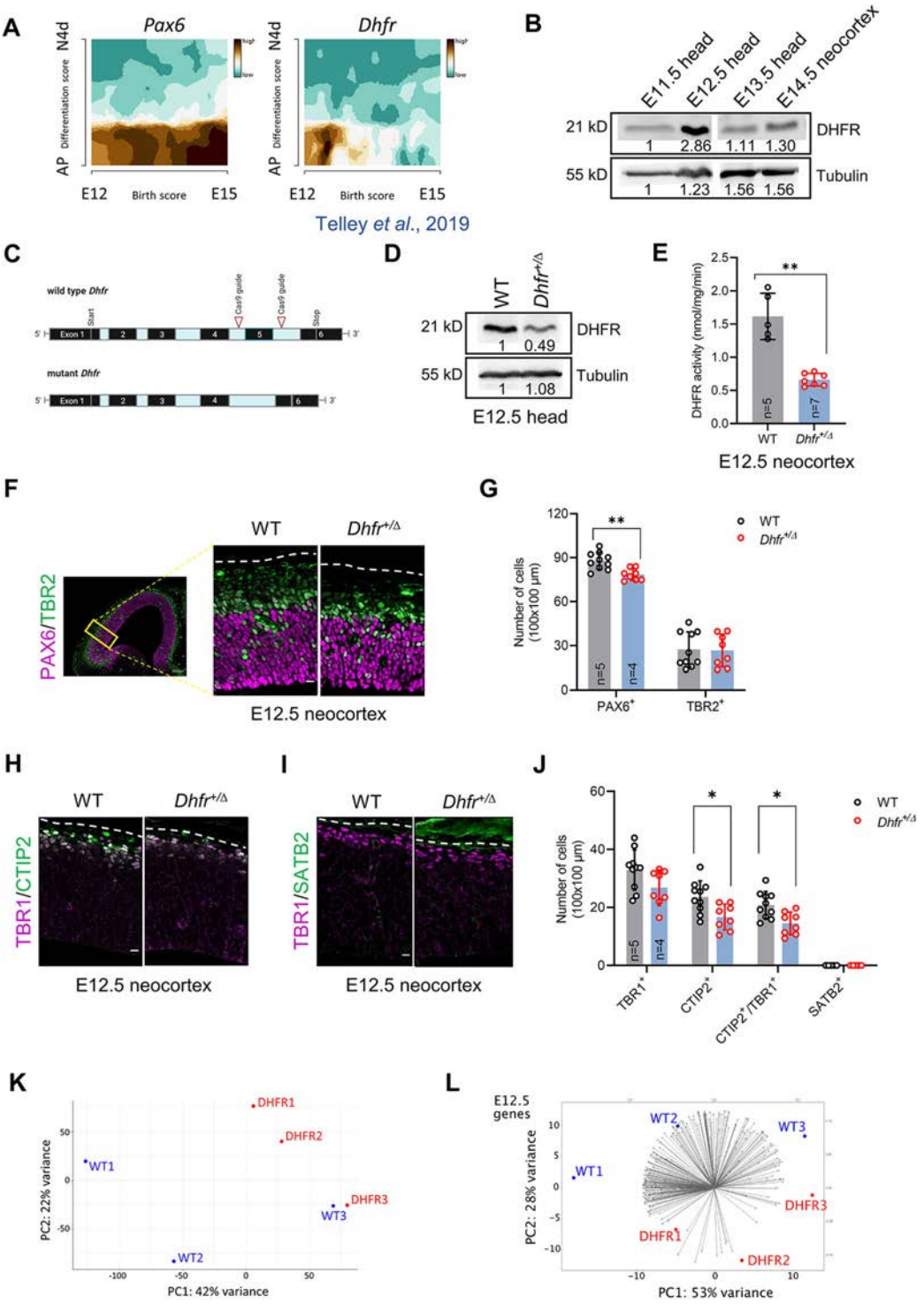

Fig. 1. *Dhfr* heterozygous mutant mice exhibits early neurodevelopmental delay. (A) *Dhfr* mRNA expression in the developing mouse neocortex (data collected from http://genebrowser.unige.ch/telagirdon/). AP, apical progenitors; E, embryonic day; N4d, 4-day-old neurons. (B) Western blot analysis of wild-type tissue extracts at different developmental stages (n=2). Primary antibodies are indicated on the right. Tubulin was used as a loading control. Numbers indicate relative levels over time. (C) Schematic representation of the wild-type *Dhfr* gene and the mutant allele obtained by deleting exon 5 with CRISPR-Cas9 engineering. (D) Representative western blot analysis of wild-type and $Dhfr^{+/\Delta}$ E12.5 head extracts (n=4). Primary antibodies are indicated on the right. Tubulin was used as a loading control. Numbers indicate relative levels. (E) DHFR activity in wild-type and $Dhfr^{+/\Delta}$ E12.5 neocortex was measured with a DHFR assay kit (Sigma-Aldrich). Enzymatic reaction kinetics were measured by spectrophotometric absorbance. (F,G) Representative images and quantification of neocortex coronal sections of E12.5 wild-type and $Dhfr^{+/\Delta}$ embryos immunostained for PAX6 and TBR2. Scale bars: 10 µm. The location of regions of interest (ROIs) (yellow box) used for quantification is indicated in the low-magnification image on the left. (H-J) Representative images and quantification of neocortex coronal sections of E12.5 wild-type and $Dhfr^{+/\Delta}$ embryos immunostained for TBR1, CTIP2 and SATB2. Scale bars: 10 µm. (K) PCA plot showing the distribution of wild-type ($Dhfr^{+/+}$) and DHFR ($Dhfr^{+/\Delta}$) embryos based on whole-genome expression profiles. (L) PCA bi-plot showing the comparison of wild-type ($Dhfr^{+/+}$) and DHFR ($Dhfr^{+/\Delta}$) embryos based on a subset of 258 genes specific to the E12.5 neocortex (data collected from Di Bella et al., 2021). Data are mean±s.d. and statistical analysis was carried out using a Mann–Whitney test.

Development (2023) 150, dev201696. doi:10.1242/dev.201696

composition. These results indicate that loss of DHFR activity promotes the generation of TBR2$^+$ progenitors at mid-corticogenesis and favors the production of SATB2$^+$ neurons by indirect neurogenesis at the expense of direct production of CTIP2$^+$ neurons.

DHFR deficiency modulates histone methylation

DHFR is a key enzyme in the one-carbon/folate metabolic pathway that has two distinct outputs: purine synthesis, which is required for DNA synthesis and cell proliferation; and synthesis of methyl groups, which is required for methylation reactions (Fig. 4A). Because it has been shown that perturbation of the methionine cycle leads to a decrease in H3K4 trimethylation, which in turn impacts gene expression (Fawal et al., 2018; Mentch et al., 2015; Shiraki et al., 2014; Shyh-Chang et al., 2013), we hypothesized that DHFR deficiency affects neurogenesis by modulating the production of methyl groups and methylation reactions. To test this, we performed biochemical assays to measure levels of THF and of the universal methyl donor SAM, and observed that both metabolites were significantly reduced in E12.5 *Dhfr*$^{+/\Delta}$ head extracts compared with wild-type samples (Fig. 4B,C). In fact, SAM levels were affected the most, halving in *Dhfr*$^{+/\Delta}$ samples (Fig. 4C). It has been shown previously that depletion in SAM levels leads to a decrease in H3K4me3 *in vitro* and this correlated with altered gene expression (Mentch et al., 2015). To test whether altered SAM levels correlated with decreased H3K4me3 in the neocortex *in vivo*, we performed western blot analysis which revealed a global loss of H3K4me3 in *Dhfr*$^{+/\Delta}$ samples compared with wild type (Fig. 4D). To go a step further, we decided to investigate whether DHFR deficiency led to changes in H3K4me3 at specific genes. To do this, we performed H3K4me3 ChIP-sequencing on neural progenitors subjected to pharmacological inhibition of DHFR *in vitro* using methotrexate (MTX), a powerful DHFR inhibitor. Our rationale for using this *in vitro* system was to ensure the observed changes in the level of H3K4me3 would be a direct consequence of inhibiting DHFR activity in neural progenitors. After DMSO or MTX treatment and ChIP-sequencing, we observed no global decrease in the level of H3K4me3 bound to neural progenitor-specific genes (Liu et al., 2017) (Fig. S4A), possibly reflecting a different sensitivity between ChIP-seq analysis and western-blot and/or a limitation due to the normalization of quantitative information using conventional ChIP-seq analysis (van Galen et al., 2016). Next, we assessed the distribution of H3K4me3 marks at sets of genes that are specific for progenitors (Kawaguchi et al., 2008) and neurons (Molyneaux et al., 2007) (Table S1). We observed a decrease in H3K4me3 binding at the TSS of VZ marker genes, while the level of H3K4me3 binding was not changed at SVZ marker genes (Fig. 4E). Concerning neuronal specification genes, some had increased H3K4me3 binding close to their TSS whereas others showed decreased H3K4me3 binding (Fig. 4E). A more detailed analysis of these neocortical layer-specific genes (Molyneaux et al., 2007) indicated a reduction in H3K4me3 on a subset of deep layer-specific genes, while the majority of upper layer-specific genes exhibited a slight increase in H3K4me3 marks in the MTX treated samples (Fig. 4F). As an example, qualitative profiling analysis revealed a substantial loss of H3K4me3 peaks at the *Bcl11b* (which encodes CTIP2) promoter in MTX-treated conditions (Fig. 4G). To confirm the effect of MTX treatment *in vivo*, we performed intraventricular *in utero* injection of MTX (20 µM) at E13.5 and analyzed the number of TBR1-, CTIP2- and SATB2-positive cells at E16.5. This analysis revealed no change in the number of TBR1$^+$ neurons with a significant reduction in the number of CTIP2$^+$ neurons at E16.5 (Fig. 4H,I), while a modest increase in the number of SATB2$^+$ neurons was observed in the lateral intermediate zone (IZ) of MTX-treated samples (Fig. S4B,C). Altogether, these findings suggest that DHFR deficiency alters epigenetic landscapes in mouse neural progenitors and this correlates with a switch in neuronal subtypes generated.

Inhibition of DHFR activity in human neural organoids promotes neurogenesis

Similar to the mouse, expression of human *DHFR* mRNA is highest in progenitors at early stages of fetal development (Fig. S5A) (Klingler et al., 2021) and at early stages of HNO development (Fig. S5B) (Kanton et al., 2019). To assess the role of human DHFR in developing neural tissue, we generated cerebral organoids, which we refer to as HNOs to follow recent nomenclature guidelines (Pasca et al., 2022), using the Lancaster protocol (Lancaster and Knoblich, 2014) and exposed them to MTX (2 µM). To specifically target neural progenitors, we treated 7 days *in vitro* (div7) neural aggregates with MTX for a duration of 3 days, with subsequent steps of HNO maturation carried out in absence of MTX (Fig. 5A). Measurement of DHFR activity in control HNOs showed a developmental reduction in DHFR activity, which is higher at div10 than at div20 (Fig. 5B), in line with the single-cell mRNA expression data (Fig. S5B). Acute 3-day MTX treatment transiently inhibited DHFR, as DHFR activity was undetectable in MTX-treated div10 HNOs but was partially recovered at div20 (Fig. 5B). Western blot analysis of human neuroepithelial samples treated with MTX revealed that inhibition of DHFR led to a global loss of H3K4me3 marks (Fig. 5C), as was shown in mouse samples (Fig. 4D). Macroscopic observation of HNOs over a 60-day time period revealed that MTX treatment stunted HNO overall growth, consistent with the role of MTX as an anti-proliferative agent (Fig. S5D). Yet in these smaller HNOs, the thickness of neocortical-like structures was increased at div40 and div60 (Fig. S5C,E) (see Materials and Methods for a description of neocortical-like structures). In contrast, the thickness of the VZ, which reflects the size of the progenitor pool, remained unchanged at div40 and div60 (Fig. S5F), suggesting that the increase in total thickness at these stages might be due solely to the enlargement of the CP in MTX-treated HNOs. To further characterize the consequences of DHFR inhibition on HNO development and maturation, we examined specific progenitor and neuronal populations in cortical-like structures at different stages of HNO culture. Because cortical-like structures in HNOs vary in size, all quantifications were made as a percentage. At div20, MTX treatment led to a small increase in the proportion of PAX6$^+$ apical progenitors and a decrease in the proportion of immature TBR1$^+$ neurons (Fig. 5D,F). In addition, the proportion of pH3-positive cells was increased in MTX-treated HNOs (Fig. 5E,F) reflecting the increased proportion of PAX6$^+$ progenitors. Together, these results indicate that inhibition of DHFR leads to an initial reduction and/or a delay in neuronal differentiation at early stages of HNO development. In contrast, at div40, we detected a reduction in the proportion of PAX6$^+$ apical progenitors associated with an overproduction of TBR2$^+$ intermediate progenitors and early-born CTIP2$^+$ deep layer neurons (Fig. 5G-I); this altered ratio was also present at div60, as we detected a persistent deficit in PAX6$^+$ apical progenitors associated with an increase in young TBR1$^+$ neurons and early-born CTIP2$^+$ neurons (Fig. 5J,L). Furthermore, at div60, late born SATB2$^+$ neurons could be observed in MTX-treated HNO, whereas they were still rare in control samples (Fig. 5K,L), suggesting that DHFR inhibition leads to an accelerated neurogenesis. Altogether, these findings indicate that inhibition of DHFR in human neural organoids leads to an

Development (2023) 150, dev201696. doi:10.1242/dev.201696

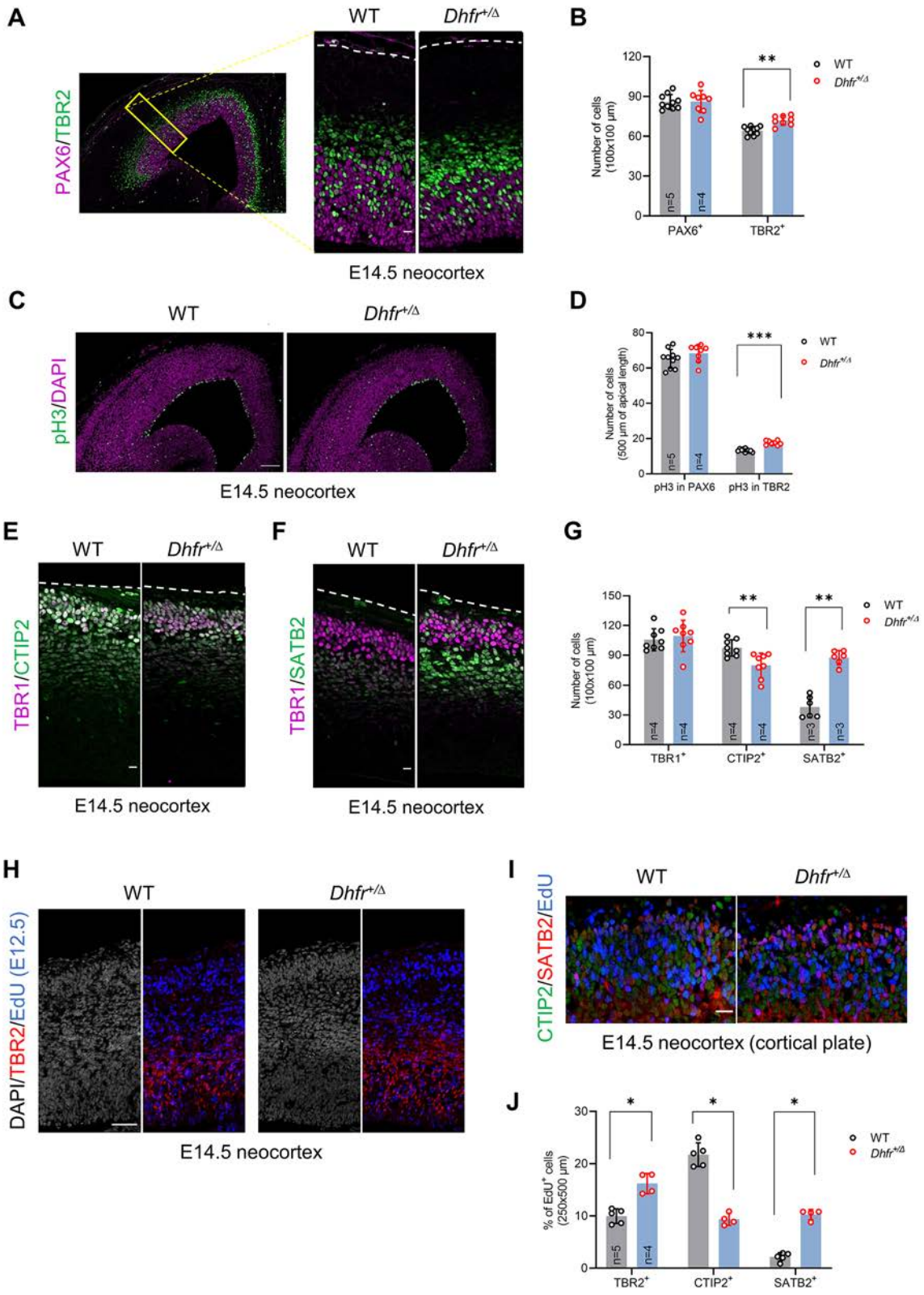

Fig. 2. Overproduction of intermediate progenitors and late-born neurons in *Dhfr*-deficient embryos. (A,B) Representative images and quantification of neocortex coronal sections of E14.5 wild-type and *Dhfr*$^{+/\Delta}$ embryos immunostained for PAX6 and TBR2. Scale bar: 10 µm. The location of regions of interest (ROIs) (yellow box) used for quantifications is indicated in the low-magnification image on the left. (C,D) Representative images and quantification of neocortex coronal sections of E14.5 wild-type and *Dhfr*$^{+/\Delta}$ embryos immunostained for pH3. Scale bar: 100 µm. (E-G) Representative images and quantification of neocortex coronal sections of E14.5 wild-type and *Dhfr*$^{+/\Delta}$ embryos immunostained for TBR1, CTIP2 and SATB2. Scale bars: 10 µm. (H-J) Representative images and quantification of neocortex coronal sections of E14.5 wild-type and *Dhfr*$^{+/\Delta}$ embryos that were injected with EdU at E12.5. Sections were immunostained for EdU, TBR2, CTIP2 and SATB2. Scale bars: 10 µm. Data are mean±s.d. and statistical analysis was carried out using a Mann–Whitney test.

Development (2023) 150, dev201696. doi:10.1242/dev.201696

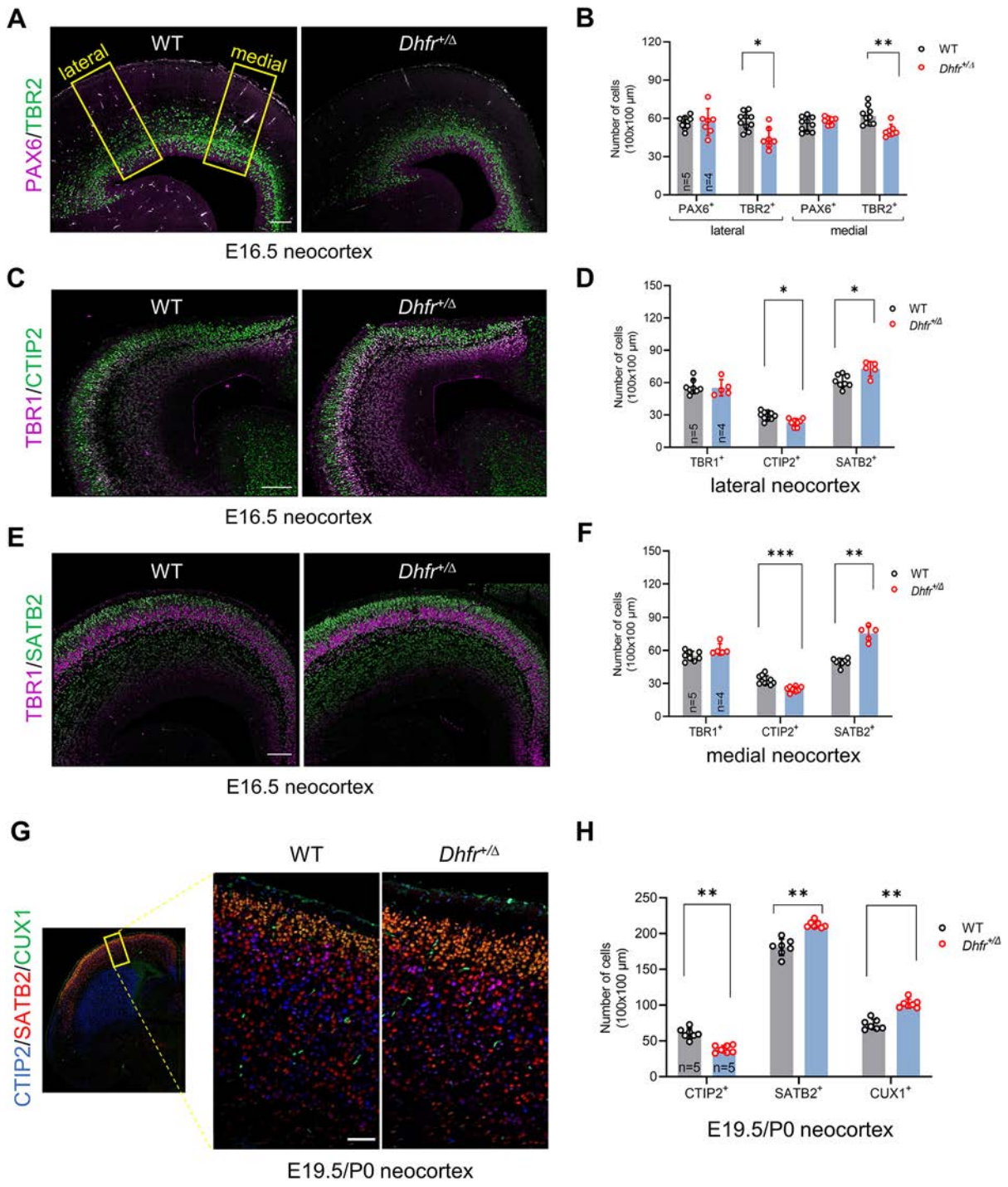

Fig. 3. Reduction in DHFR activity induces long-term changes in neocortex neuronal composition. (A-F) Representative images and quantification of neocortex coronal sections of E16.5 wild-type and *Dhfr*$^{+/\Delta}$ embryos immunostained for PAX6, TBR2, TBR1, CTIP2 and SATB2. The locations of regions of interest (ROIs) corresponding to medial and lateral neocortex used are indicated (yellow rectangles). Scale bars: 100 µm. (G,H) Representative images and quantification of neocortex coronal sections of E19.5/P0 wild-type and *Dhfr*$^{+/\Delta}$ embryos immunostained for CTIP2, SATB2 and CUX1. Scale bar: 10 µm. The ROI (yellow rectangle) used for quantifications is indicated in the low-magnification image on the left.

early developmental delay followed by increased and accelerated neuronal production.

DISCUSSION

Here, we provide evidence that DHFR, which is expressed in progenitors within a restricted time window in both mouse and human developing neocortex, plays a role in neurogenesis. Our data indicate that in both species, inhibition of DHFR activity modifies the production of neuronal subtypes by accelerating the neurogenic temporal sequence. These developmental alterations could be at the origin of altered neurodevelopment and severe neurological disorders that have been associated with mutation in DHFR or other enzymes of one-carbon/folate metabolism in humans (Cario et al., 2011; Serrano et al., 2012).

Development (2023) 150, dev201696. doi:10.1242/dev.201696

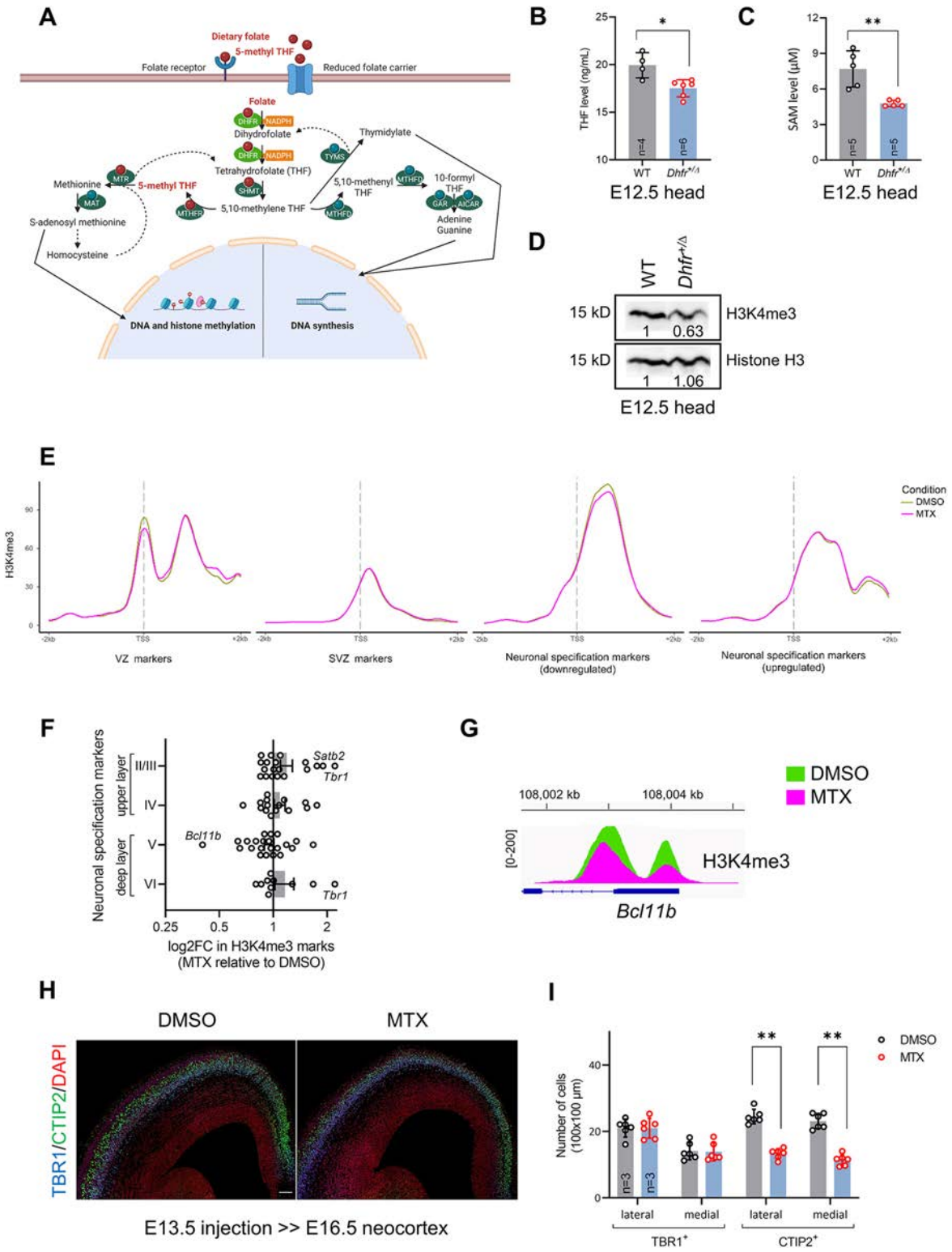

Fig. 4. DHFR inhibition modifies H3K4 trimethylation in neural progenitors. (A) Schematic representation of the 1C metabolic pathway and its outputs. Created with BioRender.com. (B,C) Levels of THF and SAM metabolites in wild-type and *Dhfr*$^{+/\Delta}$ E12.5 head extracts. THF levels were measured with a competitive inhibition enzyme immunoassay kit (Cloud-Clone) by quantifying pre-coated antibody binding with colorimetric absorbance. SAM levels were measured with Bridge-It assay kit (Mediomics) by determining DNA-MetJ protein complex formation in the presence of SAM as ligand. (D) Representative western blot analysis of wild-type and *Dhfr*$^{+/\Delta}$ E12.5 head extracts (n=4). Primary antibodies are indicated on the right. Histone H3 was used as a loading control. Numbers indicate relative levels. (E) Metagene analyses of H3K4me3 at selected marker genes after 72 h of MTX (2 µM) treatment in mouse neurosphere cultures (n=2). (F) Graphical representation of specific changes in methylation levels at neuronal specification genes. Each dot represents a gene and the mean peak intensity±s.e.m. for each layer. (G) Visualization of H3K4me3 peaks at *Bcl11b* promoter using ChIP-seq read mapping data. (H,I) Representative images and quantification of neocortex coronal sections of E16.5 DMSO and MTX (20 µM)-injected wild-type embryos immunostained for TBR1, CTIP2 and DAPI. Scale bar: 100 µm. Data are mean±s.d. and statistical analysis was carried out using a Mann–Whitney test.

Development (2023) 150, dev201696. doi:10.1242/dev.201696

We report the generation of *Dhfr*$^{+/\Delta}$ haploinsufficient embryos that exhibit alterations in neurogenesis and neuronal subtype production. In the *Dhfr*$^{+/\Delta}$ mutant mouse line, DHFR protein levels and DHFR activity are halved in the embryonic neocortex, revealing an absence of compensatory mechanisms from the wild-type allele. Absence of compensatory mechanisms also applies to humans, as a two-fold reduction in DHFR protein levels and activity was reported in individuals carrying a heterozygous point mutation in *DHFR* (Banka et al., 2011; Cario et al., 2011). Although it is generally admitted that metabolic pathways are not sensitive to gene dose due to buffering by other components of the network, this is not true for some rate-limiting enzymes (Johnson et al., 2019). Despite the important role of DHFR in DNA replication, we observed no decreased proliferation and no increased cell death in the neocortex of *Dhfr*$^{+/\Delta}$ heterozygous embryos, indicating that one copy of wild-type *Dhfr* is sufficient to sustain purine synthesis. Conversely, we observed decreased levels of SAM and H3K4 trimethylation in *Dhfr*$^{+/\Delta}$ embryonic neocortex, indicating that DHFR activity is rate-limiting for the methionine cycle and methyl group synthesis in the neural tissue. In a previously described *Dhfr* mutant mouse line (*Ora*) generated by ENU mutagenesis, it was reported that heterozygous animals, which exhibited reduced DHFR activity, survived to adulthood with tissue-specific alterations in folate abundance and distribution, and perturbed stress erythropoiesis (Thoms et al., 2016). These data, together with our data, raise the possibility that *Dhfr* is a haploinsufficient gene and suggests that human carriers of heterozygous mutations may have subtle alterations of the blood and brain compartments.

Recent single-cell RNA-sequencing data showed that *Dhfr* mRNA is expressed at high levels in neural progenitors at early stages of development and is downregulated in apical progenitors at later stages, as well as in intermediate progenitors and differentiating neurons (Di Bella et al., 2021; Kanton et al., 2019; Telley et al., 2019). This dynamic expression pattern suggests that DHFR may play a specific function in apical progenitors. Analyses of neocortex development in *Dhfr*$^{+/\Delta}$ haploinsufficient mouse embryos revealed an initial developmental delay followed by an acceleration of indirect neurogenesis, culminating in the overproduction of late-born neurons at the expense of early-born neurons. Accelerated indirect neurogenesis was also observed in HNOs treated with MTX at an early stage of development, strongly suggesting that these phenotypes are a direct consequence of DHFR inhibition in neural progenitors and not due to systemic causes. However, based on our data, we cannot completely exclude the possibility that, in mice, DHFR inhibition impacts other neural cell types that are known to influence apical progenitor behavior (Villalba et al., 2021), which then could non-autonomously contribute to the observed phenotypes. These phenotypes are reminiscent of microcephalic features observed in individuals harboring mutations *DHFR* (Banka et al., 2011), which could be due to premature differentiation leading to depletion of neural progenitor pools. Recent work studying the impact of folate-deficient diet on fetal corticogenesis in the mouse reported alterations in the production of neuronal subtypes that are similar to those observed in *Dhfr*$^{+/\Delta}$ haploinsufficient embryos (Harlan De Crescenzo et al., 2021). However, the impact of folate-deficient diet on progenitors was different and was associated with increased cell death in the neocortex (Harlan De Crescenzo et al., 2021), suggesting that a folate-deficient diet could have broad deleterious consequences on the pregnant dam that indirectly impact fetal corticogenesis.

It is well established that developmental transitions occurring during neocortex development involve chromatin and epigenetic modifications in neural progenitors (Albert et al., 2017; Hirabayashi and Gotoh, 2010; Koo et al., 2022). Here, we show that inhibition of DHFR in mouse neural progenitors *in vitro* leads to discrete changes in H3K4me3 marks on neuronal specification genes. Indeed, after MTX treatment, a number of genes expressed in early-born neurons have less H3K4me3 bound close to the TSS, whereas some genes expressed in late-born neurons have more H3K4me3 marks but these are localized further away from the TSS. Although these changes in epigenetic marks are consistent with the observed changes in neuronal subtypes in *Dhfr*$^{+/\Delta}$ embryos *in vivo*, further experiments would be needed to establish causality and to identify primary versus secondary changes in H3K4me3 levels. Nevertheless, these results suggest that variations in DHFR activity could influence the epigenetic landscape in apical progenitors and that these epigenetic modifications may set the stage for production of the different neuronal subtypes. Indeed, recent single-cell analyses of chromatin and gene-regulatory dynamics in the developing brain suggested that progenitors entering the cell cycle may be epigenetically primed toward future cell states (Trevino et al., 2021). The fact that histone modifications are stable epigenetic marks may underlie the long-term effects of inhibiting DHFR activity at early stages of neocortex development, as we have shown previously on neural progenitors *in vitro* (Fawal et al., 2018).

Our study identified a conserved function for DHFR in controlling neurogenesis. Indeed, at mid-corticogenesis, reducing DHFR activity led to increased production of SATB2$^+$ neurons in both mouse and human contexts. In the mouse, we observed a switch from CTIP2$^+$ to SATB2$^+$ neurons, whereas in the human context, we observed an increase of both types of neurons. This difference could be due to the fact that TBR2$^+$ intermediate progenitors, which are increased following DHFR inhibition both in mouse and human contexts, have different neuronal outputs in both species. Indeed, a recent lineage-tracing study in the mouse estimated that TBR2$^+$ progenitors generate ∼90% of SATB2$^+$ neurons but only ∼50% of CTIP2$^+$ neurons present in the neocortex (Huilgol et al., 2023). In humans, however, intermediate progenitors are hypothesized to give rise to the majority of projection neurons regardless of their subtype (Lui et al., 2011). In fact, in human developing embryos, TBR2$^+$ progenitors are present from the earliest stages of neurogenesis, and single-cell transcriptomics identified various subpopulations of TBR2$^+$ progenitors (Fan et al., 2020; Pebworth et al., 2021), including one subtype that may give rise to deep layer neurons (Fan et al., 2020). Although it is well known that apical progenitors generate neurons both directly and indirectly, the molecular mechanisms governing the switch from one to the other neurogenic process are not well characterized. In the mouse it was estimated that 5% of apical progenitors produce neurons (mostly CTIP2$^+$) directly at E12.5 and that the switch between direct and indirect neurogenesis involves Robo and Dll1 signaling (Cárdenas et al., 2018), as well as modifications of cell cycle parameters (Roussat et al., 2023). In the future, it would be interesting to assess the link between DHFR and these different pathways. One defining feature of indirect neurogenesis is that it is a hallmark of mammalian neocortex evolution. Indeed, direct neurogenesis with limited neuronal production dominates avian and reptilian paleocortex, whereas indirect neurogenesis predominates in mouse neocortex (Cárdenas et al., 2018). In the human neocortex, indirect neurogenesis is vastly expanded and accounts for the large increase in neuron numbers (Hansen et al., 2010; Lewitus et al., 2014; Namba and Huttner, 2017). Whether this evolutionary innovation was driven, at least in part, by evolutionary changes in 1C metabolism is an interesting question for future research (Namba et al., 2021).

Development (2023) 150, dev201696. doi:10.1242/dev.201696

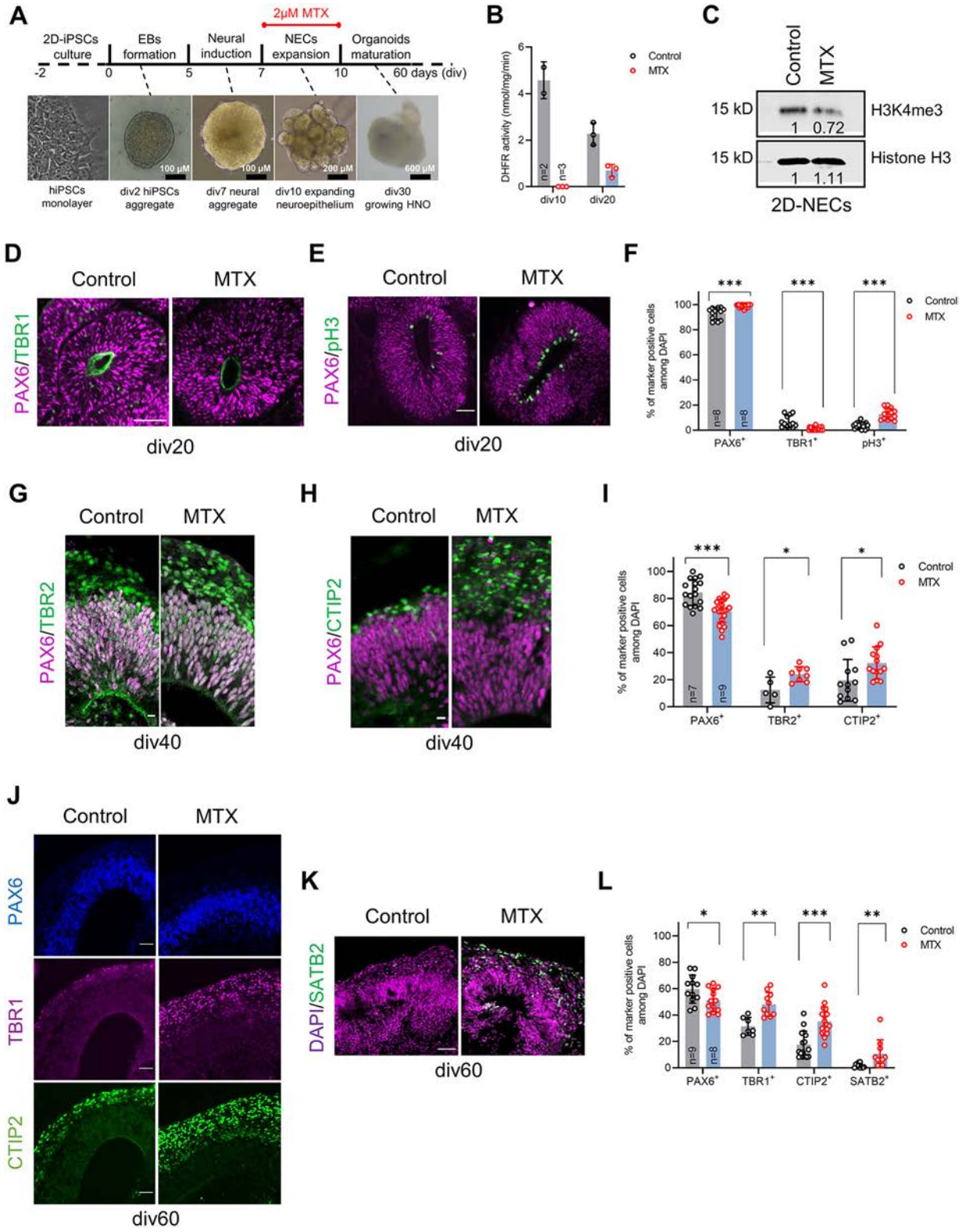

Fig. 5. DHFR deficiency accelerates the neurogenic program in HNOs. (A) Timeline of the protocol used to generate HNOs. The time window of MTX treatment is indicated in red. (B) DHFR activity in pooled DMSO- (control) or MTX-treated (*n*=2 or 3 replicates of six to eight pooled HNOs) HNOs at two different time points. DHFR activity was measured with a DHFR assay kit (Sigma-Aldrich). Enzymatic reaction kinetics were measured by spectrophotometric absorbance. (C) Representative western blot analysis of human neuroepithelial cells (2D-NECs) treated with DMSO (control) or with MTX (*n*=4). Primary antibodies are indicated on the right. Histone H3 was used as a loading control. Numbers indicate relative levels. (D-F) Representative images and quantification of control and MTX-treated HNOs immunostained for pH3, PAX6 and TBR1 at div20. Scale bars: 50 µm. (G-I) Representative images and quantification of control and MTX-treated HNO immunostained for PAX6, TBR2 and CTIP2 at div40. Scale bars: 10 µm. (J-L) Representative images and quantification of control and MTX-treated HNOs immunostained for PAX6, TBR1, CTIP2 and SATB2 at div60. Scale bars: 50 µm. Data are mean±s.d. (*n*=7-12 organoids with 15-20 cortical-like structures analyzed using a Mann–Whitney test).

Development (2023) 150, dev201696. doi:10.1242/dev.201696

MATERIALS AND METHODS

Animals

Dhfr$^{+/\Delta}$ mice were generated by CRISPR/Cas9-mediated excision of exon 5 (see supplementary Materials and Methods for further details). Mice were kept in a 129S4/C57Bl6J mixed background. The gender of embryos was not tested, littermates of each genotype were randomly assigned to experimental groups. All experimental procedures were pre-approved and carried out in compliance with the guidelines provided by the national Animal Care and Ethics Committee (APAFIS#1289-2015110609133558 v5) following Directive 2010/63/EU.

Genotyping

Genomic DNA was isolated from mouse tail and genotyping was performed using 2x PCR Taq MasterMix (abm). The PCR amplification was performed using Veriti thermal cycler (ThermoFisher) followed by agarose gel electrophoresis.

Pluripotent stem cells

Human iPSCs were obtained from Leiden University Medical Center hiPSC core facility (LUMC0004iCTRL). Cells were amplified with mTesR+ medium (STEMCELL Technologies) on h-ES qualified Matrigel (Corning) coating and stored frozen in liquid nitrogen. HNO were generated using STEMdiff cerebral organoid kit (STEMCELL Technologies) by following manufacturer instructions. Cells are tested for mycoplasma every 6 months using the mycoAlert kit (Lonza).

2D-neuroepithelial cell culture

2D-neuroepithelial cells (2D-NECs) were derived from human-iPSCs using the STEMdiff SMADi neural induction kit (STEMCELL Technologies) by following the manufacturer's instructions for the monolayer culture. They were then grown and amplified for two additional passages, using Accutase (STEMCELL Technologies) in STEMdiff neural progenitor medium (STEMCELL Technologies) on Matrigel and stored in liquid nitrogen using STEMdiff neural progenitor freezing medium (STEMCELL Technologies). For inhibition of DHFR activity in 2D-neuroepithelial cells, 50% confluent cells were treated for 3 days with 2 µM MTX diluted in growing medium.

Generation and maintenance of HNO

For every single batch of HNOs, one vial of iPSCs was defrosted every 3-4 days and cells were allowed to reach 70-80% confluence in mTesR+ medium. HNOs were generated using STEMdiff cerebral organoid kit (STEMCELL Technologies), following the manufacturer's instructions, until div60 as the final time point. For acute inhibition of DHFR activity in HNO, neuroepithelial aggregates were treated at div7 with 2 µM MTX (Sigma-Aldrich) freshly diluted in expansion medium, for 3 days.

Histochemistry

Mouse embryonic brains were embedded in paraffin wax, agarose or OCT; HNOs were embedded in OCT for microtome, vibratome or cryostat sectioning. Sections were permeabilized and incubated with antibodies diluted in blocking solution (1-3% BSA, 1-3% FBS, 0.5-1% Tween 20 and PBS) overnight at 4°C (see Table S3 for antibody details). For birthdating experiments, EdU (dissolved in PBS at 5 mg/ml, 25 µg/g body weight) was injected intraperitoneally at E12.5 and samples were collected at E14.5. Histological detection of EdU was performed using the Click-iT EdU cell proliferation kit (ThermoFisher) according to the manufacturer's instructions. For further details see supplementary Materials and Methods.

Imaging

Fluorescent images of tissue and organoid sections were captured with SP8 inverted scanning confocal microscope (Leica Biosystems) or Eclipse 80i fluorescence microscope (Nikon).

Western blot

For protein extraction, mouse and human tissues were obtained by incubating in lysis buffer [150 mM NaCl, 50 mM Tris-HCl (pH 7.4), 0.5 mM EDTA, 2 mM Na_3VO_4, 1% NP-40, 0.5 mM EGTA and 0.1 mM PMSF] supplemented with protease inhibitors for 1 h on ice. Protein lysates were vortexed, ultrasonicated for five cycles (Bioblock), and centrifuged at 16,100 ***g*** for 10 min. Protein concentration in the supernatant was determined using a DC protein assay (Bio-Rad). Lysates were then denatured by boiling in 4× loading buffer [100 mM Tris-HCl (pH 6.8), 8% SDS, 40% glycerol, 4% β-mercaptoethanol and bromophenol blue) before loading and electrophoresis on 4-20% or 12% SDS-PAGE gel using mini-PROTEAN electrophoresis chamber (Bio-Rad). Proteins were transferred onto a 0.45 µm PVDF (Millipore) or nitrocellulose membrane (GE Healthcare), which was blocked for 30 min and incubated with primary antibody in 5% nonfat dry milk in TBST [20 mM Tris, 150 mM NaCl, and 0.05% Tween 20 (pH 7.6)] overnight at 4°C. The membrane was then incubated with HRP-conjugated secondary antibodies in 5% nonfat dry milk in TBST. Immunoreactive bands were generated by adding Lumi-Light plus chemiluminescent substrates (Roche). See Table S3 for antibody details.

RNA-sequencing

Brains from E12.5 wild-type and *Dhfr*$^{+/\Delta}$ embryos were collected and the neocortex was dissected. The tissue was mechanically dissociated to form a cell pellet. RNA was isolated from the cell pellet using Trizol reagent (Invitrogen) according to the manufacturer's instructions and eluted into 35 µl nuclease-free water. Eluted RNAs were then stored at −80°C. RNA quality and integrity (RIN>7) were verified by electrophoresis using a 2100 Bioanalyzer system (Agilent). The whole procedure going from the dissociation to RNA preparation was performed on six animals (n=3 wild type and n=3 *Dhfr*$^{+/\Delta}$) obtained from two different littermates.

RNA libraries were prepared using NEBNext ultra II reagent (New England Biolabs) and RNA sequencing on neocortical samples were performed by IntegraGen (https://integragen.com) using an Illumina NovaSeq 6000 S2 sequencing system (paired-end sequencing, 100 bp reads, 35 M reads/sample).

Differential analysis was applied per genotype (wild type vs *Dhfr*$^{+/\Delta}$) by taking into consideration of litter effects using DESeq2 v1.32.0 (Love et al., 2014), available as an R package in Bioconductor (www.bioconductor.org). The raw read counts were normalized using RLE methods generating and the log2 Fold Change (log2FC) values were computed. We used principal component analysis (PCA) to cluster samples based on their expression levels. Data representation of the scaled PCA was generated using the ggplot2 package (https://ggplot2.tidyverse.org).

ChIP-sequencing

Neural progenitor cells cultured as free-floating neurospheres were treated with DMSO or 2 µM MTX for 72 h. The cells were further processed for DNA extraction according to the previously described method (Fawal et al., 2018).

GenomEast (http://genomeast.igbmc.fr) performed DNA quantification with Qubit (Invitrogen) and processed 1.5-10 ng of double-stranded purified DNA to generate libraries using MicroPlex library preparation kit v2 (Diagenode). Amplified libraries were purified with Agencourt AMPure XP beads (Beckman Coulter) and sequenced on an Illumina Hiseq 4000 sequencer (single-end sequencing, read length 50, minimum 45 M reads/sample). Sequence reads were mapped to the *Mus musculus* genome assembly (mm10) using Bowtie (Langmead et al., 2009). Peak calling was carried out using MACS v2.1.1 (Zhang et al., 2008; Feng et al., 2012). Peaks were annotated to the Ensembl release 94 using HOMER software (http://homer.ucsd.edu/homer/ngs/annotation.html). Peaks from different conditions and replicates were merged to form a consensus peak set. The read coverage for each sample was calculated with multicov function from bedtools v2.26.0 (Quinlan and Hall, 2010). Differential analysis was applied per condition (DMSO versus MTX) using DESeq2 v1.20.0 (Love et al., 2014) to calculate log2 fold change of H3K4me3 ChIP-sequencing read counts in MTX condition versus DMSO condition. Data representation of the differential binding analysis corresponds to a strong change in peak heights at the promoter or gene body. For further details see supplementary Materials and Methods.

RT-PCR and qRT-PCR

RNA was extracted from E12.5 head (for RT-PCR) or E12.5 neocortex (for qRT-PCR) using Trizol reagent according to the manufacturer's instructions. 1 µg RNA was used for reverse transcription.

Development (2023) 150, dev201696. doi:10.1242/dev.201696

For RT-PCR, 1 µl diluted cDNA (10-fold) was mixed with 2x PCR Taq MasterMix containing 1 µM of each primer, and PCR amplification was performed followed by agarose gel electrophoresis.

For quantitative PCR, cDNAs were diluted (10-, 100- and 1000-fold) and processed in triplicate for each dilution. 10 µl diluted cDNA was mixed with 10 µl premix Evagreen (Bio-Rad) containing 1 µM of each primer, and the PCR program was run for 40 cycles on CFX96 Real-Time PCR system (Bio-Rad). For further details see supplementary Materials and Methods.

Metabolic assays

DHFR activity was detected with DHFR assay kit (Sigma-Aldrich). Mouse and human tissues were suspended in 200 µl of Cellytic MT reagent (Sigma-Aldrich) supplemented with protease inhibitors and lysed mechanically using glass beads (Sigma-Aldrich). Lysates were precleared by centrifugation at 16,100 ***g*** for 10 min. The supernatant was mixed in quartz cuvette (Hellma) with 6 µl of NADPH, 5 µl of DHFA and 800 µl of assay buffer provided in the kit, and reaction kinetics were monitored by spectrophotometric absorbance at 340 nm for 2-3 min. The readouts were normalized to the protein concentration in the supernatant at 280 nm.

THF levels were analyzed based on a competitive inhibition enzyme immunoassay kit (Cloud-Clone). Dissected E12.5 head samples were suspended in 120 µl of Cellytic MT reagent supplemented with protease inhibitors followed by mechanical dissociation with a pipette tip for cell lysis and incubated on ice for 30 min. Lysates were precleared by ultrasonication and cell debris were pelleted by centrifugation at 16,100 ***g*** for 10 min. The supernatant was separated and kept with kit components at room temperature for 10 min. 50 µl of serially diluted standard or samples were added in pre-coated wells provided in the kit followed by incubation and wash steps according to the manufacturer's instructions. The absorbance was measured at 450 nm using Varioskan flash (ThermoFisher) and readouts from standard were plotted to construct a standard curve for estimating THF concentration.

SAM levels were determined by Bridge-It assay kit (Mediomics) based on biosensor fluorescence. Dissected E12.5 head samples were suspended in 100 µl of supplied CM buffer solution supplemented with protease inhibitors followed by mechanical dissociation with a pipette tip for cell lysis and incubated at room temperature for 30 min. Cell debris were pelleted by centrifugation at 16,100 ***g*** for 10 min and supernatant was separated. In a black 96-well microplate (ThermoFisher), 10 µl of standard mix (1 mM SAM) was serially diluted with Buffer S provided in the kit. 10 µl of standard mix and 50 µl of samples were then incubated with supplied assay solution at a total volume of 100 µl at room temperature for 30 min in dark. The signal intensity of fluorescence excited at 485 nm for 1 s was measured at 665 nm using Varioskan flash. The readouts from standard were plotted to construct a standard curve for estimating SAM concentration.

Quantifications and statistical analyses

Fluorescent images were captured with SP8 inverted scanning confocal microscope (Leica Biosystems) or Eclipse 80i fluorescence microscope (Nikon). The microscopic and macroscopic images were acquired with Eclipse TS100 inverted microscope (Nikon) and SMZ18 stereomicroscope (Nikon), respectively. Images were exported as TIFF files and quantification was performed manually with ImageJ (NIH) on defined regions of interest (ROIs). For mouse embryos, one ROI was counted at E12.5 and E14.5, and two ROIs were counted at E16.5 (positioning of ROI at each stage is shown in main figures). Embryos were collected from different litters and 100-500 cells were counted per hemisphere using multiple sections. Counts were normalized to an area of 100 µm of apical surface×100 µm of radial length. For organoids, quantifications were performed on cortical-like structures that were selected based on morphometric parameters (structures located at the periphery of the organoids, presence of a lumen, elongated shape of pseudostratified nuclei and a densely packed ventricular zone at least five nuclei thick). We confirmed that these morphometric parameters identified cortical-like structures by performing EMX1 immunostaining (Fig. S5C). One ROI was counted for each cortical-like structure, 100-500 cells were counted on different cortical-like structures from different HNOs and quantifications were expressed as percentage (using DAPI to count total cell number). For western blots, tissue lysates were collected from four mouse embryos for each genotype and the western blots were carried out twice with independent samples. For metabolic assays, tissue extracts were obtained from at least four to seven mouse embryos for each genotype. The exact number of samples for each experiment is provided in each graph and in Table S2. For experiments involving a pair of conditions, statistical significance between the two sets of data were analyzed with Mann–Whitney test with Holm-Šidák adjusted *P*-values using Prism9 (GraphPad). Statistically significant differences are reported at $*P<0.05$, $**P<0.01$ and $***P<0.001$.

Acknowledgements

We thank Alain Vincent and Eric Agius for critical reading of the manuscript. We acknowledge the help and contribution of the ANEXPLO mouse facility and the TRI imaging platform at the CBI. We also thank the CBI-bigA facility engineers for their help and feedback during the raw data processing, the statistical analysis and the data visualization of sequencing data. Sequencing for the ChIP-Seq analysis was performed by the GenomEast platform, which is a member of the 'France Génomique' consortium (ANR-10-INBS-0009). Both CNRS and Université de Toulouse provided core funding.

Competing interests

The authors declare no competing or financial interests.

Author contributions

Conceptualization: S.S., T.J., M.F., A.D.; Methodology: S.S., T.J., C.A., T.Y., M.F.; Software: D.O., T.Y.; Validation: S.S., T.J., M.F., A.D.; Formal analysis: S.S., T.J., D.O., C.A., T.Y., M.F., A.D.; Investigation: S.S., T.Y., M.F.; Resources: T.J., A.D.; Data curation: S.S., T.J., D.O., C.A., T.Y., M.F., A.D.; Writing - original draft: S.S., A.D.; Writing - review & editing: T.J., D.O., C.A., M.F., A.D.; Visualization: D.O., C.A., M.F.; Supervision: T.J., A.D.; Project administration: T.J., M.F., A.D.; Funding acquisition: A.D.

Funding

This work was funded by the Fondation pour la Recherche Médicale (DEQ20180339174) and the Agence Nationale de la Recherche (ANR-21-CE16-0024-01). S.S. is the recipient of a 3-year PhD scholarship from the Ministère de l'Enseignement Supérieur et de la Recherche Scientifique. Open Access funding provided by the Agence Nationale de la Recherche. Deposited in PMC for immediate release.

Data availability

RNA-Seq and ChIP-Seq data have been deposited in GEO under accession numbers GSE206406 and GSE206407.

Peer review history

The peer review history is available online at https://journals.biologists.com/dev/lookup/doi/10.1242/dev.201696.reviewer-comments.pdf.

References

Albert, M., Kalebic, N., Florio, M., Lakshmanaperumal, N., Haffner, C., Brandl, H., Henry, I. and Huttner, W. B. (2017). Epigenome profiling and editing of neocortical progenitor cells during development. *EMBO J.* **36**, 2642-2658. doi:10.15252/embj.201796764

Banka, S., Blom, H. J., Walter, J., Aziz, M., Urquhart, J., Clouthier, C. M., Rice, G. I., de Brouwer, A. P. M., Hilton, E., Vassallo, G. et al. (2011). Identification and characterization of an inborn error of metabolism caused by dihydrofolate reductase deficiency. *Am. J. Hum. Genet.* **88**, 216-225. doi:10.1016/j.ajhg.2011.01.004

Cárdenas, A., Villalba, A., De Juan Romero, C., Picó, E., Kyrousi, C., Tzika, A. C., Tessier-Lavigne, M., Ma, L., Drukker, M., Cappello, S. et al. (2018). Evolution of cortical neurogenesis in amniotes controlled by robo signaling levels. *Cell* **174**, 590-606.e21. doi:10.1016/j.cell.2018.06.007

Cario, H., Smith, D. E. C., Blom, H., Blau, N., Bode, H., Holzmann, K., Pannicke, U., Hopfner, K.-P., Rump, E.-M., Ayric, Z. et al. (2011). Dihydrofolate reductase deficiency due to a homozygous DHFR mutation causes megaloblastic anemia and cerebral folate deficiency leading to severe neurologic disease. *Am. J. Hum. Genet.* **88**, 226-231. doi:10.1016/j.ajhg.2011.01.007

Clare, C. E., Brassington, A. H., Kwong, W. Y. and Sinclair, K. D. (2018). One-carbon metabolism: linking nutritional biochemistry to epigenetic programming of long-term development. *Annu. Rev. Anim. Biosci.* **7**, 263-287. doi:10.1146/annurev-animal-020518-115206

Di Bella, D. J., Habibi, E., Stickels, R. R., Scalia, G., Brown, J., Yadollahpour, P., Yang, S. M., Abbate, C., Biancalani, T., Macosko, E. Z. et al. (2021). Molecular logic of cellular diversification in the mouse cerebral cortex. *Nature* **595**, 554-559. doi:10.1038/s41586-021-03670-5

Ducker, G. S. and Rabinowitz, J. D. (2017). One-carbon metabolism in health and disease. *Cell Metab.* **25**, 27-42. doi:10.1016/j.cmet.2016.08.009

Eze, U. C., Bhaduri, A., Haeussler, M., Nowakowski, T. J. and Kriegstein, A. R. (2021). Single-cell atlas of early human brain development highlights heterogeneity of human neuroepithelial cells and early radial glia. *Nat. Neurosci.* **24**, 584-594. doi:10.1038/s41593-020-00794-1

Fan, X., Fu, Y., Zhou, X., Sun, L., Yang, M., Wang, M., Chen, R., Wu, Q., Yong, J., Dong, J. et al. (2020). Single-cell transcriptome analysis reveals cell lineage specification in temporal-spatial patterns in human cortical development. *Sci. Adv.* **6**, eaaz2978. doi:10.1126/sciadv.aaz2978

Fawal, M.-A., Jungas, T., Kischel, A., Audouard, C., Iacovoni, J. S. and Davy, A. (2018). Cross talk between one-carbon metabolism, Eph signaling, and histone methylation promotes neural stem cell differentiation. *Cell Rep.* **23**, 2864-2873.e7. doi:10.1016/j.celrep.2018.05.005

Fawal, M.-A., Jungas, T. and Davy, A. (2021). Inhibition of DHFR targets the self-renewing potential of brain tumor initiating cells. *Cancer Lett.* **503**, 129-137. doi:10.1016/j.canlet.2021.01.026

Feder, J. N., Assaraf, Y. G., Seamer, L. C. and Schimke, R. T. (1989). The pattern of dihydrofolate reductase expression through the cell cycle in rodent and human cultured cells. *J. Biol. Chem.* **264**, 20583-20590. doi:10.1016/S0021-9258(19)47102-0

Feng, J., Liu, T., Qin, B., Zhang, Y. and Liu, X. S. (2012). Identifying ChIP-seq enrichment using MACS. *Nat. Protoc.* **7**, 1728-1740. doi:10.1038/nprot.2012.101

Götz, M., Stoykova, A. and Gruss, P. (1998). Pax6 controls radial glia differentiation in the cerebral cortex. *Neuron* **21**, 1031-1044. doi:10.1016/S0896-6273(00)80621-2

Hansen, D. V., Lui, J. H., Parker, P. R. L. and Kriegstein, A. R. (2010). Neurogenic radial glia in the outer subventricular zone of human neocortex. *Nature* **464**, 554-561. doi:10.1038/nature08845

Harlan De Crescenzo, A., Panoutsopoulos, A. A., Tat, L., Schaaf, Z., Racherla, S., Henderson, L., Leung, K.-Y., Greene, N. D. E., Green, R. and Zarbalis, K. S. (2021). Deficient or excess folic acid supply during pregnancy alter cortical neurodevelopment in mouse offspring. *Cereb. Cortex* **31**, 635-649. doi:10.1093/cercor/bhaa248

Haubensak, W., Attardo, A., Denk, W. and Huttner, W. B. (2004). Neurons arise in the basal neuroepithelium of the early mammalian telencephalon: a major site of neurogenesis. *Proc. Natl. Acad. Sci. USA* **101**, 3196-3201. doi:10.1073/pnas.0308600100

Hirabayashi, Y. and Gotoh, Y. (2010). Epigenetic control of neural precursor cell fate during development. *Nat. Rev. Neurosci.* **11**, 377-388. doi:10.1038/nrn2810

Huilgol, D., Levine, J. M., Galbavy, W., Wang, B.-S., He, M., Suryanarayana, S. M. and Huang, Z. J. (2023). Direct and indirect neurogenesis generate a mosaic of distinct glutamatergic projection neuron types in cerebral cortex. *Neuron*. doi:10.1016/j.neuron.2023.05.021

Johnson, A. F., Nguyen, H. T. and Veitia, R. A. (2019). Causes and effects of haploinsufficiency. *Biol. Rev. Camb. Philos. Soc.* **94**, 1774-1785. doi:10.1111/brv.12527

Kanton, S., Boyle, M. J., He, Z., Santel, M., Weigert, A., Sanchís-Calleja, F., Guijarro, P., Sidow, L., Fleck, J. S., Han, D. et al. (2019). Organoid single-cell genomic atlas uncovers human-specific features of brain development. *Nature* **574**, 418-422. doi:10.1038/s41586-019-1654-9

Kawaguchi, A., Ikawa, T., Kasukawa, T., Ueda, H. R., Kurimoto, K., Saitou, M. and Matsuzaki, F. (2008). Single-cell gene profiling defines differential progenitor subclasses in mammalian neurogenesis. *Development* **135**, 3113-3124. doi:10.1242/dev.022616

Klingler, E., Francis, F., Jabaudon, D. and Cappello, S. (2021). Mapping the molecular and cellular complexity of cortical malformations. *Science* **371**, eaba4517. doi:10.1126/science.aba4517

Koo, B., Lee, K.-H., Ming, G.-L., Yoon, K.-J. and Song, H. (2022). Setting the clock of neural progenitor cells during mammalian corticogenesis. *Semin. Cell Dev. Biol.* **142**, 43-53. doi:10.1016/j.semcdb.2022.05.013

Lancaster, M. A. and Knoblich, J. A. (2014). Generation of cerebral organoids from human pluripotent stem cells. *Nat. Protoc.* **9**, 2329-2340. doi:10.1038/nprot.2014.158

Langmead, B., Trapnell, C., Pop, M. and Salzberg, S. L. (2009). Ultrafast and memory-efficient alignment of short DNA sequences to the human genome. *Genome Biol.* **10**, R25. doi:10.1186/gb-2009-10-3-r25

Lewitus, E., Kelava, I., Kalinka, A. T., Tomancak, P. and Huttner, W. B. (2014). An adaptive threshold in mammalian neocortical evolution. *PLoS Biol.* **12**, e1002000. doi:10.1371/journal.pbio.1002000

Liu, J., Wu, X., Zhang, H., Pfeifer, G. P. and Lu, Q. (2017). Dynamics of RNA Polymerase II Pausing and Bivalent Histone H3 Methylation during Neuronal Differentiation in Brain Development. *Cell Rep.* **20**, 1307-1318. doi:10.1016/j.celrep.2017.07.046

Love, M. I., Huber, W. and Anders, S. (2014). Moderated estimation of fold change and dispersion for RNA-seq data with DESeq2. *Genome Biol.* **15**, 550. doi:10.1186/s13059-014-0550-8

Lui, J. H., Hansen, D. V. and Kriegstein, A. R. (2011). Development and evolution of the human neocortex. *Cell* **146**, 18-36. doi:10.1016/j.cell.2011.06.030

Mentch, S. J., Mehrmohamadi, M., Huang, L., Liu, X., Gupta, D., Mattocks, D., Gómez Padilla, P., Ables, G., Bamman, M. M., Thalacker-Mercer, A. E. et al. (2015). Histone methylation dynamics and gene regulation occur through the sensing of one-carbon metabolism. *Cell Metab.* **22**, 861-873. doi:10.1016/j.cmet.2015.08.024

Miyata, T., Kawaguchi, A., Saito, K., Kawano, M., Muto, T. and Ogawa, M. (2004). Asymmetric production of surface-dividing and non-surface-dividing cortical progenitor cells. *Development* **131**, 3133-3145. doi:10.1242/dev.01173

Molyneaux, B. J., Arlotta, P., Menezes, J. R. L. and Macklis, J. D. (2007). Neuronal subtype specification in the cerebral cortex. *Nat. Rev. Neurosci.* **8**, 427-437. doi:10.1038/nrn2151

Namba, T. and Huttner, W. B. (2017). Neural progenitor cells and their role in the development and evolutionary expansion of the neocortex. *Wiley Interdiscip. Rev. Dev. Biol.* **6**, e256. doi:10.1002/wdev.256

Namba, T., Nardelli, J., Gressens, P. and Huttner, W. B. (2021). Metabolic regulation of neocortical expansion in development and evolution. *Neuron* **109**, 408-419. doi:10.1016/j.neuron.2020.11.014

Noctor, S. C., Flint, A. C., Weissman, T. A., Dammerman, R. S. and Kriegstein, A. R. (2001). Neurons derived from radial glial cells establish radial units in neocortex. *Nature* **409**, 714-720. doi:10.1038/35055553

Noctor, S. C., Martínez-Cerdeño, V., Ivic, L. and Kriegstein, A. R. (2004). Cortical neurons arise in symmetric and asymmetric division zones and migrate through specific phases. *Nat. Neurosci.* **7**, 136-144. doi:10.1038/nn1172

Paşca, S. P., Arlotta, P., Bateup, H. S., Camp, J. G., Cappello, S., Gage, F. H., Knoblich, J. A., Kriegstein, A. R., Lancaster, M. A., Ming, G.-L. et al. (2022). A nomenclature consensus for nervous system organoids and assembloids. *Nature* **609**, 907-910. doi:10.1038/s41586-022-05219-6

Pebworth, M.-P., Ross, J., Andrews, M., Bhaduri, A. and Kriegstein, A. R. (2021). Human intermediate progenitor diversity during cortical development. *Proc. Natl. Acad. Sci. USA* **118**, e2019415118. doi:10.1073/pnas.2019415118

Quinlan, A. R. and Hall, I. M. (2010). BEDTools: a flexible suite of utilities for comparing genomic features. *Bioinformatics* **26**, 841-842. doi:10.1093/bioinformatics/btq033

Rakic, P. (1972). Mode of cell migration to the superficial layers of fetal monkey neocortex. *J. Comp. Neurol.* **145**, 61-83. doi:10.1002/cne.901450105

Roussat, M., Jungas, T., Audouard, C., Omerani, S., Medevielle, F., Agius, E., Davy, A., Pituello, F. and Bel-Vialar, S. (2023). Control of G2 phase duration by CDC25B modulates the switch from direct to indirect neurogenesis in the neocortex. *J. Neurosci. Off. J. Soc. Neurosci.* **43**, 1154-1165. doi:10.1523/JNEUROSCI.0825-22.2022

Serrano, M., Pérez-Dueñas, B., Montoya, J., Ormazabal, A. and Artuch, R. (2012). Genetic causes of cerebral folate deficiency: clinical, biochemical and therapeutic aspects. *Drug Discov. Today* **17**, 1299-1306. doi:10.1016/j.drudis.2012.07.008

Sessa, A., Mao, C. A., Hadjantonakis, A.-K., Klein, W. H. and Broccoli, V. (2008). Tbr2 directs conversion of radial glia into basal precursors and guides neuronal amplification by indirect neurogenesis in the developing neocortex. *Neuron* **60**, 56-69. doi:10.1016/j.neuron.2008.09.028

Shiraki, N., Shiraki, Y., Tsuyama, T., Obata, F., Miura, M., Nagae, G., Aburatani, H., Kume, K., Endo, F. and Kume, S. (2014). Methionine metabolism regulates maintenance and differentiation of human pluripotent stem cells. *Cell Metab.* **19**, 780-794. doi:10.1016/j.cmet.2014.03.017

Shyh-Chang, N., Locasale, J. W., Lyssiotis, C. A., Zheng, Y., Teo, R. Y., Ratanasirintrawoot, S., Zhang, J., Onder, T., Unternaehrer, J. J., Zhu, H. et al. (2013). Influence of threonine metabolism on S-adenosylmethionine and histone methylation. *Science* **339**, 222-226. doi:10.1126/science.1226603

Telley, L., Agirman, G., Prados, J., Amberg, N., Fièvre, S., Oberst, P., Bartolini, G., Vitali, I., Cadilhac, C., Hippenmeyer, S. et al. (2019). Temporal patterning of apical progenitors and their daughter neurons in the developing neocortex. *Science* **364**, eaav2522. doi:10.1126/science.aav2522

Thoms, J. A. I., Knezevic, K., Liu, J. J., Glaros, E. N., Thai, T., Qiao, Q., Campbell, H., Packham, D., Huang, Y., Papathanasiou, P. et al. (2016). Arrested hematopoiesis and vascular relaxation defects in mice with a mutation in Dhfr. *Mol. Cell. Biol.* **36**, 1222-1236. doi:10.1128/MCB.01035-15

Trevino, A. E., Müller, F., Andersen, J., Sundaram, L., Kathiria, A., Shcherbina, A., Farh, K., Chang, H. Y., Paşca, A. M., Kundaje, A. et al. (2021). Chromatin and gene-regulatory dynamics of the developing human cerebral cortex at single-cell resolution. *Cell* **184**, 5053-5069.e23. doi:10.1016/j.cell.2021.07.039

Van Galen, P., Viny, A. D., Ram, O., Ryan, R. J. H., Cotton, M. J., Donohue, L., Sievers, C., Drier, Y., Liau, B. B., Gillespie, S. M. et al. (2016). A multiplexed system for quantitative comparisons of chromatin landscapes. *Mol. Cell* **61**, 170-180. doi:10.1016/j.molcel.2015.11.003

Vasistha, N. A., Garcia-Moreno, F., Arora, S., Cheung, A. F. P., Arnold, S. J., Robertson, E. J. and Molnar, Z. (2015). Cortical and clonal contribution of Tbr2 expressing progenitors in the developing mouse brain. *Cereb. Cortex* **25**, 3290-3302. doi:10.1093/cercor/bhu125

Villalba, A., Götz, M. and Borrell, V. (2021). Chapter One - The regulation of cortical neurogenesis. In *Current Topics in Developmental Biology* (ed. G. J. Bashaw), pp. 1-66. Academic Press.

Visel, A., Thaller, C. and Eichele, G. (2004). GenePaint.org: an atlas of gene expression patterns in the mouse embryo. *Nucleic Acids Res.* **32**, D552-D556. doi:10.1093/nar/gkh029

Zhang, Y., Liu, T., Meyer, C. A., Eeckhoute, J., Johnson, D. S., Bernstein, B. E., Nusbaum, C., Myers, R. M., Brown, M., Li, W. et al. (2008). Model-based analysis of ChIP-Seq (MACS). *Genome Biol.* **9**, R137. doi:10.1186/gb-2008-9-9-r137

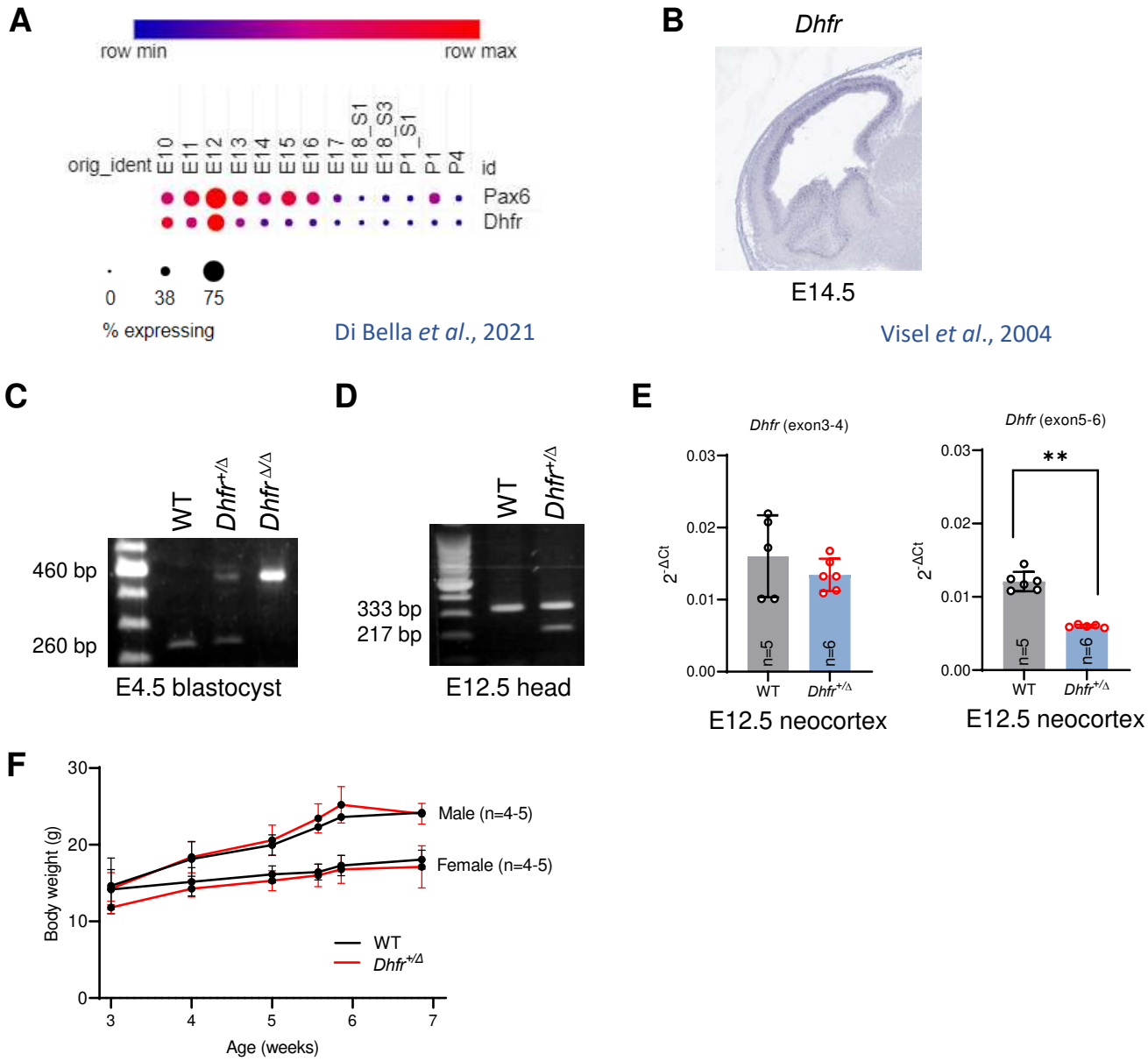

Fig. S1. *Dhfr* expression in wild type and mutant mice

(A) *Dhfr* mRNA expression in the developing mouse neocortex (data collected from https://singlecell.broadinstitute.org/single_cell/study/SCP1290/molecular-logic-of-cellular-diversification-in-the-mammalian-cerebral-cortex). Abbreviations: E, embryonic day; P, postnatal day.

(B) *In situ* hybridization of *Dhfr*, mainly located in the ventricular zone of E14.5 neocortex (data collected from GenePaint set ID: EH608, https://gp3.mpg.de/).

(C) Representative genotyping results of WT (*Dhfr*$^{+/+}$), *Dhfr*$^{+/\Delta}$ and *Dhfr*$^{\Delta/\Delta}$ E4.5 embryos. The 260 bp band corresponds to the wild type allele and the 460 bp band corresponds to the edited allele.

(D) RT-PCR on mRNA extracted from WT and *Dhfr*$^{+/\Delta}$ E12.5 embryos was used to detect expression of the wild type and edited alleles of *Dhfr*.

(E) qRT-PCR analysis of *Dhfr* expression. Two sets of primers were used to amplify either exon3-4 (not sensitive to the excision, amplification from the two alleles) or exon5-6 (sensitive to the excision, amplification from the wild type allele only).

(F) Measurement of body weight of WT and *Dhfr*$^{+/\Delta}$ pups from weaning to adult stage.

Data are reported as mean ± SD and statistical analysis was performed using Mann-Whitney test.

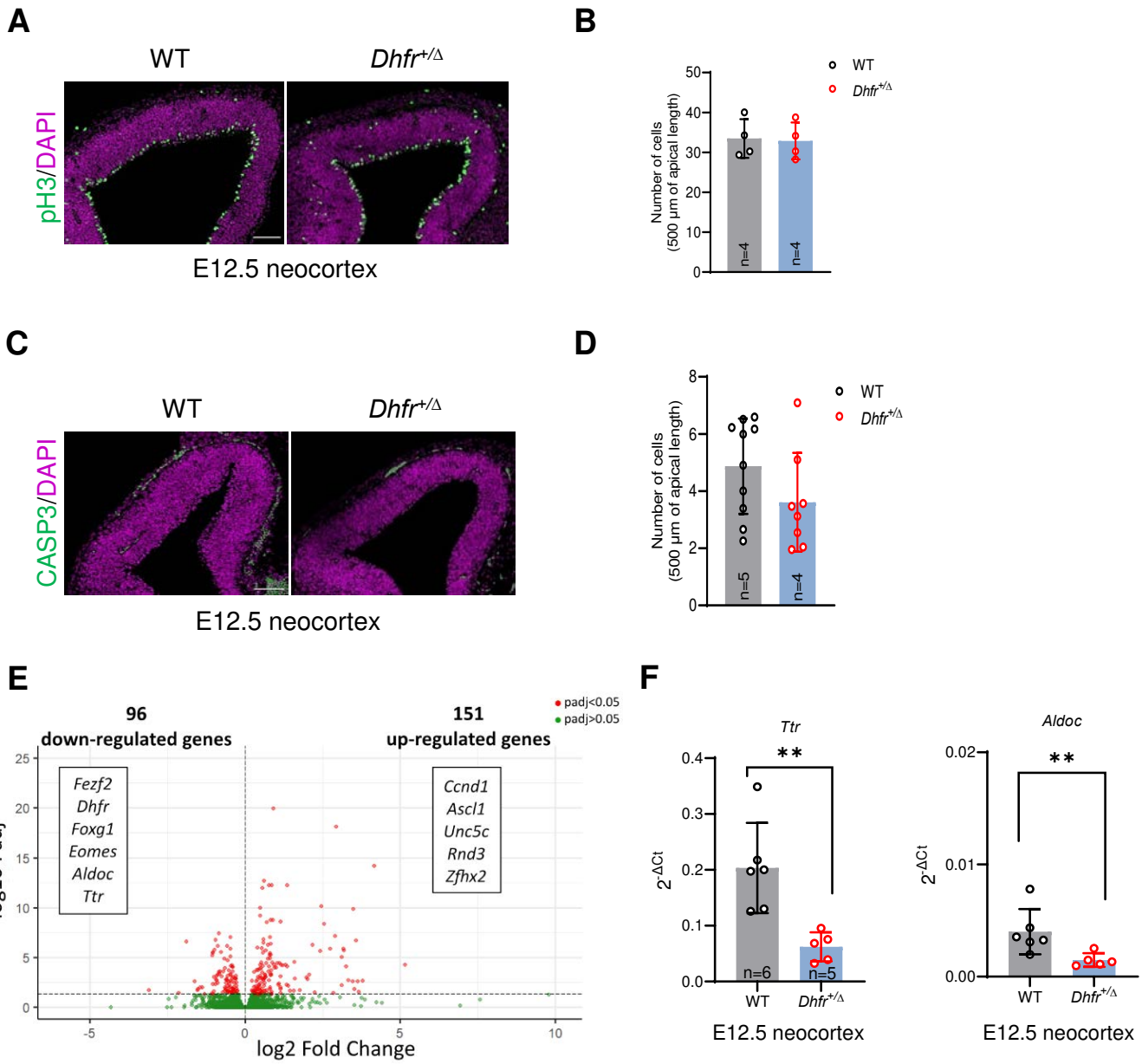

Fig. S2. Developmental phenotypes in E12.5 *Dhfr* deficient embryos

(A, B) Representative images and quantification of neocortex coronal sections of E12.5 WT and *Dhfr*$^{+/\Delta}$ embryos immunostained for phospho-Histone H3 (pH3). Scale bars, 100 µm.

(C, D) Representative images and quantification of neocortex coronal sections of E12.5 WT and *Dhfr*$^{+/\Delta}$ embryos immunostained for cleaved Caspase-3 (CASP3). Scale bars, 100 µm.

(E) Numbers of genes significantly up-regulated and down-regulated at E12.5 in *Dhfr*$^{+/\Delta}$ are indicated in red dots.

(F) qRT-PCR analysis of selected genes.

Data are reported as mean ± SD and statistical analysis was performed using Mann-Whitney test.

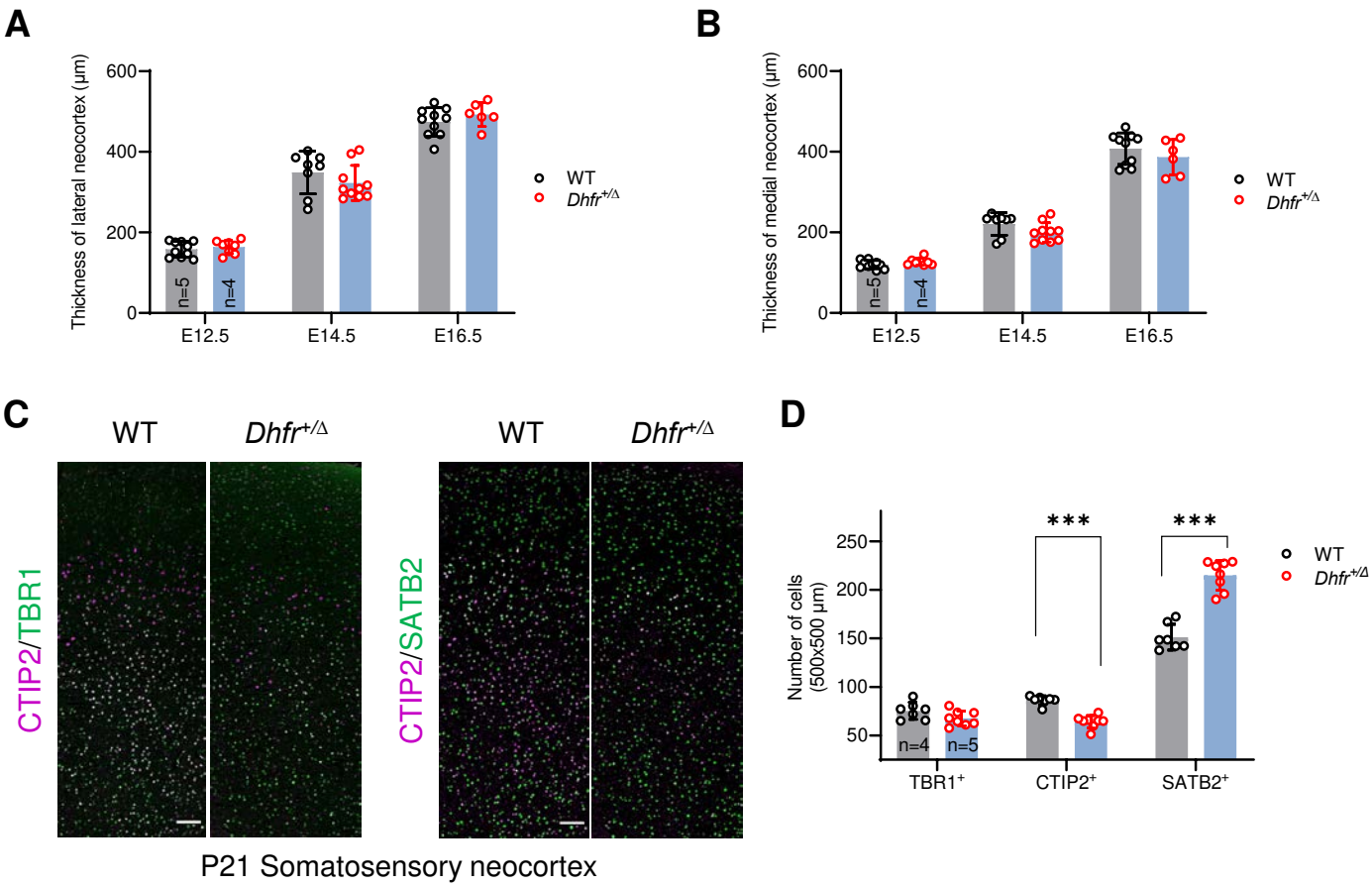

Fig. S3. DHFR deficiency does not modify neocortical thickness but irreversibly alters mouse neocortical composition

(A, B) Measurement of relative neocortical thickness at medial and lateral positions.

(C, D) Representative images and quantification of neocortex coronal sections of somatosensory cortex of P21 WT and *Dhfr*$^{+/\Delta}$ pups immunostained for TBR1, CTIP2 and SATB2. Scale bars, 100 µm.

Data are presented as mean ± SD and statistical analysis was performed using Mann-Whitney test.

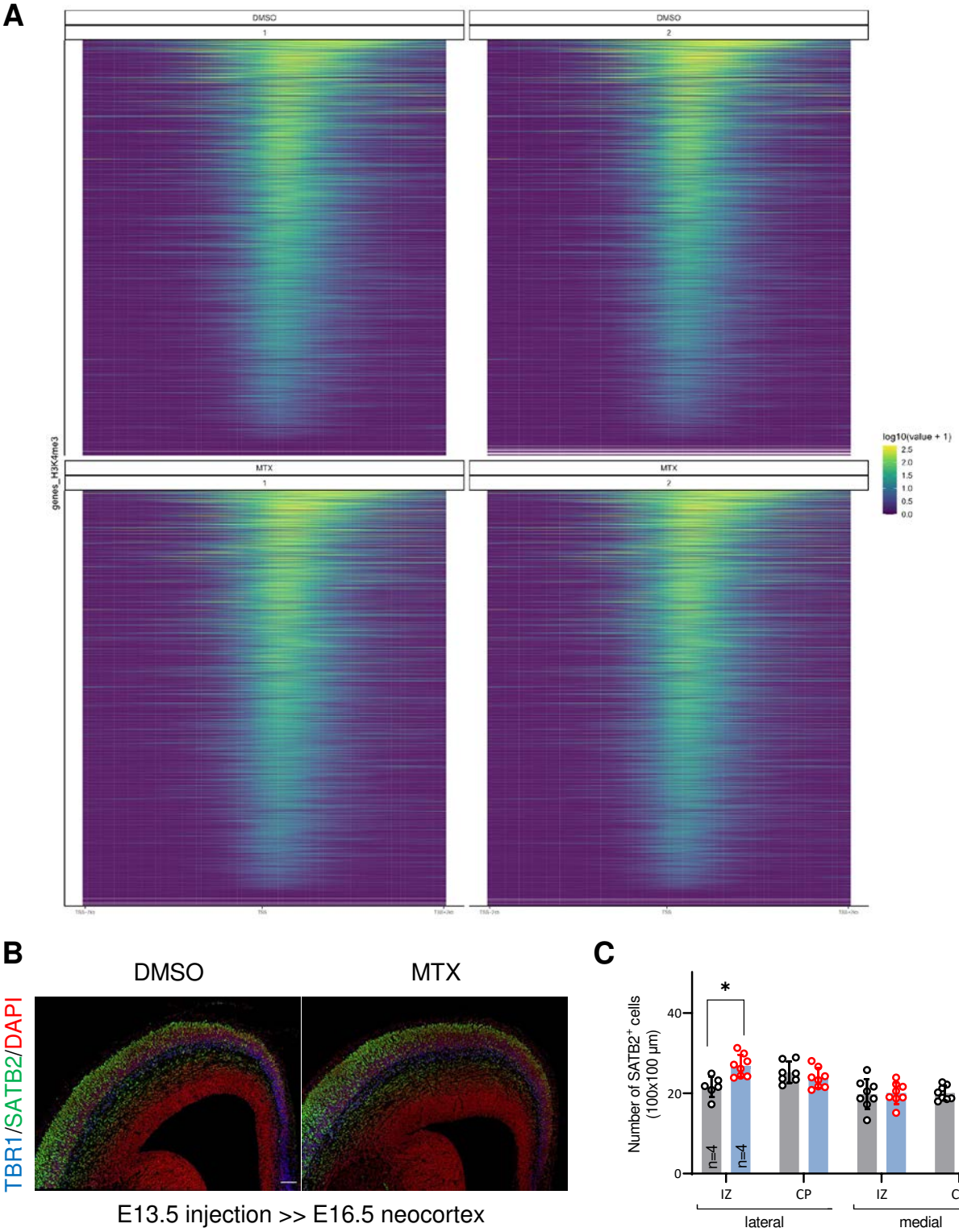

Fig. S4. No global alterations of H3K4me3 binding but modification of neocortex neuronal composition following MTX treatment in mouse

(A) Heatmap of global H3K4me3 level (at neural progenitor-specific genes) in neurospheres treated with DMSO (top) and MTX (bottom) (n=2).

(B, C) Representative images of neocortex coronal sections of E16.5 DMSO and MTX (20 µM)-injected WT embryos immunostained for TBR1, SATB2 and DAPI. Scale bars, 100 µm. Quantification of SATB2+ cells in the intermediate zone (IZ) and the cortical plate (CP).

Data are reported as mean ± SD and statistical analysis was performed using Mann-Whitney test.

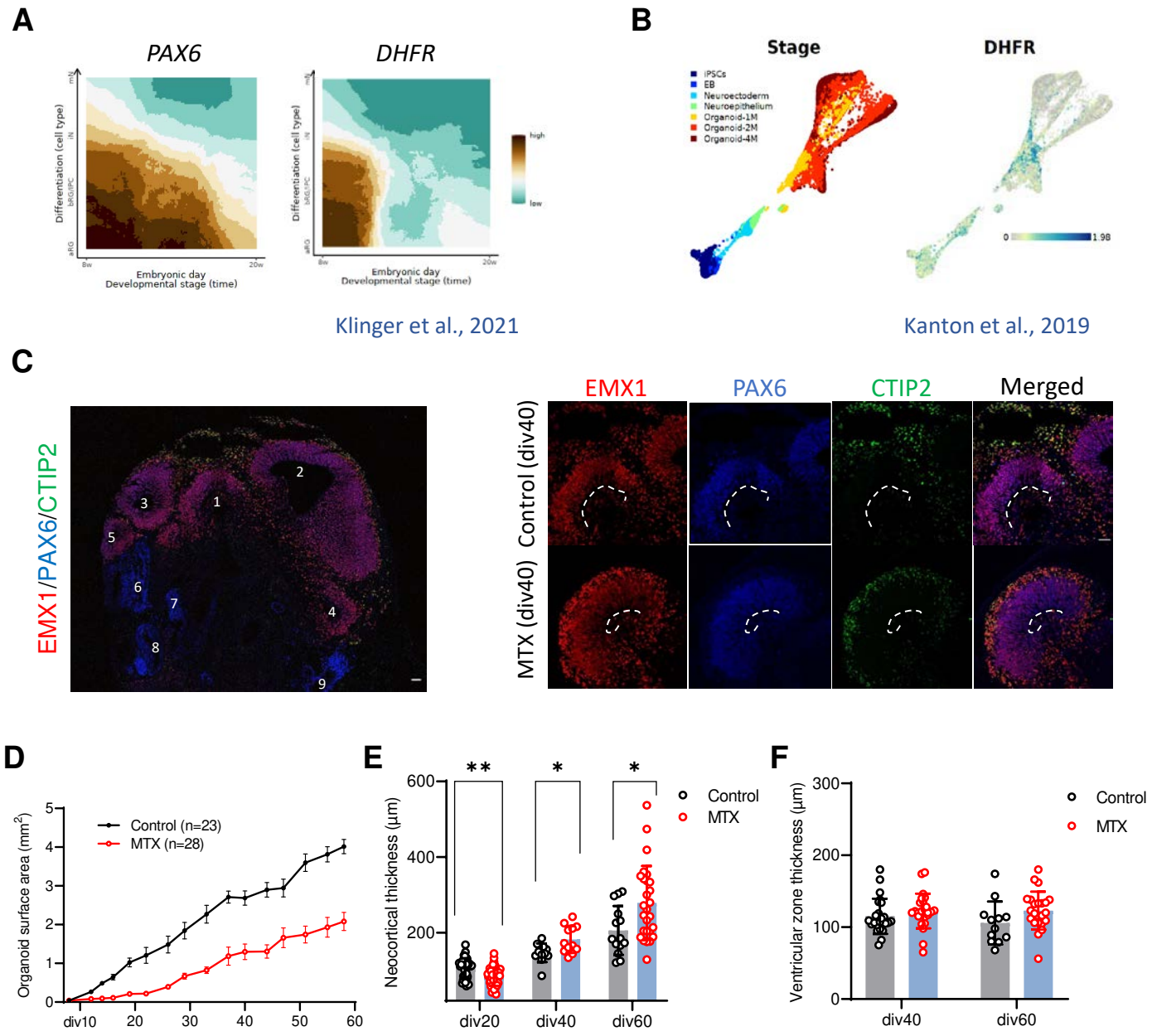

Fig. S5. *DHFR* expression and inhibition in HNO

(A) *DHFR* mRNA expression in the developing human fetal neocortex (data collected from http://www.humous.org).

(B) *DHFR* mRNA expression over the course of HNO development and maturation (data collected from https://bioinf.eva.mpg.de/shiny/sample-apps/scApeX/).

(C) Representative images of div40 HNO immunostained for EMX1, PAX6 and CTIP2. Left: low resolution image showing cortical-like structures (number 1-5) that are EMX1+ and non cortical-like structures (number 6-9) that are EMX1-. Right: High resolution images of EMX1+ cortical structures. Scale bars, 50 µm.

(D) Quantification of the size of control and MTX-treated HNO over time.

(E, F) Measurement of the relative thickness of the neocortex and ventricular zone in control and MTX-treated HNO.

Data are presented as (D) mean ± SEM or (E, F) mean ± SD (n = 7–12 organoids with 15–20 cortical-like structures analyzed with Mann-Whitney test).

Table S1. Marker genes used for ChIP-Seq analyses

Click here to download Table S1

Table S2. Raw data and statistical analyses

Click here to download Table S2

Table S3. List of Reagents

Click here to download Table S3

MATERIALS AND METHODS

ANIMALS

Wild type and *Dhfr*$^{+/\Delta}$ mice were kept in a 129S4/C57Bl6J mixed background. Mice were maintained on a standard 12 hours day:night cycle and given ad libitum access to food and water. Timed pregnancies were obtained by detecting vaginal plugs.

CRISPR/Cas9-mediated *Dhfr* deletion in mice

Using the publicly available design program CRISPOR (http://crispor.tefor.net), we designed 2 CRISPR-Cas9 crRNA targeting intronic sequences flanking *Dhfr* exon5: 5′-GGATTAGCAACTAGGTAATAAGG-3′ and 5′-TCCAAGCTGGCCCCATGTTTGGG-3′. Each crRNA was complexed with tracrRNA to generate gRNA and Cas9-ribonucleoprotein complexes (Integrated DNA Technologies), which were microinjected in 129S4/C57Bl6J 1-cell embryos. Injected embryos were re-implanted in pseudo-pregnant dams and a heterozygote founder progeny was identified with a 844 bp deletion corresponding to *Dhfr* exon5 by DNA sequencing (primer Fw: 5′-GTGATTCCATAGCCTCTTCCAG-3′, Rev: 5′-TAGCACACATGCTCCTTTCC-3′). We tested 4 predictive off-target site and designed primers to amplify the corresponding regions. By sequencing, we eliminated the likelihood of indel formation in the 4 off-target sites analyzed. All genome editing experimental procedures were pre-approved and carried out in compliance with the guidelines provided by the national Animal Care and Ethics Committee (APAFIS #11931 2017102511049339) following Directive 2010/63/EU.

Histochemistry

Mouse brains at stages E14.5 and older were collected and fixed with 4% Paraformaldehyde overnight at 4°C followed by paraffin embedding with Spin tissue processor (Myr) for 5 µm coronal sections on Microtome (Microm). Due to their small size, embryos at E12.5 were embedded in agarose for 60 µm coronal sections on Vibratome (Leica Biosystems). Paraffin-embedded sections were deparaffined, rehydrated, followed by antigen retrieval involving steam heating for 45 minutes. Coronal sections were permeabilized and incubated in blocking solution (1-3% BSA, 1-3% FBS, 0.5-1% Tween 20 and PBS) for 2 hours at room temperature.

HNO were collected and fixed with 4% Paraformaldehyde overnight at 4°C and transferred to 30% Sucrose solution at 4°C. After sinking, HNO were embedded in OCT (Sakura) in plastic mold and stored at -80°C until serial 15 µm thickness sectioning was performed using Cryostat (Leica Biosystems). Sections were incubated in blocking solution (1% BSA, 1% FBS, 0.5% Tween 20 and PBS) for 30 minutes at room temperature.

Mounted sections on Superfrost plus slides (Thermoscientific) were covered with blocking solution containing primary antibodies mix (Table S1) for an overnight at 4°C in wet atmosphere. After 3 washes for 5 minutes in PBS, sections were covered with blocking solution containing secondary antibodies (Table S1) and DAPI mix for 2 hours at room temperature, washed again 3 times in PBS and mounted with coverslips (Menzel-Gläser) and mounting medium (4.8% wt/vol Mowiol and 12% wt/vol Glycerol in 50 mM Tris [pH 8.5]).

ChIP-sequencing

E13.5 neocortical tissues were dissociated mechanically in PBS. The single-cell suspension was collected in growing medium (DMEM/F12 medium containing 0.6% Glucose, 5 mM HEPES, 1 mM Putrescine, 5 ng/ml FGF-2, 20 ng/ml EGF, 10 ng/ml Insulin-transferrin-sodium selenite supplement and 2% B27 supplement in 5% CO_2 incubator at 37°C. Neural progenitor cells were then cultured as free-floating neurospheres, which were treated with DMSO or 2 µM MTX for 72 hours. The cells were further processed for DNA extraction according to the previously described method (Fawal et al., 2018).

RT-PCR and qRT-PCR

Genomic DNA was degraded with 1 µl DNase (Promega) for 20 minutes at 37°C in 20 µl Nuclease-free water, and the reaction was stopped by adding 1 µl of Stop solution under heat inactivation at 65°C for 10 minutes. 2 µl of 10 mM dNTPs (Promega) and 2 µl of 100 mM OligodTs (Integrated DNA Technologies) were added for 5 minutes at 65°C, then 8 µl of 5x buffer, 2 µl RNasin (Roche), and 4 µl of 100 mM DTT (Promega) were added for 2 minutes at 42°C. The mix was divided into equal volumes in a RT–negative control tube with addition of 1 µl Nuclease-free water and in a RT–positive tube with 1 µl Superscript enzyme and placed at 42°C for 1 hour. The reaction was stopped at 70°C for 15 minutes, and cDNAs were synthesized.

For RT-PCR, 1 µl diluted cDNA (10-fold) was mixed with 2x PCR Taq MasterMix containing 1 µM of each primer, and PCR amplification was performed followed by agarose gel electrophoresis.

mRNA relative expression levels were calculated using the $2^{-\Delta Cts}$ method with specific primers (*Dhfr* exon3-4 Fw: 5'-CCATTCCTGAGAAGAATCGACC-3' and Rev: 5'-CTTTACTTGCCAATTCCGGTTG-3', *Dhfr* exon5-6 Fw: 5'-CAGGCCACCTCAGACTCTTT-3' and Rev: 5'-CCTTTTTCCTCCTGGACCTC-3', *Ttr* Fw: 5'-CACCAAATCGTACTGGAAGACA-3' and Rev: 5'-GTCGTTGGCTGTGAAAACCAC-3', *Aldoc* Fw: 5'-ACCATGACCTCAAACGTTGC-3' and Rev: 5'-TTGAGCAGAGTCCCTTCGAG-3', *Gapdh* as reference gene Fw: 5'-GGCCTTCCGTGTTCCTAC-3' and Rev: 5'-CTGTTGCTGTAGCCGTATTCA-3').

Manuscript 2 (in preparation): Acute dietary methionine restriction highlights sensitivity of neocortex development to metabolic variations

Aims: Exposing developing embryos to dietary methionine restriction (MR) to target the neurogenic phases of neocortex development for 5 or 10 days, we compared brain growth with other vital organs, including the liver and heart during gestation.

Rationale: Methionine and its metabolite SAM are essential for cell proliferation, stem cell maintenance and epigenetic regulation, three processes that are central to embryonic development. While MR serves beneficial effects in adults, MR during gestation could have detrimental consequences on the development.

Main results:

1) Dietary MR for 10 days leads to IUGR with a disproportionally small brain (microcephaly).
2) Reduction in neocortex growth is already detected after 5 days of dietary MR.
3) Growth of the liver and heart is unaffected which is also reflected at the molecular level (levels of methionine, DNA methylation and polysome profiling).
4) Neocortex growth reduction induced after 5 days of dietary MR, which correlates with reduced neuron numbers, is completely compensated at birth by switching back to control diet for 5 days.

Acute dietary methionine restriction highlights sensitivity of neocortex development to metabolic variations

INTRODUCTION

Methionine, an essential amino acid in mammals, is required for a number of key cellular functions, including translation, proliferation and epigenetic regulation. As a consequence, the responses to methionine restriction (MR) are pleiotropic but converge on an evolutionary conserved lifespan extension (Ables & Johnson, 2017). At the cellular level, MR leads to cell cycle arrest in proliferating cells (Lauinger & Kaiser, 2021) while in pluripotent stem cells, it promotes differentiation (Shiraki et al., 2014). In fact, several studies have shown that methionine metabolism controls pluripotency and stem cell self-renewal, by sustaining histone methylation (Ozawa et al., 2023; Shiraki et al., 2014; Tang et al., 2017; Zhu et al., 2020). The latter is explained by the fact that the first metabolite produced by 1C metabolic conversion of methionine is the universal methyl donor S-Adenosyl methionine (SAM), which directly links methionine levels to epigenetic regulation (Mentch et al., 2015). The methyl donor SAM is also involved in triggering MR-induced cell cycle arrest (Lin et al., 2014).

Methionine and its metabolite SAM are thus essential for cell proliferation, stem cell maintenance and epigenetic regulation, three processes that are central to embryonic development (Korsmo & Jiang, 2021). However, while the beneficial effects of MR in adults is well documented (Ables & Johnson, 2017), the consequences of MR during specific phases of embryonic or fetal development have not been extensively studied. Previous studies reported that dietary restriction of methyl donors (by restriction of choline, folate and methionine in the diet) for several weeks prior and during gestation led to reduced fetal growth at birth and had consequences on the behavior of adult rat offspring (Konycheva et al., 2011). More recently, we showed that decreasing levels of SAM in a genetically engineered mouse line (*DHFR* heterozygote) had no effect on fetal growth but altered neuronal production in the developing neocortex (Saha et al., 2023). Both studies point to a role for methionine and SAM in neocortex development, and indicate that MR could have detrimental consequences on the development or growth of this organ. However, both studies involve chronic restriction of methyl donors (either dietary or genetic) which could lead to metabolic reprogramming in the pre-pregnancy and pregnant dams and confuse the effect on the progeny. Thus, to more directly study the

impact of MR on neocortex development, we applied short-term dietary intervention of MR at critical windows of accelerated organogenesis during gestation.

Development of the neocortex is a stepwise process that begins with closure of the anterior neural plate and formation of the telencephalon. At this stage, around E9 (9 days postfertilization), the dorsal telencephalic wall is composed of pseudostratified neuroepithelial cells that quickly give rise to neural progenitors called apical radial glial cells (aRGC) (Rakic, 1972). Around E10.5, aRGC start to divide asymmetrically thus self-renewing and producing neurons by direct differentiation. From this stage on, direct differentiation of aRGC into neurons is progressively replaced by production of intermediate progenitors that subsequently give rise to neurons (Götz et al., 1998; Sessa et al., 2008). There are thus two broad types of progenitors in the developing cortex, aRGC that express the transcription factor PAX6 and intermediate progenitors that express the transcription factor TBR2. Collectively, these progenitors give rise to two broad categories of neurons, early born neurons that express the transcription factor CTIP2 and late born neurons (which start to be produced at E14.5) expressing the DNA binding protein SATB2. Proliferation, self-renewal/differentiation and epigenetic remodeling must be coordinated throughout this developmental process to ensure proper neuronal production both in term of number and subtypes (Hippenmeyer, 2023). Here, we designed a dietary MR regime to target the neurogenic phases of neocortex development (after E9.5), either for 5 days or for 10 days, and analyzed neocortex growth as well as neuronal production. In addition, we set out to compare brain growth with other vital organs, including the liver and heart during gestation.

Our results indicate that dietary MR for 10 days leads to intrauterine growth restriction (IUGR) with a disproportionally small brain (microcephaly). Reduction in neocortex growth is already detected after 5 days of dietary MR, revealing an extremely fast adaptation of this tissue to metabolic conditions. Further, growth of the liver and heart is unaffected highlighting an organ-specific response to MR which is also detected at the molecular level (levels of methionine, DNA methylation and polysome profiling). Strikingly, neocortex growth reduction induced after 5 days of dietary MR, which correlates with reduced neuron numbers, is completely compensated at birth by switching back to control diet for 5 days. Altogether, our data show that short term dietary MR has severe consequences on neocortex growth and development and uncovers a mechanism of catch-up growth for neuronal production in the neocortex.

RESULTS

Embryonic organ-specific responses to dietary MR

Methionine is an essential amino acid that fuels 1C metabolism and the generation of the methyl donor SAM (Fig.1A). Methionine is provided by nutrition, it is thus possible to impose MR by dietary intervention. To effect such MR, we used modified chow that contains no methionine and normal ranges of folate and choline levels (SupTable1). First, we fed adult mice control or modified chow and observed that intake of control and MR chow by both virgin adult females and pregnant dams was equivalent (Fig1B, C). Despite equivalent food intake, MR diet led to severe weight loss after 3 weeks which was completely compensated within one week of control diet (Fig1D). With the objective to assess the consequences of dietary MR on neurogenic transitions and neuronal production, we designed dietary interventions such that early phases of embryonic development would be spared. For this, we started dietary MR at E9.5, concomitant with neurogenesis in the telencephalon (Fig1E). Pregnant females were then kept in dietary MR for 10 days until E19.5/P0 or for 5 days until E14.5 (Fig1E). Dietary MR for 10 days led to IUGR shown by decreased body weight (Fig1F). Surprisingly, a survey of different organs indicated that brain weight was decreased unlike liver and heart weights (Fig1F) revealing an organ-specific response to dietary MR. Next, we analyzed the consequences of dietary MR for 5 days by analyzing E14.5 embryos. At this stage, no IUGR could be detected, yet a small decrease in brain weight was already present, while no difference in liver or heart weight could be detected (Fig1G). To ascertain that dietary MR led to changes in methionine levels in these organs, we measured steady-state methionine levels by ELISA and observed that 5 days dietary MR led to a decrease in methionine levels in the neocortex and in the liver but not the heart of E14.5 embryos (Fig1H). This data supported the notion of an organ-specific response to dietary MR and indicated that the brain might be more sensitive to MR than other organs.

To explore the potential molecular and cellular consequences of decreased methionine levels, we quantified global DNA methylation by ELISA (enzyme-linked immunosorbent assay), analyzed translation using polysome profiling and assessed cell cycle parameters by cytometry. While none of these tested parameters were modified in the heart (Fig1I-K), polysome profiling indicated that dietary MR for 5 days modified translation in the liver but not in the neocortex

(Fig1I). Conversely, we observed a significant decrease in global DNA methylation in the neocortex but not in the liver of E14.5 embryos subjected to dietary MR for 5 days (Fig1J). Lastly, cytometry analyses indicated that cell distribution in the cell cycle was modified only in the neocortex in E14.5 embryos subjected to dietary MR for 5 days (Fig1K). Specifically, in the neocortex, the fraction of cells in S and G2/M phases of the cell cycle was increased at the expense of cells in G1 yet there was no increase in the proportion of cells positive for the mitotic marker phospho-Histone 3 (pH3). This data suggested that neocortical cells may be arrested or delayed in the S and G2/M phases of the cell cycle in response to dietary MR for 5 days. Alternatively, this data could indicate that dietary MR for 5 days modified the ratio between proliferating progenitors and terminally differentiated neurons.

MR leads to neocortex growth defects and microcephaly

Next, we characterized the consequences of the dietary interventions described above (Fig2A) on neocortex growth and on neuronal production. As shown previously (Fig1F), MR for 10 days led to a reduction in brain growth observable macroscopically (Fig2B). This reduction in neocortex growth was quantified on coronal sections by measuring radial thickness and tangential extension of the neocortex (Fig2C). To assess whether this reduction in growth following 10 days of MR correlates with the loss of specific neuronal populations, we performed immunostaining with markers of newborn neurons (TBR1), deep layer neurons (CTIP2) or late born neurons (SATB2) (Fig2D, E). Quantification of the different markers revealed that MR for 10 days led to a global reduction of all neuronal subtypes in the neocortex (Fig2F).

After 5 days of MR, radial thickness of the neocortex was already decreased (Fig2G) and the number of all neuronal subtypes was already strongly reduced (Fig2H-J). This decrease was not observed after 3 days of MR (FigS1A, B). To uncover the potential causes of the reduction in neuron numbers after 5 days of MR, we performed immunostaining with the apoptotic marker activated caspase-3 and performed TUNEL (terminal deoxynucleotidyl transferase dUTP nick end labeling) assay and detected no change in apoptosis (FigS2A, B). We then used markers of apical progenitors (PAX6) and intermediate basal progenitors (TBR2) (Fig2K). Quantification of the two markers indicated that both populations of progenitors are decreased after 5 days of MR (Fig2L). It is thus likely that modification of cell cycle parameters within neocortical progenitors (Fig1K) are at the origin of the stunted neuronal production following 5 days of

MR. Altogether these results indicate that dietary MR leads to severe neocortex growth defects and microcephaly within 5 days, by altering the cycling properties of neural progenitors.

Catch-up growth allows complete recovery of neuron numbers at birth

It has been shown previously that neuronal production in the developing neocortex is a plastic process and can adapt to a transient loss of cells or to a lower rate of differentiation (Freret-Hodara et al., 2017; Kischel et al., 2020; Toma et al., 2014). To assess whether restricted growth of the neocortex induced by 5 days of MR can be rescued, we designed a regimen in which after 5 days of MR, the pregnant dams were switched back to control diet (Fig3A) and brain and neocortex growth were assessed at E19.5/P0. With this regimen, no gross difference in brain size was detected at E19.5/P0 (Fig3B), tangential growth of the neocortex was rescued (Fig3C) and radial growth of the tissue was less severely decreased compared to 10 days of MR (Fig2C). No difference of neuron numbers was observed between control regimen and the switch MR regimen (Fig3D-F), indicating that all three neuronal subtypes were completely rescued despite the severe microcephaly that was present at E14.5 (Fig2G-J).

Neural progenitors quickly respond to MR by adjusting their cycling and differentiation behavior

In order to uncover the consequences of MR on neural progenitors behavior, we used cell cohort tracing approaches in combination with diet regimen (Fig4A). We labeled a cohort of neural progenitors at E12.5 with EdU (neural progenitors in S-phase) and in the same pregnant dam, we labeled a cohort of neural progenitors at E14.5 using Flashtag/CFSE (mitotic neural progenitors abutting the ventricle) (Govindan et al., 2018; Salic & Mitchison, 2008). In this set of experiments, the switch between MR and control diet was done at E14, 15 hours before Flashtag injection, in order to catch progenitor behavior in the rescue phase (Fig4A). Injected embryos were then analyzed by immunofluorescence 2 days later, at E16.5 (Fig4B). The proportion of EdU+ and Flashtag (FT)+ cells was quantified in the different layers of the neocortex (ventricular zone (VZ), intermediary zone (IZ), cortical plate (CP)). Focusing on EdU+ cells, the quantification shows that in the control situation, a large proportion of neural progenitors that were cycling at E12.5 have differentiated into deep layer neurons (EdU+ in the CP) but some EdU+ cells have remained progenitors (EdU+ in the VZ) (Fig4C). Following 7 days of MR, EdU+ progenitors have massively differentiated into deep layer neurons and very few EdU+ cells are still present in the VZ (Fig4C). In the switched regimen, the behavior of

EdU+ cells is comparable to that of the control situation (Fig4C). These results indicate that MR promotes the neuronal differentiation of E12.5 progenitor pools.

Focusing on FT+ cells, the quantification shows that in the control situation, a large proportion of neural progenitors that were undergoing mitosis at E14.5 have differentiated, and are already positioned in the upper layers of the CP while many FT+ cells are located in the IZ (Fig4C). Very few FT+ cells have remained in the VZ. Following 7 days of MR, a large proportion of FT+ cells are still located in the VZ and none have reached the CP (Fig4C) indicating defects and delay in differentiation. In the switched regimen, while many FT+ cells are still present in the VZ, a large proportion of them has reached the CP (Fig4C), indicating that switching back to control diet has allowed FT+ cells to quickly resume differentiation. Altogether, these results suggest that MR has opposite consequences on early and mid-to-late progenitors; while MR promotes direct differentiation of early neural progenitors, it delays differentiation of mid-to-late neural progenitors.

DISCUSSION

Here, we present the consequences of short term dietary MR focusing on neocortex development and report that the response to dietary MR is extremely fast in the brain tissues, with a severe deficit in neuronal production. Unexpectedly, catch-up growth restores neocortex neuronal numbers of different subtypes.

A suboptimal nutritional supply in utero often leads to fetal growth adaptations with vital organs exhibiting differential growth outcomes (Dobbing & Sands, 1973; Gruenwald, 1963; Serpente et al., 2021). This asymmetric pattern of organ growth is known as organ sparing, which either reflect compartmentalized regulation or promote fetal survival. In our study, the 10 days restricted fetus with microcephaly were stillborn and restriction did not prolong their gestation window, strengthening the notion of genetic determinants shaping the gestation duration in mice (Murray et al., 2010). It remains unclear which malformations affected fetal survival; however, the developing brain appears to be more sensitive to MR than liver and heart, supporting a possible compartmentalized metabolism for meeting its growth requirements. Differential sensitivity to MR could be due to differential expression of enzymes of the 1C metabolic cycle that allow for remethylation of homocysteine to methionine (Cardoso-Moreira

et al., 2019; Imbard et al., 2021), and thus liver and heart growth may differentially compensate for low methionine supply in the diet. However, this may not be the only explanation since we observed low methionine levels in the liver with a potential impact on translation, yet this has no effects on the liver growth. Interestingly, heart growth seems to be independent of amino acids level (Hennig et al., 2019), suggesting the cardiovascular system might be protected in challenging microenvironments. In contrast, brain is considered as an expensive organ (Aiello & Wheeler, 1995), our data indicates that developing such tissue might be more adaptive and proportional to the methionine content. Since maternal supply and fetal liver increases nutrient bioavailability in the brain, it would be interesting to find out how inter-organ methionine supply is hierarchically organized during gestation.

The link between chronic restriction in methyl donors such as folate or choline and alteration of brain development and cognitive functions is well documented (Korsmo & Jiang, 2021). However, very few studies have analyzed the effects of dietary methyl donor restriction on the short term. One study reported that dietary folate restriction in the rat from E11 to E17 led to decreased proliferation and increased apoptosis in the forebrain (Craciunescu et al., 2004). The overall growth of the forebrain was not analyzed in this study but presumably decreased proliferation and increased apoptosis that was observed should lead to microcephaly, similar to our data following 10 days of dietary MR during gestation in the mouse. The response to dietary MR is extremely fast, within 5 days of MR there are already severe consequences in terms of growth and differentiation Similarly, catch-up growth is extremely fast, within 2 days of switching back to normal diet, the system has resumed and even accelerated its differentiation. Catch-up growth is defined by the accelerated growth of a tissue to reach a certain target size appropriate for age. This concept has been largely explored with respect to bone growth (Kagan & Rosello-Diez, 2021). One hypothesis to explain catch-up growth is the “sizostat” mechanism, which was originally formulated for whole body growth and implied a neuroendocrine loop (Tanner, 1963). This mechanism implicates a growth inhibitor and its receptor that dose-dependently inhibit proliferation. Adapted to local catch-up growth, this mechanism would posit that differentiated progeny release the growth inhibitor while progenitors express its receptor and that progenitors adapt their proliferating rate to the dose of growth inhibitor. In the developing neocortex, this concept has not been deeply explored, although previous studies have shown that neocortex growth and development is plastic and is able to adapt to cell loss (Freret-Hodara et al., 2017; Toma et al., 2014). These studies invoked the presence of negative

feedback loops on the production of neuronal subtypes. The striking pattern of the catch-up growth in our study is the fact that the proportion of the different neuronal subtypes was rescued despite the fact that the temporal windows were shifted. In the neocortex, production of the different neuronal subtypes is sequential, with early born (mostly DL) neurons generated from E11.5 to E14.5 and late born (mostly UL) neurons generated after E14.5. In the switch back experiment when control diet is provided after E14.5, we could have expected that catch-up growth would produce mostly late born neurons. Such a scenario has been observed following genetically induced cell death in the neocortex from E11.5 to E14.5 which led to an increase in UL CUX1+ neurons (Freret-Hodara et al., 2017). Alternatively, we could have expected a prolonged production of early born DL neurons at the expense of late born UL neurons, as was shown following genetic ablation of early born DL neurons (Toma et al., 2014). One possible explanation for the different outcome that we observed resides in the fact that in our study, there is no massive loss of cells by cell death at E14.5, but rather a lag in cell production. Lastly, it would be of interest to examine the glial population following catch-up growth. Indeed, neuronal and glial cells are produced from the same pool of progenitors and neuronal catch-up growth might exhaust this pool.

MATERIALS AND METHODS

Animals

Wild type mice were kept in a 129S4/C57Bl6J mixed background. The gender of embryos was not tested and littermates were randomly assigned to replicate experiments. Mice were maintained on a standard 12 hours day:night cycle and given ad libitum access to food and water. Mice were either fed a methionine-restricted diet (SAFE AIN 2g Choline #U8958 Version 330) or a control diet (SAFE #AO4) during pregnancy. Timed pregnancies were obtained by detecting vaginal plugs in the morning and samples were collected in the afternoon. All experimental procedures were pre-approved and carried out in compliance with the guidelines provided by the national Animal Care and Ethics Committee (APAFIS #35692-2022082409293050 v6) following Directive 2010/63/EU.

Evaluation of food intake

To measure food intake, a group of 2-3 non-pregnant or pregnant females (3-5 months old) were kept in a cage. A defined amount of food was provided to the mice, the remaining food was weighed at 2 days interval for the calculation of average food intake.

Weight measurement

Body weight was measured after the removal of placenta. The wet weight of fresh organ samples was recorded as soon as it is removed from the body cavity.

Immunohistochemistry

Mouse brains at stages E14.5 and older were collected and fixed with 4% Paraformaldehyde overnight at 4°C followed by paraffin or OCT embedding. The paraffin embedding was obtained with Spin tissue processor (Myr) for 5 µm coronal sections on Microtome (Microm). For OCT embedding, the samples were transferred to 30% Sucrose solution overnight at 4°C before OCT (Sakura) inclusion for performing 20 µm coronal sections using Cryostat (Leica Biosystems). Paraffin-embedded sections were exclusively deparaffined, rehydrated, followed by antigen retrieval involving steam heating for 45 minutes. Coronal sections were permeabilized and incubated in blocking solution (1-3% BSA, 1-3% FBS, 0.5-1% Tween 20 and PBS) for 2 hours at room temperature. Sections were permeabilized and incubated with antibodies diluted in blocking solution (1-3% BSA, 1-3% FBS, 0.5-1% Tween 20 and PBS) overnight at 4°C.

For birthdating experiments, EdU (dissolved in PBS at 5 mg/ml, 25 µg/g body weight) was injected intraperitoneally at E12.5. Histological detection of EdU was performed using the Click-iT EdU cell proliferation kit (ThermoFisher) according to the manufacturer's instructions. A stock of 10mM FT (CFDA-SE, STEMCELL Technologies) was prepared by dissolving the CFDA-SE in dimethyl sulfoxide (DMSO) (Euromedex) for an in utero injection. The fresh working solution of 1mM was diluted in HEPES-buffered saline solution (HBSS, ThermoFisher), in which Fast Green dye was added for monitoring successful injection.

Imaging and quantification

The macroscopic images were acquired with SMZ18 stereomicroscope (Nikon) and fluorescent images were captured with SP8 inverted scanning confocal microscope (Leica Biosystems). Images were exported as TIFF files and quantification was performed manually with ImageJ

(NIH) on defined regions of interest (ROIs). For E14.5 and E16.5 mouse embryos, one ROI in the dorsolateral region was chosen for manual counting. Embryos were collected from different litters and 100-500 cells were counted per hemisphere using multiple sections. Counts were normalized to an area of 100 µm of apical surface×100 µm of radial length. For E19.5/P0 mouse embryos, a custom script was developed for automated cell quantification in ImageJ. We defined a threshold to identify positive cells in the DAPI channel that creates a mask of all positive cell nuclei. Using image filtering on fluorescent channels, we further considered two parameters (>50 μm^2 area of the fluorescence signal and >0.6 circularity index) to identify the positive nuclei across the entire neocortical hemisphere.

Methionine assay

Methionine levels were determined by a fluorometric assay kit (Abcam) based on an enzymatic mechanism coupled with the generation of hydrogen peroxide. Dissected E14.5 tissue samples were mechanically dissociated with a pipette tip and suspended in 200 µl of supplied assay buffer. Liver samples were specifically pre-treated by adding 4 µl supplied Sample Clean-Up Mix in the assay buffer for 30 minutes incubation at 37°C. For neocortex and heart, cell debris were pelleted by centrifugation at 13,000 g for 15 min at 4°C and supernatant was collected. All samples were then filtered through a 10kD spin column (Abcam) by centrifugation at 10,000 g for 10 min at 4°C. In a black 96-well microplate (ThermoFisher), 20 µl of the ultra-filtrate were mixed with the assay buffer for a total volume of 50 µl sample. 10 µl of standard stock (10 mM methionine) was serially diluted with the assay buffer. 50 µl of standard mix and samples were then incubated with supplied Reaction Mix at a total volume of 100 µl at 37°C for 30 minutes in dark. The signal intensity of fluorescence excited at 535 nm for 1 second was measured at 587 nm using Varioskan flash (ThermoFisher). The readouts from standard were plotted to construct a standard curve for estimating methionine concentration.

DNA methylation assay

DNA was extracted from 10 mg of dissected E14.5 tissue samples using the DNeasy blood & tissue kit (Qiagen) according to the manufacturer's instructions. The amount of isolated DNA was quantified using Nanodrop spectrophotometer (ThermoFisher). 100 ng was used as input DNA for detecting global DNA methylation status by MethylFlash methylated 5mC DNA quantification kit (EpigenTek) based on an ELISA-like colorimetric reaction. The input DNA

was added to supplied strip wells with high DNA affinity. The methylated fraction of DNA was detected using supplied capture and detection antibodies and then quantified from the absorbance measurement at 450 nm in Multiskan GO microplate reader (ThermoFisher). The amount of methylated DNA is proportional to the OD intensity readouts, which were used for estimating the relative methylation status by the calculation of percentage of 5-methylcytosine (5mC) in total DNA.

Polysome profiling

E14.5 fresh tissue samples were collected in ice-cold HBSS, followed by a pull down of 5-6 samples. The neocortical dissection was carried out in ice-cold neurobasal medium (ThermoFisher). Dissected tissues were incubated in Cycloheximide-containing HBSS or neurobasal medium (100 µg/ml, Sigma-Aldrich) at 37°C for 10 minutes, followed by centrifugation at 500 g for 5 minutes at 4°C. The supernatant was discarded and pellets were washed twice with ice-cold Cycloheximide-containing PBS (100 µg/ml). Tissue pellets were incubated on ice for 10 minutes in the following lysis buffer: 200 mM HEPES, 100 mM KCl, 5 mM MgCl2, 1% Triton X-100, 0.5% Sodium deoxycholate, 1 mM Dithiothreitol (DTT), Cycloheximide (100 µg/ml), supplemented with Protease inhibitor (Roche), Phosphatase inhibitor (Roche), and RNasin inhibitor (Promega). Tissue lysates were clarified by centrifugation at 2000 g for 5 minutes at 4°C and supernatant collection, followed by another round of centrifugation at 13000 g for 5 minutes at 4°C and supernatant collection. RNA concentration was estimated by Nanodrop spectrophotometer and was further considered to normalize the sample loading. 10 to 50% sucrose gradients were prepared in RNase-free conditions with ultra-clear tubes. Clear supernatants (50-300 µg) were loaded into the sucrose gradients and centrifuged at 390000 RPM (SW41 Ti rotor, Beckman Coulter) for 100 minutes at 4°C. The gradient fractions were separated and the absorbance profiles of the RNPs (ribonucleoprotein particles), 40S, 60S, 80S, and polysome fractions were monitored at 254 nm.

Cell cycle analysis by flow cytometry

E14.5 fresh tissue samples were collected in ice-cold PBS. Heart samples were pulled down from 4 embryos, all samples were transferred into individual tubes in ice-cold FCS-containing PBS (1%). The samples were further processed for cell dissociation and staining for DAPI and phospho-Histone 3 (pH3) according to the methodology described in a previous study (Jungas

et al., 2020). The tissue lysates were loaded in Cytoflex-S flow cytometer (Beckman Coulter) and data were collected and analyzed using CytExpert software (Beckman Coulter). A range of 30,000–50,000 events was acquired with a minimal flow rate (<1000 events/s) from each sample. For analysis, clumps, debris, and doublets were eliminated and positive fluorescent signal was defined with staining controls for the primary and secondary antibodies. For cell cycle analysis, DNA content histograms from DAPI incorporation were used for a manual determination of G1/G0, S, and G2/M phases (Darzynkiewicz et al., 2010).

Statistical analyses

For each assay/experiment, tissue samples were obtained from at least four to eight mouse embryos per condition. For experiments involving a pair of conditions, statistical significance between the two sets of data were analyzed with unpaired t test or Mann–Whitney test with Holm-Šidák adjusted P-values using Prism10 (GraphPad). Statistically significant differences are reported at *P<0.05, **P<0.01 and ***P<0.001.

FIGURE LEGENDS

Figure 1. Organ-specific response to methionine restriction, brain is not spared. (A) Schematic representation of the 1C metabolism and its outputs. Created with BioRender.com. (B,C) Measurement of daily dietary intake for adult female and pregnant mice over a 5-week and pregnancy period (n= 3 mice per group). (D) Trajectories of normalized body weight of adult female mice on control (SAFE #A04) and MR (SAFE AIN 2g Choline #U8958 Version 330) diet (n= 3 mice per group). (E) Schematic of study design. MR were introduced at E9.5 to the pregnant mice. (F) Fetal body and organ weights at E19.5/P0 from dams fed on control or MR diet for 10 days (n= 4-5 embryos). (G) Fetal body and organ weights at E14.5 from dams fed on control or MR diet for 5 days (n= 4-5 embryos). (H) Levels of methionine were measured with an enzyme immunoassay kit (Abcam) in fetal tissue extracts from E14.5 (n= 5 embryos). (I) E14.5 tissue lysates were analyzed by sucrose gradient fractionation for measuring the relative abundance of ribonucleoprotein particles (RNPs), ribosomal subunits (40S and 60S), 80S ribosomes, and polysomes as a readout of global translation (n = pulldown of 5-6 samples). (J) The profile of 5mC DNA methylation profile were determined in E14.5 tissue samples by ELISA-like assay (n= 4-5 embryos). (K) Cell cycle phases were identified based on DNA

content (DAPI incorporation) and phospho-Histone 3 (pH3) staining using flow cytometric analysis of E14.5 tissue samples (n= 5-7 embryos). Data are mean±s.d. and statistical analysis was carried out using a Mann–Whitney or unpaired t test.

Figure 2. Methionine restriction leads to neocortex growth defect and microcephaly. (A) Schematic of study design illustrating dietary exposure. (B) Dorsal view of control and 10 days of MR exposed fetal brain at E19.5/P0. (C) Quantification of radial length and tangential perimeter in control and 10 days of MR exposed E19.5/P0 neocortex (n= 6-8 embryos). (D-F) Representative zoom-in images and quantification of E19.5/P0 neocortex coronal sections immunostained for TBR1, CTIP2, and SATB2. Scale bars: 50 μm. (G) Quantification of radial length in control and 5 days of MR exposed E14.5 neocortex (n= 6-7 embryos). (H-J) Representative zoom-in images and quantification of E14.5 neocortex coronal sections immunostained for TBR1, CTIP2, and SATB2 (n= 6-7 embryos). Scale bars: 25 μm. (K,L) Representative images and quantification of E14.5 neocortex coronal sections immunostained for PAX6 and TBR2 (n= 6-7 embryos). Scale bars: 50 μm. Data are mean±s.d. and statistical analysis was carried out using an unpaired t test.

Figure 3. Growth defect, including neuronal production, can be compensated in favorable nutrition conditions. (A) Schematic of study design representing dietary switch regimen. (B) Dorsal view of control and 5 days of MR exposed fetal brain at E19.5/P0. (C) Quantification of radial length and tangential perimeter in control and 5 days of MR exposed E19.5/P0 neocortex (n= 6-7 embryos). (D-F) Representative zoom-in images and quantification of E19.5/P0 neocortex coronal sections immunostained for TBR1, CTIP2, and SATB2. Scale bars: 50 μm. Data are mean±s.d. and statistical analysis was carried out using an unpaired t test.

Figure 4. Progenitors quickly respond to variations in dietary methionine. (A) Schematic of study design for coupling birthdating strategies with dietary exposure. (B-D) Representative zoom-in images and quantification of EdU and FlashTag-labelled cohort of cells born at E12.5 and E14.5, and their accumulation at ventricular zone (VZ), intermediate zone (IZ), and cortical plate (CP) in E16.5 neocortex coronal sections (n= 4 embryos). Scale bars: 50 μm.

SUPPLEMENTARY FIGURE LEGENDS

Figure S1. Onset of neurogenesis is maintained with no changes in cell death under methionine restriction. (A,B) Representative images and quantification of E12.5 neocortex coronal sections immunostained for TBR1, CTIP2, and SATB2 (n= 4-5 embryos). Scale bars: 50 μm. (C,D) Representative quantification of cell death by caspase-3 immunostaining and TUNEL assay in E14.5 neocortex coronal sections (n=3-4 embryos). Data are mean±s.d. and statistical analysis was carried out using an unpaired t test.

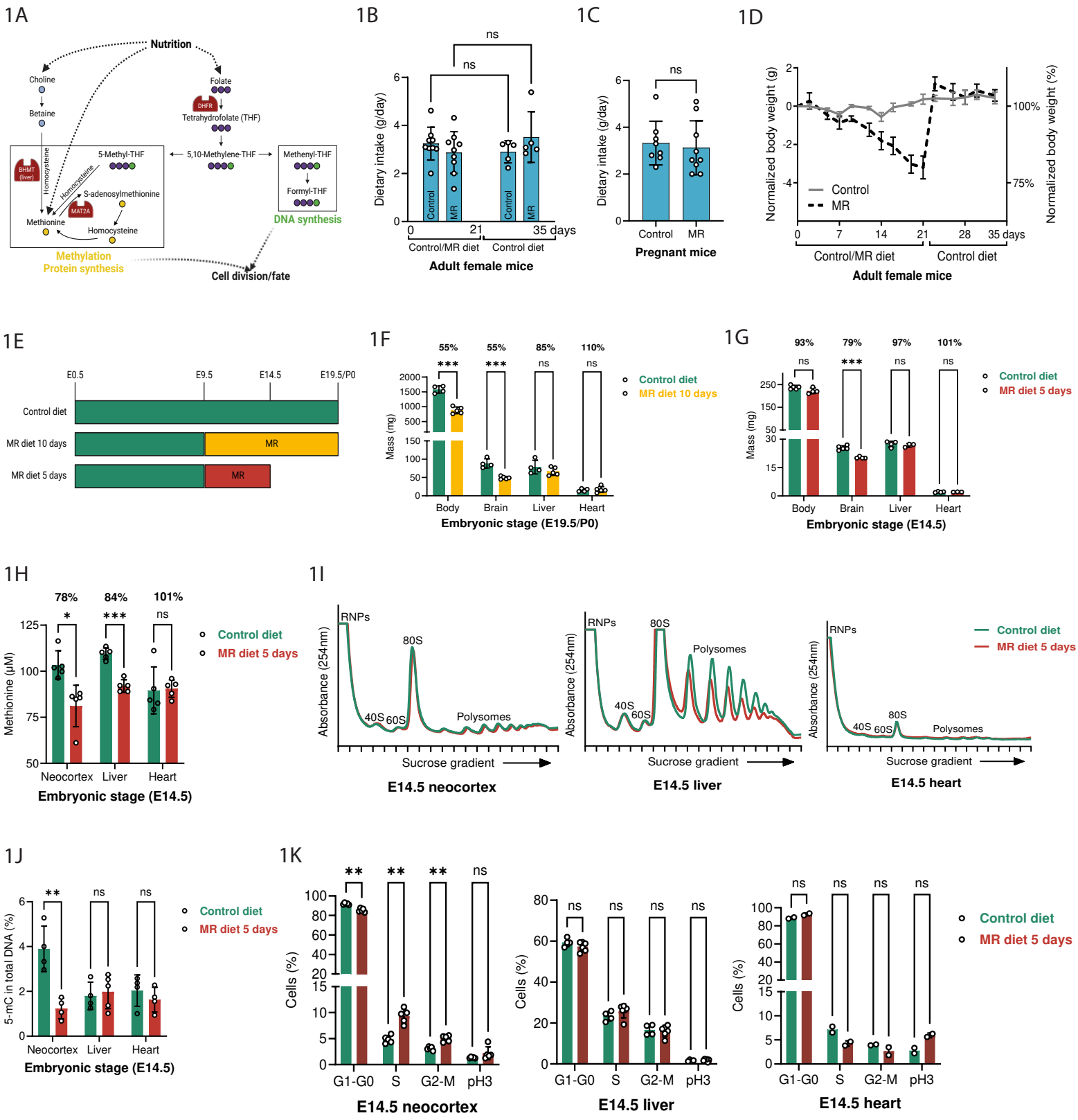

Figure 1. Organ-specific response to methionine restriction, brain is not spared.

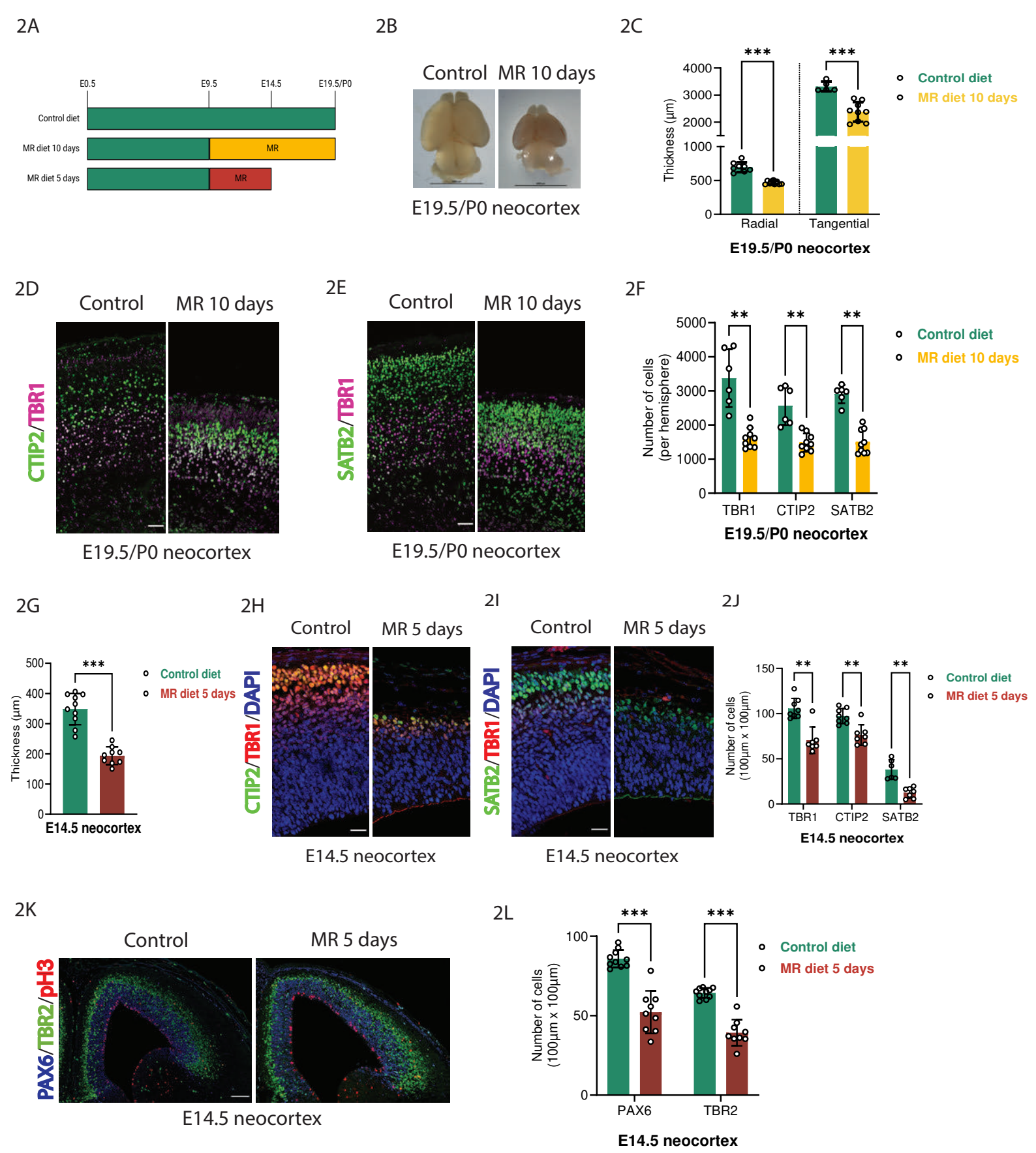

Figure 2. Methionine restriction leads to neocortex growth defect and microcephaly.

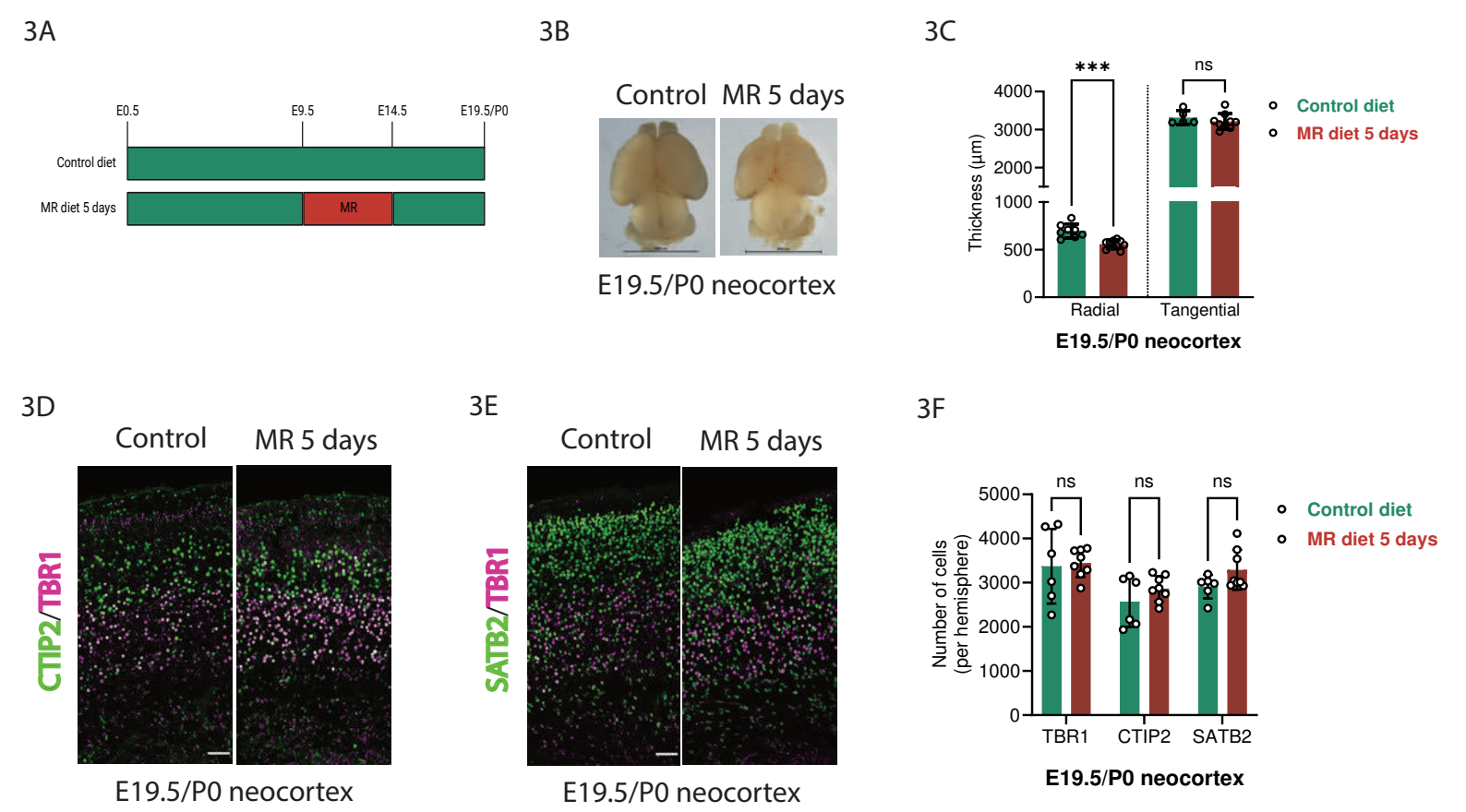

Figure 3. Growth defect, including neuronal production, can be compensated in favorable nutrition conditions.

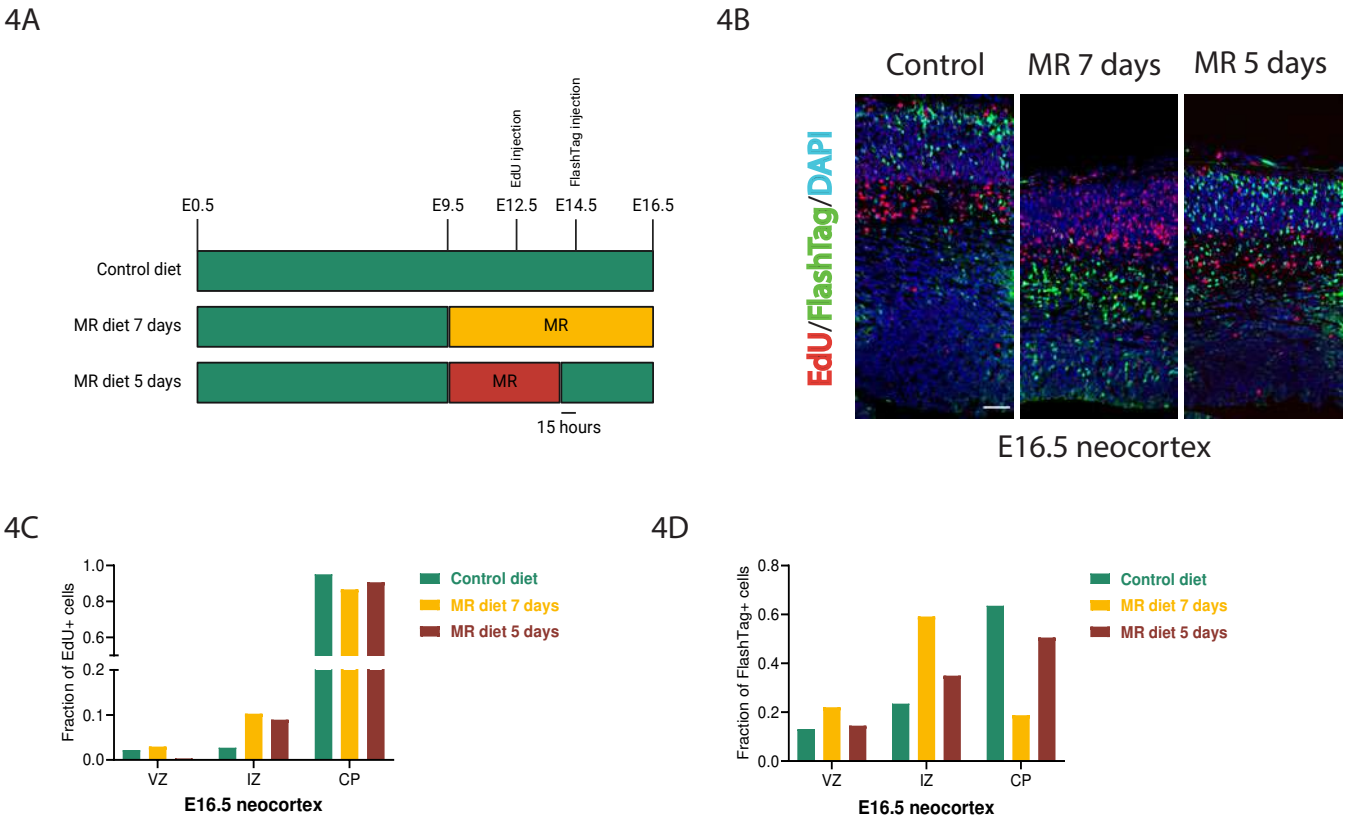

Figure 4. Progenitors quickly respond to variations in dietary methionine.

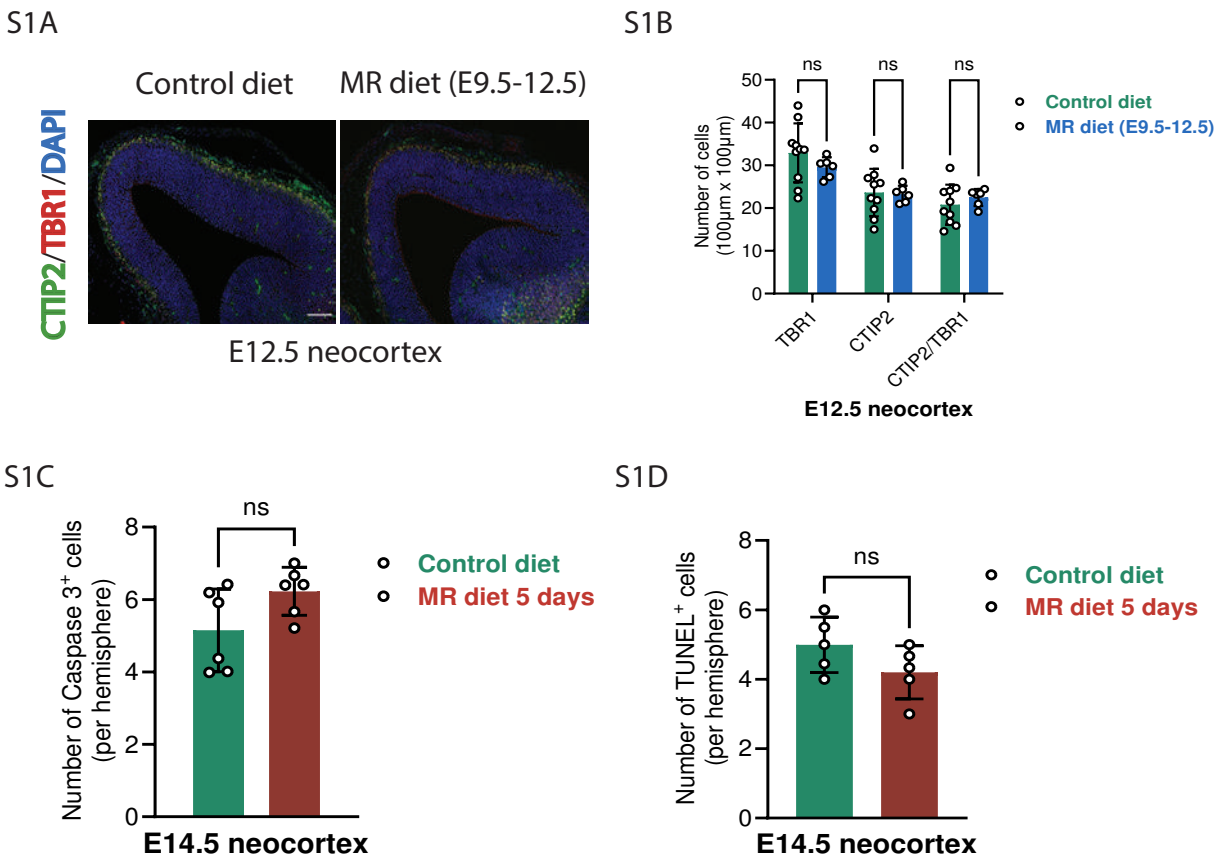

Figure S1. Onset of neurogenesis is maintained with no changes in cell death under methionine restriction.

Control diet (SAFE #AO4)

	Amount (mg per kg)	
Amino acids		
Arginine	9000	
Cystine	2500	
Lysine	7200	
Methionine	2800	
Tryptophan	1900	
Glycine	8100	
Fatty acids		
Palmitic acid	5900	
Stearic acid	600	
Palmitoleic acid	150	
Oleic acid	4800	
LA	15000	
ALA	1200	
Minerals		
Calcium	7300	
Phosphorus	5500	
Sodium	2500	
Potassium	6000	
Magnesium	1600	
Manganese	70	
Iron	270	
Copper	16	
Zinc	55	
Chlorine	4000	
Vitamins		
Vitamin A	7500 IU	
Vitamin D3	1000 IU	
Vitamin E	30 IU	
Vitamin K3	2.5	
Vitamin B1	5	
Vitamin B2	6.5	
Vitamin B3	70	
Vitamin B5	10	
Vitamin B6	3	
Vitamin B9/Folate	0.35	
Vitamin B12	0.01	
Biotin	0.08	
Choline	1600	
Energy content	**kcal per kg**	**%**
Proteins	644	19.3
Lipids	279	8.4
Carbohydrates	2416	72.4

MR diet (SAFE AIN 2g Choline #U8958 Version 330)

	Amount (mg per kg)
Amino acids	
Arginine	5880
Cystine	4116
Lysine	12696
Methionine	0
Tryptophan	2079
Glycine	2955
Fatty acids	
Palmitic acid	7420
Stearic acid	2555
Palmitoleic acid	350
Oleic acid	13020
LA	37030
ALA	5390
Sum n-3	5390
Sum n-6	37030
Sum SFA	10325
Sum UFA	55790
Sum MUFA	13370
Sum PUFA	42420
Cholesterol	1.1
Minerals	
Calcium	6333
Phosphorus	2678
Sodium	4574
Potassium	6323
Magnesium	823
Manganese	14
Iron	69
Copper	6.9
Zinc	45
Chlorine	4964
Vitamins	
Vitamin A	6437 IU
Vitamin D3	1625 IU
Vitamin E	106 IU
Vitamin K3	8
Vitamin B1	7.8
Vitamin B2	7.5
Vitamin B3	45
Vitamin B5	20
Vitamin B6	9.1
Vitamin B9/Folate	2.6

Vitamin B12	0.033	
Biotin	0.26	
Choline	2062	
Sugars		
Glucose	< 0.5 %	
Sucrose	13%	
Energy content	**kcal per kg**	**%**
Proteins	561.4	14.6
Lipids	640.4	16.6
Carbohydrates	2647.4	68.8

General discussion

In this work, we studied the making of an organ under metabolic restriction, which is characterized by genetic conditions of deficiency and poor nutritional intake during gestational development. Gestation is a critical moment for both mother and embryo, the fertilized embryo goes from a relatively inactive metabolic state to a rapid metabolic state during and after implantation (Tippetts et al., 2023). Stem/progenitor cells in the postimplantation tissues become partially autonomous due to the constraints in metabolic genes, but exogenous supply of nutrients stay relevant for their direct contributions to the metabolic networks. While pregnant mother carries out a species-specific strategy for the optimal fetal growth (Wade & Schneider, 1992), consistent evidences support that metabolic restriction adversely impacts fetal brain developmental processes, including the proliferation, differentiation, synaptogenesis, and dendritic arborization in many regions of the brain (Georgieff, 2007). In this work, I showed that 1C metabolic deficiency affect the timing of neurodevelopmental processes, including the proliferation and differentiation in the mouse and human experimental models of neocortex. This perturbation results in specific changes in NPC fate dynamics and neuronal differentiation output, creating a scope for vulnerable brain growth.

During development, the fate of NPC is influenced by specific transcription factors and epigenetic machinery. This machinery is a driving force of developmental processes, and understanding how nutrition controls the cellular metabolic networks and impacts tissue growth and body plan across species requires further exploration. Our results from both folate and methionine perturbations pinpoint that epigenetic machinery is sensitive at the onset of neurogenesis, because it is assumed that it sets the differentiation pace and output (Albert et al., 2017; Ciceri et al., 2024). Genetic perturbation of key epigenetic regulators revealed distinct morphological and transcriptional developmental delays (Grosswendt et al., 2020), highlighting how developmental growth is influenced in the absence of epigenetic coordination. In our perturbations, developmental delay was observed both under folate and methionine deficiency. Nevertheless, genetic folate deficiency did not impact mouse tissue growth, it did alter the precise differentiation trajectory and laminar distribution of excitatory projection neurons. A

comparison of the laminar organization shows inter-species variations across mammals (Graïc et al., 2022), prompting inquiries into whether intrinsic metabolic cues have undergone phylogenetic adaptations for this specific purpose. In contrast, dietary methionine deficiency resulted in IUGR, defined by insufficient/delayed growth in relation to its genetic potential, which is often associated with risks of stillbirth and neonatal death, neurodevelopmental and metabolic disorders (Sharma et al., 2016). IUGR is classified as symmetric (20-30%) or asymmetric (70-80%), based on the growth of head circumference (Fleiss et al., 2019). Asymmetric IUGR is considered to be a result of brain sparing, a process whereby brain growth is spared with the redistribution of blood flow maximizing oxygen and nutrient supply (Godfrey et al., 2012; Shin et al., 2023). Remarkably, brain sparing is observed from *Drosophila* to human (Beukers et al., 2017; Cheng et al., 2011; Serpente et al., 2021), yet the contributions of specific nutrients have not been identified until now. Our finding highlights that organ growth can be modified through methionine-dependent plastic responses to changing nutrition. Brain growth appears sensitive to methionine deficiency, while other organs are not affected, leading to altered body proportions under persistent methionine deficiency. The brain growth defects, including the diversity and number of neurons, were largely recovered with the reintroduction of methionine during critical embryonic development. It remains to be determined whether specific tissues control their growth through local nutrient sensing. SAMTOR, a sensor for SAM, is a promising candidate capable of detecting methionine levels and potentially coordinating the systemic regulation of mTORC1 signaling for tissue growth (Gu et al., 2017).

The recovery of neuronal diversity and numbers is quite interesting in the context of temporal fate plasticity. In *Drosophila,* neuronal diversity under protein deprivation was maintained at the expense of appropriate number (Lanet et al., 2013). NPC pool is reduced under such nutritional deprivation, yet understanding how the mammalian brain possesses a capacity to generate neuron diversity and numbers is important. Neurogenesis is strictly regulated by an integrated interplay between extrinsic and intrinsic cues acting on balancing the NPC proliferation and differentiation. This interplay aims at generating stereotypical number and type of neurons, through the timing of cell-cycle length and division mode. After introducing methionine-restricted diet at a window containing early RGC and observing developmental plasticity in later stages, it becomes intriguing to explore the impacts on late RGC which tends to be more extrinsically controlled as development proceeds (Telley et al., 2019). In our context,

the term “developmental plasticity” distinguishes irreversible phenotypic changes from reversible ones induced by environmental perturbations (Forsman, 2015), specifically referring to neuronal diversity and numbers. In addition and importantly, what developmental costs are incurred as a consequence of the observed plasticity? In compensating neuronal production, the shared RGC pool is possibly accomplishing a remarkable feat through an overconsumption for neurogenesis at the expense of gliogenesis.

Development sculpts the size and connections of the brain, which is dependent on the stereotyped production of correct number of neuronal and glial populations. An imbalance in neuronal and glial populations may lead to autism spectrum disorder (ASD) and microcephaly (Li et al., 2017), and 1C metabolic deficiency has been linked to ASD and microcephaly cases in humans (Serrano et al., 2012). Nutritional changes do not only affect the birth and migration of neurons and survival of NPC progeny, but also neuronal maturation process in later stages. In order for a neuron to become fully mature and participate in neuronal circuitry, it must develop axonal projections to targets, extend its dendrites, form synapses, and be able to release neurotransmitter. A recent study revealed that folate metabolism not only affects the generation of deep layer neurons but also their morphology (Tat et al., 2023). There seems to be a noticeable delay in the generation of excitatory neurons and reduction in the complexity of excitatory neurons. The functional consequences of 1C metabolic processes may extend to the circuit level concerning neuronal interconnectivity. Together, 1C metabolic deficiency alters the neuronal production dynamics, a mechanism possibly responsible for the etiology of ASD and microcephaly.

In *Drosophila*, type II neuroblasts in the optic lobe share many similarities to the neocortical RGC and a recent study revealed that 1C metabolism is involved in stage-specific cellular productions in the optic lobe (Silva et al., 2023). Perhaps most importantly, folate metabolism is essential for early-born neuronal progeny across species. The likelihood that a synergistic regulation of 1C metabolism and methylation-dependent neuronal diversification contributes to this phenomenon can be inferred from the high expression of MAT2A in early-born deep layer neurons (Micali et al., 2023). In addition, low folate intake has been linked to exhibit significant abnormalities in tissue growth due to the impaired DNA synthesis (Blatch et al., 2015; Harlan De Crescenzo et al., 2021). This suggests 1C metabolism is crucial and conserved in many aspects of neurodevelopment across species, which can be pinpointed to the availability of

folate and methionine nutrition in the diet across the animal kingdom. However, it remains unclear how such metabolic traits are positively selected and linked to the diet content. Kleiber's law, a widely accepted principle, asserts that as the mass of organs increases, they become more metabolically efficient (Kleiber, 1932), but it is challenging to trace the selection pressure on the metabolic strategies. In long-lived species, low methionine content is thought to be one of the molecular adaptations (Mota-Martorell et al., 2021); however, adult specimens might not represent the influences on the constituent parts of neurodevelopment. One possibility to examine the metabolic strategies during postnatal brain development by studying the composition of milk during lactation. Since lactation serves all nutrients to the offspring, protein concentration were identified across mammals, with human milk having the lowest amount (approximately 8 g/L) (Davis et al., 1994). Interestingly, amino acid patterns were similar: essential amino acids (40%), branched-chain amino acids (20%), and sulfur amino acids (4%) of the total amino acids across all species. In contrast to ungulates, carnivores, and rodents, primates displayed low methionine content in their milk. Considering that slow-growing larger species put more efforts on the maintenance, it becomes intriguing to ask whether the low methionine content correlates with slower growth rates. The results of the present study show a remarkable brain growth delay in the methionine-restricted mouse embryos that we analyzed. Metabolism, to a large extent, determines the tissue growth and so challenges the existing constraints. How genetic (e.g, enzyme) and non-genetic component (e.g., diet) acts together on an evolutionary innovation is largely unknown. Despite being omnivores and possessing two copies of the DHFR gene, rhesus macaques do not exhibit the dynamic pattern of DHFR expression observed in the mouse and human developing neocortex (Cardoso-Moreira et al., 2019; Di Bella et al., 2021; Klingler et al., 2021; Micali et al., 2023), giving rise to a question of scaling mechanism for 1C metabolism among primates. Growing evidences support that enhanced metabolism are associated with an extended proliferation output, a key hallmark in the evolutionary expansion of the neocortex (Namba et al., 2020; Pinson et al., 2022). In particular, mitochondria is considered as a key determinant of species-specific metabolic strategies in neurodevelopment (Iwata et al., 2020, 2023; Rangaraju et al., 2019). The mitochondria harbors many duplicated 1C enzymes (Ducker & Rabinowitz, 2017), it remains to be defined how parallel metabolic networks can be advantageous for a species. Future studies across species in a developmental context might reveal a better understanding of metabolic contributions to neocortical evolution.

While essential amounts of folate and methionine are accessible from the diet, micronutrient status and dietary habits vary throughout the world (Gilsing et al., 2010; Sanderson et al., 2019; Schmidt et al., 2016). Especially women in developing countries are at risk of micronutrient deficiencies (Torheim et al., 2010). Interventions, including recommendations on intake and supplements, have been widely applied to support health of the fetus (Gernand et al., 2016). For instance, recommended folate levels and intake of folic acid (synthetic folate)-fortified foods are made available to prevent brain congenital malformations such as neural tube defects. It is also recommended to follow a total protein intake of approximately 71 g/day in pregnancy (Hanson et al., 2015). Despite these attempts, a detailed recommendation for micronutrients like methionine is yet to be proposed. Since a vegan diet, being limited to plant-based products with low methionine content, increases the risk for low birthweight and IUGR (Avnon et al., 2021), the modeling of methionine restriction in a human context is required to understand the specific contributions of this nutrient in human organ growth. Organoids provide a unique opportunity; however, such in vitro based approaches still miss many aspects of inter-organ communications during development. Neural organoids in principles could model brain development with a restricted growth medium, but contrasting evidences are questioning the metabolic state in organoids (Bhaduri et al., 2020; Klingler et al., 2021; Uzquiano et al., 2022). Compared to primary tissue, organoid cells may lack accurate matching of metabolic gene expressions in a spatiotemporal manner. Nevertheless, in the future, organoids could enable us to validate a threshold point at which a micronutrient deficiency results in brain growth defects.

To date, metabolic conditions are detected by prenatal and newborn genomic and biochemical screening. It is critical to note, we lack defined markers for the detection of a past metabolic condition of a non-genetic origin. More precisely, identifying DNA and histone methylation-related transient or permanent alterations that impact specific target genes frequently proves challenging. DNA methylation is mainly categorized into two categories: CpG and non-CpG (CH). CH methylation is rare in fetal brains and accumulates during neuronal maturation after birth (Lister et al., 2013). It is currently unknown whether adaptive mechanisms enable maturing neurons to actively restore their functional epigenomes from metabolic perturbations. A recent study suggested that certain epigenetic marks are recovered through SAM partitioning during methyl-metabolite depletion (Haws et al., 2020). While maternal diet status is linked

with the establishment of DNA methylation at metastable epialleles in the mouse offspring (Waterland et al., 2006). This persistent and systemic epigenetic changes has also been observed at human metastable epialleles (Dominguez-Salas et al., 2014). In a recent comprehensive analysis of the epigenome in twin pairs, distinct differentially methylated loci associated with vegan and omnivore diets were revealed, providing insights into the influenced pathways within eight weeks (Dwaraka et al., 2023). Hypermethylated sites in vegans showed enrichment in neuroprotective mechanisms. Conversely, hypermethylation in omnivores was associated with cell division and genetic regulation. The cohort also demonstrated differential methylation in neurodevelopmental genes, including DHFR and CTIP2/BCL11B, when comparing the two experimental groups.

In summary, folate and methionine are interdependent metabolites in the 1C metabolic pathway, where folate provides the necessary one-carbon units, and methionine utilizes these units for important cellular processes. A collaboration between folate and methionine is widely known for contributions to the essential processes, including the DNA and protein synthesis, and methylation reactions in the cells. This study suggests that folate and methionine may independently respond to the neurodevelopmental metabolic demands during neurogenesis. Consequently, they orchestrate a fraction of growth and differentiation output in the embryonic brain, creating a critical window of vulnerability to metabolic challenges.

Bibliography

Ables, G. P., & Johnson, J. E. (2017). Pleiotropic responses to methionine restriction. *Experimental Gerontology*, *94*, 83–88. https://doi.org/10.1016/j.exger.2017.01.012

Adams, M., Lucock, M., Stuart, J., Fardell, S., Baker, K., & Ng, X. (2007). Preliminary evidence for involvement of the folate gene polymorphism 19bp deletion-DHFR in occurrence of autism. *Neuroscience Letters*, *422*(1), 24–29. https://doi.org/10.1016/j.neulet.2007.05.025

Aiello, L. C., & Wheeler, P. (1995). The Expensive-Tissue Hypothesis: The Brain and the Digestive System in Human and Primate Evolution. *Current Anthropology*, *36*(2), 199–221. https://doi.org/10.1086/204350

Albert, M., Kalebic, N., Florio, M., Lakshmanaperumal, N., Haffner, C., Brandl, H., Henry, I., & Huttner, W. B. (2017). Epigenome profiling and editing of neocortical progenitor cells during development. *The EMBO Journal*, *36*(17), 2642–2658. https://doi.org/10.15252/embj.201796764

Anderson, S. A., Eisenstat, D. D., Shi, L., & Rubenstein, J. L. R. (1997). Interneuron Migration from Basal Forebrain to Neocortex: Dependence on Dlx Genes. *Science*, *278*(5337), 474–476. https://doi.org/10.1126/science.278.5337.474

Arvanitis, D. N., Béhar, A., Tryoen-Tóth, P., Bush, J. O., Jungas, T., Vitale, N., & Davy, A. (2013). Ephrin B1 maintains apical adhesion of neural progenitors. *Development*, *140*(10), 2082–2092. https://doi.org/10.1242/dev.088203

Assimacopoulos, S., Grove, E. A., & Ragsdale, C. W. (2003). Identification of a Pax6-Dependent Epidermal Growth Factor Family Signaling Source at the Lateral Edge of the Embryonic Cerebral Cortex. *Journal of Neuroscience*, *23*(16), 6399–6403. https://doi.org/10.1523/JNEUROSCI.23-16-06399.2003

Avnon, T., Paz Dubinsky, E., Lavie, I., Ben-Mayor Bashi, T., Anbar, R., & Yogev, Y. (2021). The impact of a vegan diet on pregnancy outcomes. *Journal of Perinatology*, *41*(5), Article 5. https://doi.org/10.1038/s41372-020-00804-x

Azevedo, F. A. C., Carvalho, L. R. B., Grinberg, L. T., Farfel, J. M., Ferretti, R. E. L., Leite, R. E. P., Filho, W. J., Lent, R., & Herculano-Houzel, S. (2009). Equal numbers of neuronal and nonneuronal cells make the human brain an isometrically scaled-up primate brain. *Journal of Comparative Neurology*, *513*(5), 532–541. https://doi.org/10.1002/cne.21974

Bahous, R. H., Jadavji, N. M., Deng, L., Cosín-Tomás, M., Lu, J., Malysheva, O., Leung, K.-Y., Ho, M.-K., Pallàs, M., Kaliman, P., Greene, N. D. E., Bedell, B. J., Caudill, M. A., & Rozen, R. (2017). High dietary folate in pregnant mice leads to pseudo-MTHFR deficiency and altered methyl metabolism, with embryonic growth delay and short-term memory impairment in offspring. *Human Molecular Genetics*, *26*(5), 888–900. https://doi.org/10.1093/hmg/ddx004

Bain, G., Kitchens, D., Yao, M., Huettner, J. E., & Gottlieb, D. I. (1995). Embryonic Stem Cells Express Neuronal Properties in Vitro. *Developmental Biology*, *168*(2), 342–357. https://doi.org/10.1006/dbio.1995.1085

Bandler, R. C., Vitali, I., Delgado, R. N., Ho, M. C., Dvoretskova, E., Ibarra Molinas, J. S., Frazel, P. W., Mohammadkhani, M., Machold, R., Maedler, S., Liddelow, S. A., Nowakowski, T. J., Fishell, G., & Mayer, C. (2022). Single-cell delineation of lineage and genetic

identity in the mouse brain. *Nature*, *601*(7893), Article 7893. https://doi.org/10.1038/s41586-021-04237-0

Banka, S., Blom, H. J., Walter, J., Aziz, M., Urquhart, J., Clouthier, C. M., Rice, G. I., de Brouwer, A. P. M., Hilton, E., Vassallo, G., Will, A., Smith, D. E. C., Smulders, Y. M., Wevers, R. A., Steinfeld, R., Heales, S., Crow, Y. J., Pelletier, J. N., Jones, S., & Newman, W. G. (2011). Identification and characterization of an inborn error of metabolism caused by dihydrofolate reductase deficiency. *American Journal of Human Genetics*, *88*(2), 216–225. https://doi.org/10.1016/j.ajhg.2011.01.004

Barger, G., & Coyne, F. P. (1928). The amino-acid methionine; constitution and synthesis. *Biochemical Journal*, *22*(6), 1417–1425.

Barker, D. J. P. (2004). The developmental origins of adult disease. *Journal of the American College of Nutrition*, *23*(6 Suppl), 588S-595S. https://doi.org/10.1080/07315724.2004.10719428

Barnabé-Heider, F., Wasylnka, J. A., Fernandes, K. J. L., Porsche, C., Sendtner, M., Kaplan, D. R., & Miller, F. D. (2005). Evidence that Embryonic Neurons Regulate the Onset of Cortical Gliogenesis via Cardiotrophin-1. *Neuron*, *48*(2), 253–265. https://doi.org/10.1016/j.neuron.2005.08.037

Beattie, R., Postiglione, M. P., Burnett, L. E., Laukoter, S., Streicher, C., Pauler, F. M., Xiao, G., Klezovitch, O., Vasioukhin, V., Ghashghaei, T. H., & Hippenmeyer, S. (2017). Mosaic Analysis with Double Markers Reveals Distinct Sequential Functions of Lgl1 in Neural Stem Cells. *Neuron*, *94*(3), 517-533.e3. https://doi.org/10.1016/j.neuron.2017.04.012

Beukers, F., Aarnoudse-Moens, C. S. H., van Weissenbruch, M. M., Ganzevoort, W., van Goudoever, J. B., & van Wassenaer-Leemhuis, A. G. (2017). Fetal Growth Restriction

with Brain Sparing: Neurocognitive and Behavioral Outcomes at 12 Years of Age. *The Journal of Pediatrics*, *188*, 103-109.e2. https://doi.org/10.1016/j.jpeds.2017.06.003

Bhaduri, A., Andrews, M. G., Mancia Leon, W., Jung, D., Shin, D., Allen, D., Jung, D., Schmunk, G., Haeussler, M., Salma, J., Pollen, A. A., Nowakowski, T. J., & Kriegstein, A. R. (2020). Cell stress in cortical organoids impairs molecular subtype specification. *Nature*, *578*(7793), Article 7793. https://doi.org/10.1038/s41586-020-1962-0

Blatch, S. A., Stabler, S. P., & Harrison, J. F. (2015). The effects of folate intake on DNA and single-carbon pathway metabolism in the fruit fly Drosophila melanogaster compared to mammals. *Comparative Biochemistry and Physiology Part B: Biochemistry and Molecular Biology*, *189*, 34–39. https://doi.org/10.1016/j.cbpb.2015.07.007

Boehr, D. D., McElheny, D., Dyson, H. J., & Wright, P. E. (2006). The Dynamic Energy Landscape of Dihydrofolate Reductase Catalysis. *Science*, *313*(5793), 1638–1642. https://doi.org/10.1126/science.1130258

Borello, U., & Pierani, A. (2010). Patterning the cerebral cortex: Traveling with morphogens. *Current Opinion in Genetics & Development*, *20*(4), 408–415. https://doi.org/10.1016/j.gde.2010.05.003

Briscoe, J., Pierani, A., Jessell, T. M., & Ericson, J. (2000). A Homeodomain Protein Code Specifies Progenitor Cell Identity and Neuronal Fate in the Ventral Neural Tube. *Cell*, *101*(4), 435–445. https://doi.org/10.1016/S0092-8674(00)80853-3

Briscoe, S. D., Albertin, C. B., Rowell, J. J., & Ragsdale, C. W. (2018). Neocortical Association Cell Types in the Forebrain of Birds and Alligators. *Current Biology*, *28*(5), 686-696.e6. https://doi.org/10.1016/j.cub.2018.01.036

Brown, B., & Wright, C. (2020). Safety and efficacy of supplements in pregnancy. *Nutrition Reviews*, *78*(10), 813–826. https://doi.org/10.1093/nutrit/nuz101

Campbell, K. (2003). Dorsal-ventral patterning in the mammalian telencephalon. *Current Opinion in Neurobiology*, *13*(1), 50–56. https://doi.org/10.1016/S0959-4388(03)00009-6

Cárdenas, A., Villalba, A., de Juan Romero, C., Picó, E., Kyrousi, C., Tzika, A. C., Tessier-Lavigne, M., Ma, L., Drukker, M., Cappello, S., & Borrell, V. (2018). Evolution of Cortical Neurogenesis in Amniotes Controlled by Robo Signaling Levels. *Cell*, *174*(3), 590-606.e21. https://doi.org/10.1016/j.cell.2018.06.007

Cardoso-Moreira, M., Halbert, J., Valloton, D., Velten, B., Chen, C., Shao, Y., Liechti, A., Ascenção, K., Rummel, C., Ovchinnikova, S., Mazin, P. V., Xenarios, I., Harshman, K., Mort, M., Cooper, D. N., Sandi, C., Soares, M. J., Ferreira, P. G., Afonso, S., … Kaessmann, H. (2019). Gene expression across mammalian organ development. *Nature*, *571*(7766), Article 7766. https://doi.org/10.1038/s41586-019-1338-5

Cario, H., Smith, D. E. C., Blom, H., Blau, N., Bode, H., Holzmann, K., Pannicke, U., Hopfner, K.-P., Rump, E.-M., Ayric, Z., Kohne, E., Debatin, K.-M., Smulders, Y., & Schwarz, K. (2011). Dihydrofolate reductase deficiency due to a homozygous DHFR mutation causes megaloblastic anemia and cerebral folate deficiency leading to severe neurologic disease. *American Journal of Human Genetics*, *88*(2), 226–231. https://doi.org/10.1016/j.ajhg.2011.01.007

Cheatham, C. L. (2020). Nutritional Factors in Fetal and Infant Brain Development. *Annals of Nutrition and Metabolism*, *75*(Suppl. 1), 20–32. https://doi.org/10.1159/000508052

Cheng, L. Y., Bailey, A. P., Leevers, S. J., Ragan, T. J., Driscoll, P. C., & Gould, A. P. (2011). Anaplastic lymphoma kinase spares organ growth during nutrient restriction in Drosophila. *Cell*, *146*(3), 435–447. https://doi.org/10.1016/j.cell.2011.06.040

Cheroni, C., Trattaro, S., Caporale, N., López-Tobón, A., Tenderini, E., Sebastiani, S., Troglio, F., Gabriele, M., Bressan, R. B., Pollard, S. M., Gibson, W. T., & Testa, G. (2022). Benchmarking brain organoid recapitulation of fetal corticogenesis. *Translational Psychiatry*, *12*(1), Article 1. https://doi.org/10.1038/s41398-022-02279-0

Chiaradia, I., & Lancaster, M. A. (2020). Brain organoids for the study of human neurobiology at the interface of in vitro and in vivo. *Nature Neuroscience*, *23*(12), Article 12. https://doi.org/10.1038/s41593-020-00730-3

Ciceri, G., Baggiolini, A., Cho, H. S., Kshirsagar, M., Benito-Kwiecinski, S., Walsh, R. M., Aromolaran, K. A., Gonzalez-Hernandez, A. J., Munguba, H., Koo, S. Y., Xu, N., Sevilla, K. J., Goldstein, P. A., Levitz, J., Leslie, C. S., Koche, R. P., & Studer, L. (2024). An epigenetic barrier sets the timing of human neuronal maturation. *Nature*, 1–10. https://doi.org/10.1038/s41586-023-06984-8

Coquand, L., Macé, A.-S., Farcy, S., Avalos, C. B., Cicco, A. D., Lampic, M., Bessières, B., Attie-Bitach, T., Fraisier, V., Guimiot, F., & Baffet, A. (2022). *A cell fate decision map reveals abundant direct neurogenesis in the human developing neocortex* (p. 2022.02.01.478661). bioRxiv. https://doi.org/10.1101/2022.02.01.478661

Craciunescu, C. N., Brown, E. C., Mar, M.-H., Albright, C. D., Nadeau, M. R., & Zeisel, S. H. (2004). Folic Acid Deficiency During Late Gestation Decreases Progenitor Cell Proliferation and Increases Apoptosis in Fetal Mouse Brain. *The Journal of Nutrition*, *134*(1), 162–166. https://doi.org/10.1093/jn/134.1.162

Cusick, S. E., & Georgieff, M. K. (2016). The Role of Nutrition in Brain Development: The Golden Opportunity of the "First 1000 Days." *The Journal of Pediatrics*, *175*, 16–21. https://doi.org/10.1016/j.jpeds.2016.05.013

Darzynkiewicz, Z., Halicka, H. D., & Zhao, H. (2010). Analysis of Cellular DNA Content by Flow and Laser Scanning Cytometry. *Advances in Experimental Medicine and Biology*, *676*, 137–147.

Davis, T. A., Nguyen, H. V., Garcia-Bravo, R., Fiorotto, M. L., Jackson, E. M., Lewis, D. S., Lee, D. R., & Reeds, P. J. (1994). Amino acid composition of human milk is not unique. *The Journal of Nutrition*, *124*(7), 1126–1132. https://doi.org/10.1093/jn/124.7.1126

DeBerardinis, R. J., & Thompson, C. B. (2012). Cellular Metabolism and Disease: What Do Metabolic Outliers Teach Us? *Cell*, *148*(6), 1132–1144. https://doi.org/10.1016/j.cell.2012.02.032

Dehorter, N., & Del Pino, I. (2020). Shifting Developmental Trajectories During Critical Periods of Brain Formation. *Frontiers in Cellular Neuroscience*, *14*. https://www.frontiersin.org/articles/10.3389/fncel.2020.00283

Delgado, R. N., Allen, D. E., Keefe, M. G., Mancia Leon, W. R., Ziffra, R. S., Crouch, E. E., Alvarez-Buylla, A., & Nowakowski, T. J. (2022). Individual human cortical progenitors can produce excitatory and inhibitory neurons. *Nature*, *601*(7893), Article 7893. https://doi.org/10.1038/s41586-021-04230-7

Di Bella, D. J., Habibi, E., Stickels, R. R., Scalia, G., Brown, J., Yadollahpour, P., Yang, S. M., Abbate, C., Biancalani, T., Macosko, E. Z., Chen, F., Regev, A., & Arlotta, P. (2021). Molecular logic of cellular diversification in the mouse cerebral cortex. *Nature*, *595*(7868), Article 7868. https://doi.org/10.1038/s41586-021-03670-5

Dobbing, J., & Sands, J. (1973). Quantitative growth and development of human brain. *Archives of Disease in Childhood*, *48*(10), 757–767.

Dominguez-Salas, P., Moore, S. E., Baker, M. S., Bergen, A. W., Cox, S. E., Dyer, R. A., Fulford, A. J., Guan, Y., Laritsky, E., Silver, M. J., Swan, G. E., Zeisel, S. H., Innis, S. M., Waterland, R. A., Prentice, A. M., & Hennig, B. J. (2014). Maternal nutrition at conception modulates DNA methylation of human metastable epialleles. *Nature Communications*, *5*(1), Article 1. https://doi.org/10.1038/ncomms4746

Douglas, R. J., & Martin, K. A. C. (2004). Neuronal Circuits of the Neocortex. *Annual Review of Neuroscience*, *27*(1), 419–451. https://doi.org/10.1146/annurev.neuro.27.070203.144152

Ducker, G. S., & Rabinowitz, J. D. (2017). One-Carbon Metabolism in Health and Disease. *Cell Metabolism*, *25*(1), 27–42. https://doi.org/10.1016/j.cmet.2016.08.009

Dwaraka, V. B., Aronica, L., Carreras-Gallo, N., Robinson, J. L., Hennings, T., Lin, A., Turner, L., Smith, R., Mendez, T. L., Went, H., Ebel, E. R., Carter, M. M., Sonnenburg, E. D., Sonnenburg, J. L., & Gardner, C. D. (2023). *Unveiling the Epigenetic Impact of Vegan vs. Omnivorous Diets on Aging: Insights from the Twins Nutrition Study (TwiNS)* (p. 2023.12.26.23300543). medRxiv. https://doi.org/10.1101/2023.12.26.23300543

Edmondson, A. C., Salant, J., Ierardi-Curto, L. A., & Ficicioglu, C. (2016). Missed Newborn Screening Case of Carnitine Palmitoyltransferase-II Deficiency. *JIMD Reports*, *33*, 93–97. https://doi.org/10.1007/8904_2016_528

Eiraku, M., Watanabe, K., Matsuo-Takasaki, M., Kawada, M., Yonemura, S., Matsumura, M., Wataya, T., Nishiyama, A., Muguruma, K., & Sasai, Y. (2008). Self-Organized Formation of Polarized Cortical Tissues from ESCs and Its Active Manipulation by

Extrinsic Signals. *Cell Stem Cell*, *3*(5), 519–532. https://doi.org/10.1016/j.stem.2008.09.002

Emery, A. E., Timson, J., & Watson-Williams, E. J. (1969). Pathogenesis of spina bifida. *Lancet (London, England)*, *2*(7626), 909–910. https://doi.org/10.1016/s0140-6736(69)92371-x

Englund, C., Fink, A., Lau, C., Pham, D., Daza, R. A. M., Bulfone, A., Kowalczyk, T., & Hevner, R. F. (2005). Pax6, Tbr2, and Tbr1 are expressed sequentially by radial glia, intermediate progenitor cells, and postmitotic neurons in developing neocortex. *The Journal of Neuroscience: The Official Journal of the Society for Neuroscience*, *25*(1), 247–251. https://doi.org/10.1523/JNEUROSCI.2899-04.2005

Fabra-Beser, J., Araujo, J. A. M. de, Marques-Coelho, D., Goff, L. A., Costa, M. R., Müller, U., & Gil-Sanz, C. (2021). Differential Expression Levels of Sox9 in Early Neocortical Radial Glial Cells Regulate the Decision between Stem Cell Maintenance and Differentiation. *Journal of Neuroscience*, *41*(33), 6969–6986. https://doi.org/10.1523/JNEUROSCI.2905-20.2021

Fan, G., Martinowich, K., Chin, M. H., He, F., Fouse, S. D., Hutnick, L., Hattori, D., Ge, W., Shen, Y., Wu, H., ten Hoeve, J., Shuai, K., & Sun, Y. E. (2005). DNA methylation controls the timing of astrogliogenesis through regulation of JAK-STAT signaling. *Development (Cambridge, England)*, *132*(15), 3345–3356. https://doi.org/10.1242/dev.01912

Fang, H., Stone, K. P., Wanders, D., Forney, L. A., & Gettys, T. W. (2022). The Origins, Evolution, and Future of Dietary Methionine Restriction. *Annual Review of Nutrition*, *42*(1), 201–226. https://doi.org/10.1146/annurev-nutr-062320-111849

Farber, S., & Diamond, L. K. (1948). Temporary remissions in acute leukemia in children produced by folic acid antagonist, 4-aminopteroyl-glutamic acid. *The New England Journal of Medicine*, *238*(23), 787–793. https://doi.org/10.1056/NEJM194806032382301

Farkas, L. M., Haffner, C., Giger, T., Khaitovich, P., Nowick, K., Birchmeier, C., Pääbo, S., & Huttner, W. B. (2008). Insulinoma-associated 1 has a panneurogenic role and promotes the generation and expansion of basal progenitors in the developing mouse neocortex. *Neuron*, *60*(1), 40–55. https://doi.org/10.1016/j.neuron.2008.09.020

Fawal, M.-A., Jungas, T., Kischel, A., Audouard, C., Iacovoni, J. S., & Davy, A. (2018). Cross Talk between One-Carbon Metabolism, Eph Signaling, and Histone Methylation Promotes Neural Stem Cell Differentiation. *Cell Reports*, *23*(10), 2864-2873.e7. https://doi.org/10.1016/j.celrep.2018.05.005

Fleiss, B., Wong, F., Brownfoot, F., Shearer, I. K., Baud, O., Walker, D. W., Gressens, P., & Tolcos, M. (2019). Knowledge Gaps and Emerging Research Areas in Intrauterine Growth Restriction-Associated Brain Injury. *Frontiers in Endocrinology*, *10*. https://www.frontiersin.org/articles/10.3389/fendo.2019.00188

Forsman, A. (2015). Rethinking phenotypic plasticity and its consequences for individuals, populations and species. *Heredity*, *115*(4), Article 4. https://doi.org/10.1038/hdy.2014.92

Franco, S. J., Gil-Sanz, C., Martinez-Garay, I., Espinosa, A., Harkins-Perry, S. R., Ramos, C., & Müller, U. (2012). Fate-Restricted Neural Progenitors in the Mammalian Cerebral Cortex. *Science*, *337*(6095), 746–749. https://doi.org/10.1126/science.1223616

Freinkel, N. (1980). Banting Lecture 1980. Of pregnancy and progeny. *Diabetes*, *29*(12), 1023–1035. https://doi.org/10.2337/diab.29.12.1023

Freret-Hodara, B., Cui, Y., Griveau, A., Vigier, L., Arai, Y., Touboul, J., & Pierani, A. (2017). Enhanced Abventricular Proliferation Compensates Cell Death in the Embryonic Cerebral Cortex. *Cerebral Cortex*, *27*(10), 4701–4718. https://doi.org/10.1093/cercor/bhw264

Fukuchi-Shimogori, T., & Grove, E. A. (2001). Neocortex Patterning by the Secreted Signaling Molecule FGF8. *Science*, *294*(5544), 1071–1074. https://doi.org/10.1126/science.1064252

Furuta, Y., Piston, D. W., & Hogan, B. L. M. (1997). Bone morphogenetic proteins (BMPs) as regulators of dorsal forebrain development. *Development*, *124*(11), 2203–2212. https://doi.org/10.1242/dev.124.11.2203

Ganetzky, R. D., Bedoukian, E., Deardorff, M. A., & Ficicioglu, C. (2016). Argininosuccinic Acid Lyase Deficiency Missed by Newborn Screen. *JIMD Reports*, *34*, 43–47. https://doi.org/10.1007/8904_2016_2

Gao, P., Postiglione, M. P., Krieger, T. G., Hernandez, L., Wang, C., Han, Z., Streicher, C., Papusheva, E., Insolera, R., Chugh, K., Kodish, O., Huang, K., Simons, B. D., Luo, L., Hippenmeyer, S., & Shi, S.-H. (2014). Deterministic Progenitor Behavior and Unitary Production of Neurons in the Neocortex. *Cell*, *159*(4), 775–788. https://doi.org/10.1016/j.cell.2014.10.027

Garrod, A. E. (1908). *Inborn Errors of Metabolism*.

Gaspard, N., Bouschet, T., Hourez, R., Dimidschstein, J., Naeije, G., van den Ameele, J., Espuny-Camacho, I., Herpoel, A., Passante, L., Schiffmann, S. N., Gaillard, A., & Vanderhaeghen, P. (2008). An intrinsic mechanism of corticogenesis from

embryonic stem cells. *Nature*, *455*(7211), Article 7211. https://doi.org/10.1038/nature07287

Georgieff, M. K. (2007). Nutrition and the developing brain: Nutrient priorities and measurement2. *The American Journal of Clinical Nutrition*, *85*(2), 614S-620S. https://doi.org/10.1093/ajcn/85.2.614S

Gernand, A. D., Schulze, K. J., Stewart, C. P., West, K. P., & Christian, P. (2016). Micronutrient deficiencies in pregnancy worldwide: Health effects and prevention. *Nature Reviews. Endocrinology*, *12*(5), 274–289. https://doi.org/10.1038/nrendo.2016.37

Giandomenico, S. L., Mierau, S. B., Gibbons, G. M., Wenger, L. M. D., Masullo, L., Sit, T., Sutcliffe, M., Boulanger, J., Tripodi, M., Derivery, E., Paulsen, O., Lakatos, A., & Lancaster, M. A. (2019). Cerebral organoids at the air–liquid interface generate diverse nerve tracts with functional output. *Nature Neuroscience*, *22*(4), Article 4. https://doi.org/10.1038/s41593-019-0350-2

Gilsing, A. M. J., Crowe, F. L., Lloyd-Wright, Z., Sanders, T. a. B., Appleby, P. N., Allen, N. E., & Key, T. J. (2010). Serum concentrations of vitamin B12 and folate in British male omnivores, vegetarians and vegans: Results from a cross-sectional analysis of the EPIC-Oxford cohort study. *European Journal of Clinical Nutrition*, *64*(9), Article 9. https://doi.org/10.1038/ejcn.2010.142

Ginhoux, F., Greter, M., Leboeuf, M., Nandi, S., See, P., Gokhan, S., Mehler, M. F., Conway, S. J., Ng, L. G., Stanley, E. R., Samokhvalov, I. M., & Merad, M. (2010). Fate Mapping Analysis Reveals That Adult Microglia Derive from Primitive Macrophages. *Science*, *330*(6005), 841–845. https://doi.org/10.1126/science.1194637

Godfrey, K. M., Haugen, G., Kiserud, T., Inskip, H. M., Cooper, C., Harvey, N. C. W., Crozier, S. R., Robinson, S. M., Davies, L., Group, the S. W. S. S., & Hanson, M. A. (2012). Fetal Liver Blood Flow Distribution: Role in Human Developmental Strategy to Prioritize Fat Deposition versus Brain Development. *PLOS ONE*, *7*(8), e41759. https://doi.org/10.1371/journal.pone.0041759

Götz, M., Stoykova, A., & Gruss, P. (1998). Pax6 Controls Radial Glia Differentiation in the Cerebral Cortex. *Neuron*, *21*(5), 1031–1044. https://doi.org/10.1016/S0896-6273(00)80621-2

Govindan, S., Oberst, P., & Jabaudon, D. (2018). In vivo pulse labeling of isochronic cohorts of cells in the central nervous system using FlashTag. *Nature Protocols*, *13*(10), Article 10. https://doi.org/10.1038/s41596-018-0038-1

Graïc, J.-M., Peruffo, A., Corain, L., Finos, L., Grisan, E., & Cozzi, B. (2022). The primary visual cortex of Cetartiodactyls: Organization, cytoarchitectonics and comparison with perissodactyls and primates. *Brain Structure and Function*, *227*(4), 1195–1225. https://doi.org/10.1007/s00429-021-02392-8

Greig, L. C., Woodworth, M. B., Galazo, M. J., Padmanabhan, H., & Macklis, J. D. (2013). Molecular logic of neocortical projection neuron specification, development and diversity. *Nature Reviews Neuroscience*, *14*(11), Article 11. https://doi.org/10.1038/nrn3586

Grosswendt, S., Kretzmer, H., Smith, Z. D., Kumar, A. S., Hetzel, S., Wittler, L., Klages, S., Timmermann, B., Mukherji, S., & Meissner, A. (2020). Epigenetic regulator function through mouse gastrulation. *Nature*, *584*(7819), Article 7819. https://doi.org/10.1038/s41586-020-2552-x

Grove, E. A., Tole, S., Limon, J., Yip, L., & Ragsdale, C. W. (1998). The hem of the embryonic cerebral cortex is defined by the expression of multiple Wnt genes and is compromised in Gli3-deficient mice. *Development*, *125*(12), 2315–2325. https://doi.org/10.1242/dev.125.12.2315

Gruenwald, P. (1963). CHRONIC FETAL DISTRESS AND PLACENTAL INSUFFICIENCY. *Biologia Neonatorum. Neo-Natal Studies*, *5*, 215–265. https://doi.org/10.1159/000239870

Gu, X., Orozco, J. M., Saxton, R. A., Condon, K. J., Liu, G. Y., Krawczyk, P. A., Scaria, S. M., Harper, J. W., Gygi, S. P., & Sabatini, D. M. (2017). SAMTOR is an S-adenosylmethionine sensor for the mTORC1 pathway. *Science*, *358*(6364), 813–818. https://doi.org/10.1126/science.aao3265

Gunhaga, L., Marklund, M., Sjödal, M., Hsieh, J.-C., Jessell, T. M., & Edlund, T. (2003). Specification of dorsal telencephalic character by sequential Wnt and FGF signaling. *Nature Neuroscience*, *6*(7), Article 7. https://doi.org/10.1038/nn1068

Guo, J., Huang, X., Dou, L., Yan, M., Shen, T., Tang, W., & Li, J. (2022). Aging and aging-related diseases: From molecular mechanisms to interventions and treatments. *Signal Transduction and Targeted Therapy*, *7*(1), Article 1. https://doi.org/10.1038/s41392-022-01251-0

Hanashima, C., Shen, L., Li, S. C., & Lai, E. (2002). Brain Factor-1 Controls the Proliferation and Differentiation of Neocortical Progenitor Cells through Independent Mechanisms. *The Journal of Neuroscience*, *22*(15), 6526–6536. https://doi.org/10.1523/JNEUROSCI.22-15-06526.2002

Hanson, M. A., Bardsley, A., De-Regil, L. M., Moore, S. E., Oken, E., Poston, L., Ma, R. C., McAuliffe, F. M., Maleta, K., Purandare, C. N., Yajnik, C. S., Rushwan, H., & Morris, J.

L. (2015). The International Federation of Gynecology and Obstetrics (FIGO) recommendations on adolescent, preconception, and maternal nutrition: "Think Nutrition First." *International Journal of Gynaecology and Obstetrics: The Official Organ of the International Federation of Gynaecology and Obstetrics*, *131 Suppl 4*, S213-253. https://doi.org/10.1016/S0020-7292(15)30034-5

Harlan De Crescenzo, A., Panoutsopoulos, A. A., Tat, L., Schaaf, Z., Racherla, S., Henderson, L., Leung, K.-Y., Greene, N. D. E., Green, R., & Zarbalis, K. S. (2021). Deficient or Excess Folic Acid Supply During Pregnancy Alter Cortical Neurodevelopment in Mouse Offspring. *Cerebral Cortex*, *31*(1), 635–649. https://doi.org/10.1093/cercor/bhaa248

Haws, S. A., Yu, D., Ye, C., Wille, C. K., Nguyen, L. C., Krautkramer, K. A., Tomasiewicz, J. L., Yang, S. E., Miller, B. R., Liu, W. H., Igarashi, K., Sridharan, R., Tu, B. P., Cryns, V. L., Lamming, D. W., & Denu, J. M. (2020). Methyl-Metabolite Depletion Elicits Adaptive Responses to Support Heterochromatin Stability and Epigenetic Persistence. *Molecular Cell*, *78*(2), 210-223.e8. https://doi.org/10.1016/j.molcel.2020.03.004

Hennig, M., Ewering, L., Pyschny, S., Shimoyama, S., Olecka, M., Ewald, D., Magarin, M., Uebing, A., Thierfelder, L., Jux, C., & Drenckhahn, J.-D. (2019). Dietary protein restriction throughout intrauterine and postnatal life results in potentially beneficial myocardial tissue remodeling in the adult mouse heart. *Scientific Reports*, *9*(1), Article 1. https://doi.org/10.1038/s41598-019-51654-3

Hibbard, B. M., Hibbard, E. D., & Jeffcoate, T. N. A. (1965). Folic Acid and Reproduction. *Acta Obstetricia et Gynecologica Scandinavica*, *44*(3), 375–400. https://doi.org/10.3109/00016346509155874

Hippenmeyer, S. (2023). Principles of neural stem cell lineage progression: Insights from developing cerebral cortex. *Current Opinion in Neurobiology*, *79*, 102695. https://doi.org/10.1016/j.conb.2023.102695

Hoffman, D. J., Powell, T. L., Barrett, E. S., & Hardy, D. B. (2021). Developmental origins of metabolic diseases. *Physiological Reviews*, *101*(3), 739–795. https://doi.org/10.1152/physrev.00002.2020

Hoffman, R. M. (1984). Altered methionine metabolism, DNA methylation and oncogene expression in carcinogenesis: A review and synthesis. *Biochimica et Biophysica Acta (BBA) - Reviews on Cancer*, *738*(1), 49–87. https://doi.org/10.1016/0304-419X(84)90019-2

Horns, R. C., Dower, W. J., & Schimke, R. T. (1984). Gene amplification in a leukemic patient treated with methotrexate. *Journal of Clinical Oncology*, *2*(1), 2–7. https://doi.org/10.1200/JCO.1984.2.1.2

Huang, P. L. (2009). A comprehensive definition for metabolic syndrome. *Disease Models & Mechanisms*, *2*(5–6), 231–237. https://doi.org/10.1242/dmm.001180

Hughes, L., Carton, R., Minguzzi, S., McEntee, G., Deinum, E. E., O'Connell, M. J., & Parle-McDermott, A. (2015). An active second dihydrofolate reductase enzyme is not a feature of rat and mouse, but they do have activity in their mitochondria. *FEBS Letters*, *589*(15), 1855–1862. https://doi.org/10.1016/j.febslet.2015.05.017

Imbard, A., Schwendimann, L., Lebon, S., Gressens, P., Blom, H. J., & Benoist, J.-F. (2021). Liver and brain differential expression of one-carbon metabolism genes during ontogenesis. *Scientific Reports*, *11*(1), Article 1. https://doi.org/10.1038/s41598-021-00311-9

Iwata, R., Casimir, P., Erkol, E., Boubakar, L., Planque, M., Gallego López, I. M., Ditkowska, M., Gaspariunaite, V., Beckers, S., Remans, D., Vints, K., Vandekeere, A., Poovathingal, S., Bird, M., Vlaeminck, I., Creemers, E., Wierda, K., Corthout, N., Vermeersch, P., … Vanderhaeghen, P. (2023). Mitochondria metabolism sets the species-specific tempo of neuronal development. *Science (New York, N.Y.)*, *379*(6632), eabn4705. https://doi.org/10.1126/science.abn4705

Iwata, R., Casimir, P., & Vanderhaeghen, P. (2020). Mitochondrial dynamics in postmitotic cells regulate neurogenesis. *Science*, *369*(6505), 858–862. https://doi.org/10.1126/science.aba9760

James, S. J., Melnyk, S., Jernigan, S., Cleves, M. A., Halsted, C. H., Wong, D. H., Cutler, P., Bock, K., Boris, M., Bradstreet, J. J., Baker, S. M., & Gaylor, D. W. (2006). Metabolic endophenotype and related genotypes are associated with oxidative stress in children with autism. *American Journal of Medical Genetics Part B: Neuropsychiatric Genetics*, *141B*(8), 947–956. https://doi.org/10.1002/ajmg.b.30366

Jungas, T., Joseph, M., Fawal, M.-A., & Davy, A. (2020). Population Dynamics and Neuronal Polyploidy in the Developing Neocortex. *Cerebral Cortex Communications*, *1*(1), tgaa063. https://doi.org/10.1093/texcom/tgaa063

Kadoshima, T., Sakaguchi, H., Nakano, T., Soen, M., Ando, S., Eiraku, M., & Sasai, Y. (2013). Self-organization of axial polarity, inside-out layer pattern, and species-specific progenitor dynamics in human ES cell–derived neocortex. *Proceedings of the National Academy of Sciences*, *110*(50), 20284–20289. https://doi.org/10.1073/pnas.1315710110

Kagan, B. J., & Rosello-Diez, A. (2021). Integrating levels of bone growth control: From stem cells to body proportions. *WIREs Developmental Biology*, *10*(1), e384. https://doi.org/10.1002/wdev.384

Kang, P., Lee, H. K., Glasgow, S. M., Finley, M., Donti, T., Gaber, Z. B., Graham, B. H., Foster, A. E., Novitch, B. G., Gronostajski, R. M., & Deneen, B. (2012). Sox9 and NFIA Coordinate a Transcriptional Regulatory Cascade during the Initiation of Gliogenesis. *Neuron*, *74*(1), 79–94. https://doi.org/10.1016/j.neuron.2012.01.024

Kang, W., Wong, L. C., Shi, S.-H., & Hébert, J. M. (2009). The Transition from Radial Glial to Intermediate Progenitor Cell Is Inhibited by FGF Signaling during Corticogenesis. *Journal of Neuroscience*, *29*(46), 14571–14580. https://doi.org/10.1523/JNEUROSCI.3844-09.2009

Karimi, R., Cleven, A., Elbarbry, F., & Hoang, H. (2021). The Impact of Fasting on Major Metabolic Pathways of Macronutrients and Pharmacokinetics Steps of Drugs. *European Journal of Drug Metabolism and Pharmacokinetics*, *46*(1), 25–39. https://doi.org/10.1007/s13318-020-00656-y

Kessaris, N., Fogarty, M., Iannarelli, P., Grist, M., Wegner, M., & Richardson, W. D. (2006). Competing waves of oligodendrocytes in the forebrain and postnatal elimination of an embryonic lineage. *Nature Neuroscience*, *9*(2), Article 2. https://doi.org/10.1038/nn1620

Keuls, R. A., Finnell, R. H., & Parchem, R. J. (2023). Maternal metabolism influences neural tube closure. *Trends in Endocrinology & Metabolism*, *34*(9), 539–553. https://doi.org/10.1016/j.tem.2023.06.005

Khodosevich, K., & Sellgren, C. M. (2023). Neurodevelopmental disorders—High-resolution rethinking of disease modeling. *Molecular Psychiatry*, *28*(1), Article 1. https://doi.org/10.1038/s41380-022-01876-1

Kierdorf, K., Erny, D., Goldmann, T., Sander, V., Schulz, C., Perdiguero, E. G., Wieghofer, P., Heinrich, A., Riemke, P., Hölscher, C., Müller, D. N., Luckow, B., Brocker, T., Debowski, K., Fritz, G., Opdenakker, G., Diefenbach, A., Biber, K., Heikenwalder, M., … Prinz, M. (2013). Microglia emerge from erythromyeloid precursors via Pu.1- and Irf8-dependent pathways. *Nature Neuroscience*, *16*(3), Article 3. https://doi.org/10.1038/nn.3318

Kintaka, Y., Wada, N., Shioda, S., Nakamura, S., Yamazaki, Y., & Mochizuki, K. (2020). Excessive folic acid supplementation in pregnant mice impairs insulin secretion and induces the expression of genes associated with fatty liver in their offspring. *Heliyon*, *6*(4), e03597. https://doi.org/10.1016/j.heliyon.2020.e03597

Kischel, A., Audouard, C., Fawal, M.-A., & Davy, A. (2020). Ephrin-B2 paces neuronal production in the developing neocortex. *BMC Developmental Biology*, *20*, 12. https://doi.org/10.1186/s12861-020-00215-3

Kleiber, M. (1932). Body size and metabolism. *Hilgardia*, *6*(11), 315–353.

Klingler, E., Francis, F., Jabaudon, D., & Cappello, S. (2021). Mapping the molecular and cellular complexity of cortical malformations. *Science (New York, N.Y.)*, *371*(6527), eaba4517. https://doi.org/10.1126/science.aba4517

Knaus, L. S., Basilico, B., Malzl, D., Gerykova Bujalkova, M., Smogavec, M., Schwarz, L. A., Gorkiewicz, S., Amberg, N., Pauler, F. M., Knittl-Frank, C., Tassinari, M., Maulide, N., Rülicke, T., Menche, J., Hippenmeyer, S., & Novarino, G. (2023). Large neutral amino

acid levels tune perinatal neuronal excitability and survival. *Cell*, *186*(9), 1950-1967.e25. https://doi.org/10.1016/j.cell.2023.02.037

Konycheva, G., Dziadek, M. A., Ferguson, L. R., Krägeloh, C. U., Coolen, M. W., Davison, M., & Breier, B. H. (2011). Dietary methyl donor deficiency during pregnancy in rats shapes learning and anxiety in offspring. *Nutrition Research*, *31*(10), 790–804. https://doi.org/10.1016/j.nutres.2011.09.015

Korsmo, H. W., & Jiang, X. (2021). One carbon metabolism and early development: A diet-dependent destiny. *Trends in Endocrinology & Metabolism*, *32*(8), 579–593. https://doi.org/10.1016/j.tem.2021.05.011

Kowalczyk, T., Pontious, A., Englund, C., Daza, R. A. M., Bedogni, F., Hodge, R., Attardo, A., Bell, C., Huttner, W. B., & Hevner, R. F. (2009). Intermediate neuronal progenitors (basal progenitors) produce pyramidal-projection neurons for all layers of cerebral cortex. *Cerebral Cortex (New York, N.Y.: 1991)*, *19*(10), 2439–2450. https://doi.org/10.1093/cercor/bhn260

Kramer, A. C., Jansson, T., Bale, T. L., & Powell, T. L. (2023). Maternal-fetal cross-talk via the placenta: Influence on offspring development and metabolism. *Development*, *150*(20), dev202088. https://doi.org/10.1242/dev.202088

Kriegstein, A., Noctor, S., & Martínez-Cerdeño, V. (2006). Patterns of neural stem and progenitor cell division may underlie evolutionary cortical expansion. *Nature Reviews Neuroscience*, *7*(11), Article 11. https://doi.org/10.1038/nrn2008

Kuijpers, T. W., de Vries, A. C. H., van Leeuwen, E. M., Ermens, A. (Ton) A. M., de Pont, S., Smith, D. E. C., Wamelink, M. M. C., Mensenkamp, A. R., Nelen, M. R., Lango Allen, H., Pals, S. T., Beverloo, B. H. B., Huidekoper, H. H., & Wagner, A. (2022). Megalobastic anemia, infantile leukemia, and immunodeficiency caused by a novel homozygous

mutation in the DHFR gene. *Blood Advances*, *6*(22), 5829–5834. https://doi.org/10.1182/bloodadvances.2022007233

Laguesse, S., Creppe, C., Nedialkova, D. D., Prévot, P.-P., Borgs, L., Huysseune, S., Franco, B., Duysens, G., Krusy, N., Lee, G., Thelen, N., Thiry, M., Close, P., Chariot, A., Malgrange, B., Leidel, S. A., Godin, J. D., & Nguyen, L. (2015). A Dynamic Unfolded Protein Response Contributes to the Control of Cortical Neurogenesis. *Developmental Cell*, *35*(5), 553–567. https://doi.org/10.1016/j.devcel.2015.11.005

Lancaster, M. A., Renner, M., Martin, C.-A., Wenzel, D., Bicknell, L. S., Hurles, M. E., Homfray, T., Penninger, J. M., Jackson, A. P., & Knoblich, J. A. (2013). Cerebral organoids model human brain development and microcephaly. *Nature*, *501*(7467), Article 7467. https://doi.org/10.1038/nature12517

Lanet, E., Gould, A. P., & Maurange, C. (2013). Protection of Neuronal Diversity at the Expense of Neuronal Numbers during Nutrient Restriction in the Drosophila Visual System. *Cell Reports*, *3*(3), 587–594. https://doi.org/10.1016/j.celrep.2013.02.006

Lauinger, L., & Kaiser, P. (2021). Sensing and Signaling of Methionine Metabolism. *Metabolites*, *11*(2), Article 2. https://doi.org/10.3390/metabo11020083

Lepiemme, F., Stoufflet, J., Javier-Torrent, M., Mazzucchelli, G., Silva, C. G., & Nguyen, L. (2022). Oligodendrocyte precursors guide interneuron migration by unidirectional contact repulsion. *Science*, *376*(6595), eabn6204. https://doi.org/10.1126/science.abn6204

Li, J., Wang, L., Guo, H., Shi, L., Zhang, K., Tang, M., Hu, S., Dong, S., Liu, Y., Wang, T., Yu, P., He, X., Hu, Z., Zhao, J., Liu, C., Sun, Z. S., & Xia, K. (2017). Targeted sequencing and functional analysis reveal brain-size-related genes and their networks in autism

spectrum disorders. *Molecular Psychiatry*, *22*(9), Article 9. https://doi.org/10.1038/mp.2017.140

Lim, L., Mi, D., Llorca, A., & Marín, O. (2018). Development and Functional Diversification of Cortical Interneurons. *Neuron*, *100*(2), 294–313. https://doi.org/10.1016/j.neuron.2018.10.009

Lin, D.-W., Chung, B. P., & Kaiser, P. (2014). S-adenosylmethionine limitation induces p38 mitogen-activated protein kinase and triggers cell cycle arrest in G1. *Journal of Cell Science*, *127*(1), 50–59. https://doi.org/10.1242/jcs.127811

Lionaki, E., Ploumi, C., & Tavernarakis, N. (2022). One-Carbon Metabolism: Pulling the Strings behind Aging and Neurodegeneration. *Cells*, *11*(2), Article 2. https://doi.org/10.3390/cells11020214

Lister, R., Mukamel, E. A., Nery, J. R., Urich, M., Puddifoot, C. A., Johnson, N. D., Lucero, J., Huang, Y., Dwork, A. J., Schultz, M. D., Yu, M., Tonti-Filippini, J., Heyn, H., Hu, S., Wu, J. C., Rao, A., Esteller, M., He, C., Haghighi, F. G., … Ecker, J. R. (2013). Global Epigenomic Reconfiguration During Mammalian Brain Development. *Science*, *341*(6146), 1237905. https://doi.org/10.1126/science.1237905

Llorca, A., Ciceri, G., Beattie, R., Wong, F. K., Diana, G., Serafeimidou-Pouliou, E., Fernández-Otero, M., Streicher, C., Arnold, S. J., Meyer, M., Hippenmeyer, S., Maravall, M., & Marin, O. (2019). A stochastic framework of neurogenesis underlies the assembly of neocortical cytoarchitecture. *eLife*, *8*, e51381. https://doi.org/10.7554/eLife.51381

Lodato, S., Rouaux, C., Quast, K. B., Jantrachotechatchawan, C., Studer, M., Hensch, T. K., & Arlotta, P. (2011). Excitatory Projection Neuron Subtypes Control the Distribution

of Local Inhibitory Interneurons in the Cerebral Cortex. *Neuron*, *69*(4), 763–779. https://doi.org/10.1016/j.neuron.2011.01.015

Lunden, J. W., Durens, M., Phillips, A. W., & Nestor, M. W. (2019). Cortical interneuron function in autism spectrum condition. *Pediatric Research*, *85*(2), Article 2. https://doi.org/10.1038/s41390-018-0214-6

MacDonald, I. A., & Webber, J. (1995). Feeding, fasting and starvation: Factors affecting fuel utilization. *The Proceedings of the Nutrition Society*, *54*(1), 267–274. https://doi.org/10.1079/pns19950053

Malatesta, P., Hack, M. A., Hartfuss, E., Kettenmann, H., Klinkert, W., Kirchhoff, F., & Götz, M. (2003). Neuronal or glial progeny: Regional differences in radial glia fate. *Neuron*, *37*(5), 751–764. https://doi.org/10.1016/s0896-6273(03)00116-8

Marton, R. M., Miura, Y., Sloan, S. A., Li, Q., Revah, O., Levy, R. J., Huguenard, J. R., & Pașca, S. P. (2019). Differentiation and maturation of oligodendrocytes in human three-dimensional neural cultures. *Nature Neuroscience*, *22*(3), Article 3. https://doi.org/10.1038/s41593-018-0316-9

McConnell, S. K., & Kaznowski, C. E. (1991). Cell cycle dependence of laminar determination in developing neocortex. *Science (New York, N.Y.)*, *254*(5029), 282–285. https://doi.org/10.1126/science.254.5029.282

Mentch, S. J., Mehrmohamadi, M., Huang, L., Liu, X., Gupta, D., Mattocks, D., Gómez Padilla, P., Ables, G., Bamman, M. M., Thalacker-Mercer, A. E., Nichenametla, S. N., & Locasale, J. W. (2015). Histone Methylation Dynamics and Gene Regulation Occur through the Sensing of One-Carbon Metabolism. *Cell Metabolism*, *22*(5), 861–873. https://doi.org/10.1016/j.cmet.2015.08.024

Micali, N., Ma, S., Li, M., Kim, S.-K., Mato-Blanco, X., Sindhu, S. K., Arellano, J. I., Gao, T., Shibata, M., Gobeske, K. T., Duque, A., Santpere, G., Sestan, N., & Rakic, P. (2023). Molecular programs of regional specification and neural stem cell fate progression in macaque telencephalon. *Science*, *382*(6667), eadf3786. https://doi.org/10.1126/science.adf3786

Mitchell, H. K., Snell, E. E., & Williams, R. J. (1941). THE CONCENTRATION OF "FOLIC ACID." *Journal of the American Chemical Society*, *63*(8), 2284–2284. https://doi.org/10.1021/ja01853a512

Miyata, T., Kawaguchi, A., Saito, K., Kawano, M., Muto, T., & Ogawa, M. (2004). Asymmetric production of surface-dividing and non-surface-dividing cortical progenitor cells. *Development (Cambridge, England)*, *131*(13), 3133–3145. https://doi.org/10.1242/dev.01173

Miyazawa, H., & Aulehla, A. (2018). Revisiting the role of metabolism during development. *Development*, *145*(19), dev131110. https://doi.org/10.1242/dev.131110

Molné, M., Studer, L., Tabar, V., Ting, Y.-T., Eiden, M. V., & McKay, R. D. G. (2000). Early cortical precursors do not undergo LIF-mediated astrocytic differentiation. *Journal of Neuroscience Research*, *59*(3), 301–311. https://doi.org/10.1002/(SICI)1097-4547(20000201)59:3<301::AID-JNR3>3.0.CO;2-H

Mota-Martorell, N., Jové, M., Berdún, R., & Pamplona, R. (2021). Plasma methionine metabolic profile is associated with longevity in mammals. *Communications Biology*, *4*(1), Article 1. https://doi.org/10.1038/s42003-021-02254-3

MRC Vitamin Study Research Group. (1991). Prevention of neural tube defects: Results of the Medical Research Council Vitamin Study. MRC Vitamin Study Research Group. *Lancet (London, England)*, *338*(8760), 131–137.

Mueller, J. H. (1921). Growth-determining substances in bacteriological culture media. *Proceedings of the Society for Experimental Biology and Medicine*, *18*(7), 225–228. https://doi.org/10.3181/00379727-18-113

Murray, S. A., Morgan, J. L., Kane, C., Sharma, Y., Heffner, C. S., Lake, J., & Donahue, L. R. (2010). Mouse Gestation Length Is Genetically Determined. *PLOS ONE*, *5*(8), e12418. https://doi.org/10.1371/journal.pone.0012418

Muzio, L., & Mallamaci, A. (2003). Emx1, Emx2 and Pax6 in Specification, Regionalization and Arealization of the Cerebral Cortex. *Cerebral Cortex*, *13*(6), 641–647. https://doi.org/10.1093/cercor/13.6.641

Nadarajah, B., & Parnavelas, J. G. (2002). Modes of neuronal migration in the developing cerebral cortex. *Nature Reviews. Neuroscience*, *3*(6), 423–432. https://doi.org/10.1038/nrn845

Namba, T., Dóczi, J., Pinson, A., Xing, L., Kalebic, N., Wilsch-Bräuninger, M., Long, K. R., Vaid, S., Lauer, J., Bogdanova, A., Borgonovo, B., Shevchenko, A., Keller, P., Drechsel, D., Kurzchalia, T., Wimberger, P., Chinopoulos, C., & Huttner, W. B. (2020). Human-Specific ARHGAP11B Acts in Mitochondria to Expand Neocortical Progenitors by Glutaminolysis. *Neuron*, *105*(5), 867-881.e9. https://doi.org/10.1016/j.neuron.2019.11.027

Namba, T., Nardelli, J., Gressens, P., & Huttner, W. B. (2021). Metabolic Regulation of Neocortical Expansion in Development and Evolution. *Neuron*, *109*(3), 408–419. https://doi.org/10.1016/j.neuron.2020.11.014

Nilsson, R., Jain, M., Madhusudhan, N., Sheppard, N. G., Strittmatter, L., Kampf, C., Huang, J., Asplund, A., & Mootha, V. K. (2014). Metabolic enzyme expression highlights a key

role for MTHFD2 and the mitochondrial folate pathway in cancer. *Nature Communications*, *5*(1), Article 1. https://doi.org/10.1038/ncomms4128

Noctor, S. C., Martínez-Cerdeño, V., Ivic, L., & Kriegstein, A. R. (2004). Cortical neurons arise in symmetric and asymmetric division zones and migrate through specific phases. *Nature Neuroscience*, *7*(2), Article 2. https://doi.org/10.1038/nn1172

Oberst, P., Fièvre, S., Baumann, N., Concetti, C., Bartolini, G., & Jabaudon, D. (2019). Temporal plasticity of apical progenitors in the developing mouse neocortex. *Nature*, *573*(7774), Article 7774. https://doi.org/10.1038/s41586-019-1515-6

O'Connor, R. J. (1950). The Metabolism of Cell Division. *British Journal of Experimental Pathology*, *31*(3), 390–396.

O'Connor, R. J. (1952). Growth and Aerobic Glycolysis in the Retina of the Chicken Embryo. *Nature*. https://www.nature.com/articles/169246a0

Osborn, M. J., & Huennekens, F. M. (1958). Enzymatic Reduction of Dihydrofolic Acid. *Journal of Biological Chemistry*, *233*(4), 969–974. https://doi.org/10.1016/S0021-9258(18)64688-5

Ozawa, H., Kambe, A., Hibi, K., Murakami, S., Oikawa, A., Handa, T., Fujiki, K., Nakato, R., Shirahige, K., Kimura, H., Shiraki, N., & Kume, S. (2023). Transient Methionine Deprivation Triggers Histone Modification and Potentiates Differentiation of Induced Pluripotent Stem Cells. *Stem Cells*, *41*(3), 271–286. https://doi.org/10.1093/stmcls/sxac082

Parrettini, S., Caroli, A., & Torlone, E. (2020). Nutrition and Metabolic Adaptations in Physiological and Complicated Pregnancy: Focus on Obesity and Gestational Diabetes. *Frontiers in Endocrinology*, *11*, 611929. https://doi.org/10.3389/fendo.2020.611929

Parthasarathy, S., Srivatsa, S., Nityanandam, A., & Tarabykin, V. (2014). Ntf3 acts downstream of Sip1 in cortical postmitotic neurons to control progenitor cell fate through feedback signaling. *Development*, *141*(17), 3324–3330. https://doi.org/10.1242/dev.114173

Paşca, A. M., Sloan, S. A., Clarke, L. E., Tian, Y., Makinson, C. D., Huber, N., Kim, C. H., Park, J.-Y., O'Rourke, N. A., Nguyen, K. D., Smith, S. J., Huguenard, J. R., Geschwind, D. H., Barres, B. A., & Paşca, S. P. (2015). Functional cortical neurons and astrocytes from human pluripotent stem cells in 3D culture. *Nature Methods*, *12*(7), Article 7. https://doi.org/10.1038/nmeth.3415

Perez-Ramirez, C. A., Nakano, H., Law, R. C., Matulionis, N., Thompson, J., Pfeiffer, A., Park, J. O., Nakano, A., & Christofk, H. R. (2024). Atlas of fetal metabolism during mid-to-late gestation and diabetic pregnancy. *Cell*, *187*(1), 204-215.e14. https://doi.org/10.1016/j.cell.2023.11.011

Petryniak, M. A., Potter, G. B., Rowitch, D. H., & Rubenstein, J. L. R. (2007). Dlx1 and Dlx2 Control Neuronal versus Oligodendroglial Cell Fate Acquisition in the Developing Forebrain. *Neuron*, *55*(3), 417–433. https://doi.org/10.1016/j.neuron.2007.06.036

Pinson, A., Xing, L., Namba, T., Kalebic, N., Peters, J., Oegema, C. E., Traikov, S., Reppe, K., Riesenberg, S., Maricic, T., Derihaci, R., Wimberger, P., Pääbo, S., & Huttner, W. B. (2022). Human TKTL1 implies greater neurogenesis in frontal neocortex of modern humans than Neanderthals. *Science*, *377*(6611), eabl6422. https://doi.org/10.1126/science.abl6422

Pinto, L., Drechsel, D., Schmid, M.-T., Ninkovic, J., Irmler, M., Brill, M. S., Restani, L., Gianfranceschi, L., Cerri, C., Weber, S. N., Tarabykin, V., Baer, K., Guillemot, F.,

Beckers, J., Zecevic, N., Dehay, C., Caleo, M., Schorle, H., & Götz, M. (2009). AP2gamma regulates basal progenitor fate in a region- and layer-specific manner in the developing cortex. *Nature Neuroscience*, *12*(10), 1229–1237. https://doi.org/10.1038/nn.2399

Pizzorno, G., Mini, E., Coronnello, M., McGuire, J. J., Moroson, B. A., Cashmore, A. R., Dreyer, R. N., Lin, J. T., Mazzei, T., Periti, P., & Bertino, J. R. (1988). Impaired Polyglutamylation of Methotrexate as a Cause of Resistance in CCRF-CEM Cells after Short-Term, High-Dose Treatment with This Drug1. *Cancer Research*, *48*(8), 2149–2155.

Pollen, A. A., Nowakowski, T. J., Chen, J., Retallack, H., Sandoval-Espinosa, C., Nicholas, C. R., Shuga, J., Liu, S. J., Oldham, M. C., Diaz, A., Lim, D. A., Leyrat, A. A., West, J. A., & Kriegstein, A. R. (2015). Molecular Identity of Human Outer Radial Glia during Cortical Development. *Cell*, *163*(1), 55–67. https://doi.org/10.1016/j.cell.2015.09.004

Puelles, L., Kuwana, E., Puelles, E., Bulfone, A., Shimamura, K., Keleher, J., Smiga, S., & Rubenstein, J. L. (2000). Pallial and subpallial derivatives in the embryonic chick and mouse telencephalon, traced by the expression of the genes Dlx-2, Emx-1, Nkx-2.1, Pax-6, and Tbr-1. *The Journal of Comparative Neurology*, *424*(3), 409–438. https://doi.org/10.1002/1096-9861(20000828)424:3<409::aid-cne3>3.0.co;2-7

Qiu, R., Wang, X., Davy, A., Wu, C., Murai, K., Zhang, H., Flanagan, J. G., Soriano, P., & Lu, Q. (2008). Regulation of neural progenitor cell state by ephrin-B. *Journal of Cell Biology*, *181*(6), 973–983. https://doi.org/10.1083/jcb.200708091

Rakic, P. (1972). Mode of cell migration to the superficial layers of fetal monkey neocortex. *Journal of Comparative Neurology*, *145*(1), 61–83. https://doi.org/10.1002/cne.901450105

Rallu, M., Machold, R., Gaiano, N., Corbin, J. G., McMahon, A. P., & Fishell, G. (2002). Dorsoventral patterning is established in the telencephalon of mutants lacking both Gli3 and Hedgehog signaling. *Development*, *129*(21), 4963–4974. https://doi.org/10.1242/dev.129.21.4963

Rangaraju, V., Lewis, T. L., Hirabayashi, Y., Bergami, M., Motori, E., Cartoni, R., Kwon, S.-K., & Courchet, J. (2019). Pleiotropic Mitochondria: The Influence of Mitochondria on Neuronal Development and Disease. *Journal of Neuroscience*, *39*(42), 8200–8208. https://doi.org/10.1523/JNEUROSCI.1157-19.2019

Reillo, I., de Juan Romero, C., García-Cabezas, M. Á., & Borrell, V. (2011). A Role for Intermediate Radial Glia in the Tangential Expansion of the Mammalian Cerebral Cortex. *Cerebral Cortex*, *21*(7), 1674–1694. https://doi.org/10.1093/cercor/bhq238

Renner, M., Lancaster, M. A., Bian, S., Choi, H., Ku, T., Peer, A., Chung, K., & Knoblich, J. A. (2017). Self-organized developmental patterning and differentiation in cerebral organoids. *The EMBO Journal*, *36*(10), 1316–1329. https://doi.org/10.15252/embj.201694700

Romo, A., Carceller, R., & Tobajas, J. (2009). Intrauterine growth retardation (IUGR): Epidemiology and etiology. *Pediatric Endocrinology Reviews : PER*. https://www.semanticscholar.org/paper/Intrauterine-growth-retardation-(IUGR)%3A-and-Romo-Carceller/74478edcaaa801c354dae216bd5600b3edbc9cae

Saha, S., Jungas, T., Ohayon, D., Audouard, C., Ye, T., Fawal, M.-A., & Davy, A. (2023). Dihydrofolate reductase activity controls neurogenic transitions in the developing neocortex. *Development*, *150*(20), dev201696. https://doi.org/10.1242/dev.201696

Sahara, S., & O'Leary, D. D. M. (2009). Fgf10 Regulates Transition Period of Cortical Stem Cell Differentiation to Radial Glia Controlling Generation of Neurons and Basal Progenitors. *Neuron*, *63*(1), 48–62. https://doi.org/10.1016/j.neuron.2009.06.006

Salic, A., & Mitchison, T. J. (2008). A chemical method for fast and sensitive detection of DNA synthesis in vivo. *Proceedings of the National Academy of Sciences*, *105*(7), 2415–2420. https://doi.org/10.1073/pnas.0712168105

Sanderson, S. M., Gao, X., Dai, Z., & Locasale, J. W. (2019). Methionine metabolism in health and cancer: A nexus of diet and precision medicine. *Nature Reviews. Cancer*, *19*(11), 625–637. https://doi.org/10.1038/s41568-019-0187-8

Sanosaka, T., Imamura, T., Hamazaki, N., Chai, M., Igarashi, K., Ideta-Otsuka, M., Miura, F., Ito, T., Fujii, N., Ikeo, K., & Nakashima, K. (2017). DNA Methylome Analysis Identifies Transcription Factor-Based Epigenomic Signatures of Multilineage Competence in Neural Stem/Progenitor Cells. *Cell Reports*, *20*(12), 2992–3003. https://doi.org/10.1016/j.celrep.2017.08.086

Scardigli, R., Bäumer, N., Gruss, P., Guillemot, F., & Le Roux, I. (2003). Direct and concentration-dependent regulation of the proneural gene Neurogenin2 by Pax6. *Development*, *130*(14), 3269–3281. https://doi.org/10.1242/dev.00539

Schmidt, J. A., Rinaldi, S., Scalbert, A., Ferrari, P., Achaintre, D., Gunter, M. J., Appleby, P. N., Key, T. J., & Travis, R. C. (2016). Plasma concentrations and intakes of amino acids

in male meat-eaters, fish-eaters, vegetarians and vegans: A cross-sectional analysis in the EPIC-Oxford cohort. *European Journal of Clinical Nutrition*, *70*(3), Article 3. https://doi.org/10.1038/ejcn.2015.144

Serpente, P., Zhang, Y., Islimye, E., Hart-Johnson, S., & Gould, A. P. (2021). Quantification of fetal organ sparing in maternal low-protein dietary models. *Wellcome Open Research*, *6*, 218. https://doi.org/10.12688/wellcomeopenres.17124.2

Serrano, M., Pérez-Dueñas, B., Montoya, J., Ormazabal, A., & Artuch, R. (2012). Genetic causes of cerebral folate deficiency: Clinical, biochemical and therapeutic aspects. *Drug Discovery Today*, *17*(23), 1299–1306. https://doi.org/10.1016/j.drudis.2012.07.008

Sessa, A., Mao, C., Hadjantonakis, A.-K., Klein, W. H., & Broccoli, V. (2008). Tbr2 Directs Conversion of Radial Glia into Basal Precursors and Guides Neuronal Amplification by Indirect Neurogenesis in the Developing Neocortex. *Neuron*, *60*(1), 56–69. https://doi.org/10.1016/j.neuron.2008.09.028

Sharma, D., Shastri, S., & Sharma, P. (2016). Intrauterine Growth Restriction: Antenatal and Postnatal Aspects. *Clinical Medicine Insights: Pediatrics*, *10*, CMPed.S40070. https://doi.org/10.4137/CMPed.S40070

Shen, Q., Wang, Y., Dimos, J. T., Fasano, C. A., Phoenix, T. N., Lemischka, I. R., Ivanova, N. B., Stifani, S., Morrisey, E. E., & Temple, S. (2006). The timing of cortical neurogenesis is encoded within lineages of individual progenitor cells. *Nature Neuroscience*, *9*(6), Article 6. https://doi.org/10.1038/nn1694

Shen, Z., Lin, Y., Yang, J., Jörg, D. J., Peng, Y., Zhang, X., Xu, Y., Hernandez, L., Ma, J., Simons, B. D., & Shi, S.-H. (2021). Distinct progenitor behavior underlying neocortical

gliogenesis related to tumorigenesis. *Cell Reports*, *34*(11), 108853. https://doi.org/10.1016/j.celrep.2021.108853

Shi, Y., Kirwan, P., Smith, J., Robinson, H. P. C., & Livesey, F. J. (2012). Human cerebral cortex development from pluripotent stem cells to functional excitatory synapses. *Nature Neuroscience*, *15*(3), Article 3. https://doi.org/10.1038/nn.3041

Shin, J. A., Lee, J. Y., & Yum, S. K. (2023). Echocardiographic assessment of brain sparing in small-for-gestational age infants and association with neonatal outcomes. *Scientific Reports*, *13*(1), Article 1. https://doi.org/10.1038/s41598-023-37376-7

Shiraki, N., Shiraki, Y., Tsuyama, T., Obata, F., Miura, M., Nagae, G., Aburatani, H., Kume, K., Endo, F., & Kume, S. (2014). Methionine Metabolism Regulates Maintenance and Differentiation of Human Pluripotent Stem Cells. *Cell Metabolism*, *19*(5), 780–794. https://doi.org/10.1016/j.cmet.2014.03.017

Sidman, R. L., & Rakic, P. (1973). Neuronal migration, with special reference to developing human brain: A review. *Brain Research*, *62*(1), 1–35. https://doi.org/10.1016/0006-8993(73)90617-3

Siegenthaler, J. A., Ashique, A. M., Zarbalis, K., Patterson, K. P., Hecht, J. H., Kane, M. A., Folias, A. E., Choe, Y., May, S. R., Kume, T., Napoli, J. L., Peterson, A. S., & Pleasure, S. J. (2009). Retinoic Acid from the Meninges Regulates Cortical Neuron Generation. *Cell*, *139*(3), 597–609. https://doi.org/10.1016/j.cell.2009.10.004

Silva, E. A. B., Venda, A. M., & Homem, C. C. F. (2023). Serine hydroxymethyl transferase is required for optic lobe neuroepithelia development in Drosophila. *Development*, *150*(20), dev201152. https://doi.org/10.1242/dev.201152

Solmonson, A., Faubert, B., Gu, W., Rao, A., Cowdin, M. A., Menendez-Montes, I., Kelekar, S., Rogers, T. J., Pan, C., Guevara, G., Tarangelo, A., Zacharias, L. G., Martin-Sandoval, M.

S., Do, D., Pachnis, P., Dumesnil, D., Mathews, T. P., Tasdogan, A., Pham, A., … DeBerardinis, R. J. (2022). Compartmentalized metabolism supports midgestation mammalian development. *Nature*, *604*(7905), Article 7905. https://doi.org/10.1038/s41586-022-04557-9

Southwell, D. G., Paredes, M. F., Galvao, R. P., Jones, D. L., Froemke, R. C., Sebe, J. Y., Alfaro-Cervello, C., Tang, Y., Garcia-Verdugo, J. M., Rubenstein, J. L., Baraban, S. C., & Alvarez-Buylla, A. (2012). Intrinsically determined cell death of developing cortical interneurons. *Nature*, *491*(7422), Article 7422. https://doi.org/10.1038/nature11523

Takahashi, T., Nowakowski, R. S., & Caviness, V. S. (1993). Cell cycle parameters and patterns of nuclear movement in the neocortical proliferative zone of the fetal mouse. *Journal of Neuroscience*, *13*(2), 820–833. https://doi.org/10.1523/JNEUROSCI.13-02-00820.1993

Takizawa, T., Nakashima, K., Namihira, M., Ochiai, W., Uemura, A., Yanagisawa, M., Fujita, N., Nakao, M., & Taga, T. (2001). DNA Methylation Is a Critical Cell-Intrinsic Determinant of Astrocyte Differentiation in the Fetal Brain. *Developmental Cell*, *1*(6), 749–758. https://doi.org/10.1016/S1534-5807(01)00101-0

Tanaka, Y., Cakir, B., Xiang, Y., Sullivan, G. J., & Park, I.-H. (2020). Synthetic Analyses of Single-Cell Transcriptomes from Multiple Brain Organoids and Fetal Brain. *Cell Reports*, *30*(6), 1682-1689.e3. https://doi.org/10.1016/j.celrep.2020.01.038

Tang, S., Fang, Y., Huang, G., Xu, X., Padilla-Banks, E., Fan, W., Xu, Q., Sanderson, S. M., Foley, J. F., Dowdy, S., McBurney, M. W., Fargo, D. C., Williams, C. J., Locasale, J. W., Guan, Z., & Li, X. (2017). Methionine metabolism is essential for SIRT1-regulated mouse

embryonic stem cell maintenance and embryonic development. *The EMBO Journal*, *36*(21), 3175–3193. https://doi.org/10.15252/embj.201796708

Tanner, J. M. (1963). Regulation of Growth in Size in Mammals. *Nature*, *199*(4896), Article 4896. https://doi.org/10.1038/199845a0

Tat, L., Cannizzaro, N., Schaaf, Z., Racherla, S., Bottiglieri, T., Green, R., & Zarbalis, K. S. (2023). Prenatal folic acid and vitamin B12 imbalance alter neuronal morphology and synaptic density in the mouse neocortex. *Communications Biology*, *6*(1), Article 1. https://doi.org/10.1038/s42003-023-05492-9

Telley, L., Agirman, G., Prados, J., Amberg, N., Fièvre, S., Oberst, P., Bartolini, G., Vitali, I., Cadilhac, C., Hippenmeyer, S., Nguyen, L., Dayer, A., & Jabaudon, D. (2019). Temporal patterning of apical progenitors and their daughter neurons in the developing neocortex. *Science*, *364*(6440), eaav2522. https://doi.org/10.1126/science.aav2522

Tippetts, T. S., Sieber, M. H., & Solmonson, A. (2023). Beyond energy and growth: The role of metabolism in developmental signaling, cell behavior and diapause. *Development*, *150*(20), dev201610. https://doi.org/10.1242/dev.201610

Toma, K., Kumamoto, T., & Hanashima, C. (2014). The Timing of Upper-Layer Neurogenesis Is Conferred by Sequential Derepression and Negative Feedback from Deep-Layer Neurons. *Journal of Neuroscience*, *34*(39), 13259–13276. https://doi.org/10.1523/JNEUROSCI.2334-14.2014

Torheim, L. E., Ferguson, E. L., Penrose, K., & Arimond, M. (2010). Women in resource-poor settings are at risk of inadequate intakes of multiple micronutrients. *The Journal of Nutrition*, *140*(11), 2051S-8S. https://doi.org/10.3945/jn.110.123463

Trujillo, C. A., Gao, R., Negraes, P. D., Gu, J., Buchanan, J., Preissl, S., Wang, A., Wu, W., Haddad, G. G., Chaim, I. A., Domissy, A., Vandenberghe, M., Devor, A., Yeo, G. W., Voytek, B., & Muotri, A. R. (2019). Complex Oscillatory Waves Emerging from Cortical Organoids Model Early Human Brain Network Development. *Cell Stem Cell*, *25*(4), 558-569.e7. https://doi.org/10.1016/j.stem.2019.08.002

Tu, W. B., Christofk, H. R., & Plath, K. (2023). Nutrient regulation of development and cell fate decisions. *Development*, *150*(20), dev199961. https://doi.org/10.1242/dev.199961

Uzquiano, A., Kedaigle, A. J., Pigoni, M., Paulsen, B., Adiconis, X., Kim, K., Faits, T., Nagaraja, S., Antón-Bolaños, N., Gerhardinger, C., Tucewicz, A., Murray, E., Jin, X., Buenrostro, J., Chen, F., Velasco, S., Regev, A., Levin, J. Z., & Arlotta, P. (2022). Proper acquisition of cell class identity in organoids allows definition of fate specification programs of the human cerebral cortex. *Cell*, *185*(20), 3770-3788.e27. https://doi.org/10.1016/j.cell.2022.09.010

Vanderhaeghen, P., & Polleux, F. (2023). Developmental mechanisms underlying the evolution of human cortical circuits. *Nature Reviews. Neuroscience*, *24*(4), 213–232. https://doi.org/10.1038/s41583-023-00675-z

Velasco, S., Kedaigle, A. J., Simmons, S. K., Nash, A., Rocha, M., Quadrato, G., Paulsen, B., Nguyen, L., Adiconis, X., Regev, A., Levin, J. Z., & Arlotta, P. (2019). Individual brain organoids reproducibly form cell diversity of the human cerebral cortex. *Nature*, *570*(7762), Article 7762. https://doi.org/10.1038/s41586-019-1289-x

Verney, C., Takahashi, T., Bhide, P. G., Nowakowski, R. S., & Caviness Jr., V. S. (2000). Independent Controls for Neocortical Neuron Production and Histogenetic Cell

Death. *Developmental Neuroscience*, *22*(1–2), 125–138. https://doi.org/10.1159/000017434

Wade, G. N., & Schneider, J. E. (1992). Metabolic fuels and reproduction in female mammals. *Neuroscience & Biobehavioral Reviews*, *16*(2), 235–272. https://doi.org/10.1016/S0149-7634(05)80183-6

Wang, W., Jossin, Y., Chai, G., Lien, W.-H., Tissir, F., & Goffinet, A. M. (2016). Feedback regulation of apical progenitor fate by immature neurons through Wnt7–Celsr3–Fzd3 signalling. *Nature Communications*, *7*(1), Article 1. https://doi.org/10.1038/ncomms10936

Waterland, R. A., Dolinoy, D. C., Lin, J.-R., Smith, C. A., Shi, X., & Tahiliani, K. G. (2006). Maternal methyl supplements increase offspring DNA methylation at Axin fused. *Genesis*, *44*(9), 401–406. https://doi.org/10.1002/dvg.20230

Woodworth, M. B., Greig, L. C., Kriegstein, A. R., & Macklis, J. D. (2012). SnapShot: Cortical Development. *Cell*, *151*(4), 918-918.e1. https://doi.org/10.1016/j.cell.2012.10.004

Yang, W., Soares, J., Greninger, P., Edelman, E. J., Lightfoot, H., Forbes, S., Bindal, N., Beare, D., Smith, J. A., Thompson, I. R., Ramaswamy, S., Futreal, P. A., Haber, D. A., Stratton, M. R., Benes, C., McDermott, U., & Garnett, M. J. (2013). Genomics of Drug Sensitivity in Cancer (GDSC): A resource for therapeutic biomarker discovery in cancer cells. *Nucleic Acids Research*, *41*(Database issue), D955–D961. https://doi.org/10.1093/nar/gks1111

Zhu, Q., Cheng, X., Cheng, Y., Chen, J., Xu, H., Gao, Y., Duan, X., Ji, J., Li, X., & Yi, W. (2020). O-GlcNAcylation regulates the methionine cycle to promote pluripotency of stem

cells. *Proceedings of the National Academy of Sciences*, *117*(14), 7755–7763. https://doi.org/10.1073/pnas.1915582117